

The damage-associated molecular pattern HMGB1 is released early after clinical hepatic ischemia/reperfusion

Rowan F. van Golen¹, Megan J. Reiniers¹, Gerben Marsman², Lindy K. Alles¹, Derrick M. van Rooyen³, Björn Petri^{4,5,6}, Vincent A. Van der Mark^{1,7}, Adriaan A. van Beek⁸, Ben Meijer⁸, Martinus A. Maas¹, Sacha Zeerleder^{2,10}, Joanne Verheij⁹, Geoffrey C. Farrell³, Brenda M. Luken², Narci C. Teoh³, Thomas M. van Gulik¹, Michael P. Murphy¹¹, Michal Heger^{1*}

1 Department of Surgery (Experimental Laboratory), Academic Medical Center, University of Amsterdam, Amsterdam, the Netherlands

2 Department of Immunopathology, Sanquin Research and Landsteiner Laboratory, Academic Medical Center, University of Amsterdam, Amsterdam, the Netherlands

3 Liver Research Group, Australian National University at The Canberra Hospital, Canberra, Australia

4 Department of Microbiology, Immunology, and Infectious Diseases, Cumming School of Medicine, University of Calgary, Calgary AB T2N 1N4, Alberta, Canada

5 Department of Physiology and Pharmacology, Cumming School of Medicine, University of Calgary, Calgary AB T2N 1N4, Alberta, Canada

6 Snyder Institute for Chronic diseases, University of Calgary, Calgary, Canada

7 Tytgat Institute for Gastrointestinal and Liver Research, Academic Medical Center, University of Amsterdam, Amsterdam, the Netherlands

8 Department of Cell Biology and Immunology, Wageningen University, Wageningen, the Netherlands

9 Department of Pathology, Academic Medical Center, University of Amsterdam, Amsterdam, the Netherlands

10 Department of Hematology, Academic Medical Center, University of Amsterdam, Amsterdam, the Netherlands

11 Medical Research Council Mitochondrial Biology Unit, Cambridge, United Kingdom

***Correspondence:** Michal Heger, Department of Surgery (Experimental Laboratory), Academic Medical Center, University of Amsterdam, Meibergdreef 9, 1105 AZ Amsterdam, the Netherlands
Tel: +31 20 5665573. Fax: +31 20 6976621. Email: m.heger@amc.uva.nl.

Financial support: RVG was supported by a PhD Scholarship and The Young Talent Fund, both from the Academic Medical Center in Amsterdam. MH was supported by grants from the Dutch Anti-Cancer Foundation (Stichting Nationaal Fonds Tegen Kanker) in Amsterdam, the Phospholipid Research Center in Heidelberg, the Nijbakker-Morra Foundation in Leiden, and Stichting Technologische Wetenschap (STW). MH is currently supported by the Dutch Cancer Society (project # 10666).

Abstract

Objective and background. Activation of sterile inflammation after hepatic I/R culminates in liver injury. The route to liver damage starts with mitochondrial oxidative stress and cell death during early reperfusion. The link between mitochondrial oxidative stress, damage-associated molecular pattern (DAMP) release, and sterile immune signalling is incompletely understood and lacks clinical validation. The aim of the study was to validate this relation in a clinical liver I/R cohort and to limit DAMP release using a mitochondria-targeted antioxidant in I/R-subjected mice.

Methods. Plasma levels of the DAMPs high-mobility group box 1 (HMGB1), mitochondrial DNA, and nucleosomes were measured in 39 patients enrolled in an observational study who underwent a major liver resection with (N=29) or without (N=13) intraoperative liver ischemia. Circulating cytokine and neutrophil activation markers were also determined. In mice, the mitochondria-targeted antioxidant MitoQ was intravenously infused in attempt to limit DAMP release, reduce sterile inflammation, and suppress I/R injury.

Results. In patients, HMGB1 was elevated following liver resection with I/R compared to liver resection without I/R. HMGB1 correlated positively with ischemia duration and peak post-operative transaminase (ALT) levels. There were no differences in mitochondrial DNA, nucleosome, or cytokine release. In mice, MitoQ neutralized hepatic oxidative stress and decreased HMGB1 release by $\pm 50\%$. MitoQ suppressed transaminase release, hepatocellular necrosis, and cytokine production. Reconstituting disulfide HMGB1 during reperfusion reversed these protective effects.

Conclusion. HMGB1 seems the most pertinent DAMP in clinical hepatic I/R injury. Neutralizing mitochondrial oxidative stress may limit DAMP release after hepatic I/R and reduce liver damage.

Keywords:

Damage-associated molecular patterns

Antioxidants

Intravital microscopy

Liver resection

Sterile inflammation

Mitochondrial DNA

Abbreviations:

ALT = alanine aminotransferase

ASA = American Society of Anesthesiologists

AST = aspartate aminotransferase

BMI = body mass index

CTRL = control (group)

CRC = colorectal cancer metastasis

DAMP = damage-associated molecular pattern

dTPP = decyl-triphenylphosphonium

HCC = hepatocellular carcinoma

HMGB1 = high-mobility group box 1

I/R = ischemia/reperfusion

ICAM = intercellular adhesion molecule

IHC = intrahepatic cholangiocarcinoma

IL = interleukin

INR = international normalized ratio

IQR = interquartile range

mtDNA = mitochondrial DNA

PHCC = perihilar cholangiocarcinoma

PVE = portal vein embolization

RAGE = receptor for advanced glycation end products

ROS = reactive oxygen species

TLR = toll-like receptor

NAC = N-acetylcysteine

VIO = vascular inflow occlusion

VCAM = vascular cell adhesion protein

1. Introduction

During major liver resection, the induction of liver ischemia by surgical clamping of the afferent hepatic vasculature is used to counter the risks of excessive blood loss. This surgical technique is known as vascular inflow occlusion (VIO) or the Pringle maneuver¹. When employed within predefined time limits and in selected patients, this manoeuvre is considered safe. However, the transient lack of organ perfusion and oxygenation also inadvertently causes ischemia/reperfusion (I/R) injury²⁻⁴ and the severity of hepatic I/R injury impacts the recovery of patients after major liver surgery.

Activation of sterile inflammation is a key feature of hepatic I/R injury. During ischemia, the lack of oxygen halts oxidative phosphorylation and leads to the build-up of citric acid cycle metabolites such as succinate^{5,6}. Once the oxygen supply is restored, the consumption of accumulated succinate during the first minutes of reperfusion fuels a burst of reactive oxygen species (ROS) production by the mitochondrial electron transport chain^{5,6}. The consequent wave of ROS-induced cell death triggers the release of damage-associated molecular patterns (DAMPs) by hepatocytes. DAMPs are innocuous intracellular constituents that become potent triggers of the innate immune system once released into the circulation^{2,7}. Effector cells of the innate immune system such as neutrophils in turn confer the bulk of hepatic tissue injury. Based on this sequence of events, DAMPs occupy a crucial role in the onset of I/R injury as signal transducers and amplifiers of the sterile immune response.

Several DAMPs, including histones⁸, DNA⁹, and high-mobility group box 1 (HMGB1)¹⁰ have been causally linked to hepatic I/R injury in animal studies. DAMP release has also been measured in clinical accounts of sterile liver injury^{11,12}. However, the link between mitochondrial oxidative stress and DAMP release has not been clinically elaborated in the context of hepatic I/R injury to date, and was therefore investigated in this study. To that end, DAMP release was studied in patients undergoing liver resection with or without being subjected to I/R.

It is shown that patients who underwent major liver surgery rapidly exhibit DAMP release after resection. Of the tested DAMPs, only HMGB1 levels increased specifically in I/R-subjected patients and not in the control group operated without I/R. HMGB1 release correlated positively with ischemia time and postoperative hepatocellular injury markers. The results were back-translated to a validated mouse model¹³ to allow experimental confirmation and further elaboration. Decreasing mitochondrial oxidative

damage during early reperfusion with the mitochondria-targeted antioxidant MitoQ in mice prevented HMGB1 release and attenuated the I/R immune response. Decreasing mitochondrial oxidative damage therefore may potentially improve outcomes in patients undergoing major liver surgery.

2. Materials and methods

References to the supplemental information are indicated with the prefix 'S'.

2.1 Study participants and study design

The effect of liver surgery performed with or without intraoperative liver ischemia on DAMP release was investigated in a single-center observational trial registered at <https://ClinicalTrials.gov> under identifier NCT01700660. Eligible for participation were all patients scheduled for a major liver resection (removal of ≥ 3 Couinaud segments) that were ≥ 18 years old and had an American Society of Anesthesiology physical status score of ≤ 3 . Patients were excluded from the study when considered unresectable during surgical exploration, when the employed ischemia time was < 20 min, when they underwent an emergency operation, or when the patient was pregnant or breast-feeding. Because the decision whether or not to use vascular inflow occlusion (VIO) and thereby subject patients to I/R was made at the discretion of the performing surgeon based on the actual or anticipated amount of blood loss, participants were non-randomly assigned to either the I/R group (N=26) or the control group (N=13). Intermittent VIO was typically performed in cycles comprising 20 min of ischemia followed by 10 min of reperfusion. In a minor fraction of patients, the operative cause necessitated the use of continuous VIO (see Supplemental Table S4). All patients were operated by the same primary surgeon (TVG).

Blood samples were drawn from a central venous catheter after the induction of general anesthesia (i.e., at baseline) and 1 and 6 h after the start of reperfusion (I/R group) or completion of parenchymal transection (CTRL group). Plasma liver injury (ALT) and liver function (international normalized ratio (INR), total bilirubin) were determined as part of routine patient care. Post-operative complications were categorized according to the Clavien-Dindo grading system¹⁴. All experimental results were normalized to plasma protein content (Pierce BCA Protein Assay Kit, Life Technologies, Carlsbad, CA) to correct for hemodilution, as described¹⁵. All study protocols were approved by the Institutional Review Board and written informed consent was obtained from all participants before undergoing any study-related procedures. The study design is summarized in Supplemental Figure S1.

2.2 Circulating HMGB1

Plasma HMGB1 levels were determined in 10 μ L of EDTA-anticoagulated plasma samples by ELISA (IBL International, Hamburg, Germany) according to manufacturer's instructions. All samples were measured in duplicate in regular sensitivity mode on a Synergy HT microplate reader (BioTek Instruments, Winooski, VT).

2.3 Circulating nucleosomes and elastase- α 1-antitrypsin complexes

Nucleosome levels were assessed by ELISA as previously described¹⁶. Briefly, monoclonal antibody CLB-ANA/60 (Sanquin, Amsterdam, the Netherlands) that recognizes histone 3 was used as capture antibody. Biotinylated F(ab)₂ fragments of monoclonal antibody CLB-ANA/58 (Sanquin), which recognizes an epitope exposed on complexes of dsDNA histone 2A and histone 2B in combination with poly-horseradish peroxidase-labeled streptavidin (Sanquin) were used for detection. As a standard, we used culture supernatant of Jurkat cells (1×10^6 cells/mL), cultured for an additional week without refreshing the medium, to obtain 100% apoptotic cells. One unit is the amount of nucleosomes released by ≈ 100 Jurkat cells. The lower detection limit of the assay was 2.5 U/mL¹⁷. The reference range for circulating nucleosomes in healthy individuals is 0-10.3 U/mL.

Elastase- α 1-antitrypsin complexes (E-AT) were measured by ELISA as described¹⁸. This assay was adapted from a previously described radioimmunoassay¹⁹. Briefly, plates were coated with a polyclonal rabbit anti-human neutrophil elastase antibody (1.5 μ g/mL; Sanquin). Standard and samples were diluted in high-performance ELISA buffer (HPE; Sanquin) + 40 μ g/mL bovine IgG. Bound complexes were detected with a biotinylated monoclonal anti- α 1-antitrypsin antibody (1 μ g/mL; Sanquin) in combination with poly-horseradish peroxidase-labeled streptavidin. Results are expressed in ng/mL by reference to a standard curve of normal human citrated plasma in which EA-T were generated by incubation with porcine elastase (final concentration 2 μ g/mL; Sigma, Zwijndrecht, the Netherlands) for 15 min at room temperature. The detection limit of the assay was 2 ng/mL. The reference range for EA-T in healthy individuals is 8.5 to 55.7 ng/mL.

2.4 Circulating mitochondrial DNA

Plasma mitochondrial DNA levels were determined according to Nakahira et al.²⁰, with minor modifications. Total DNA was isolated from 190 μ L of heparin-anticoagulated plasma using the QIAamp DNA Blood Mini Kit (cat. #51106, Qiagen) according to the manufacturer's instructions. DNA was eluted in 100 μ L of elution buffer. Levels of mitochondrial DNA (mtDNA) were analyzed in duplicate by real-time quantitative PCR on a Lightcycler 480 (Roche) using a reaction volume of 10 μ L consisting of 2 μ L of DNA, 2 μ L of nuclease-free water (Qiagen), 1 μ L of primer mix (0.5 μ M final primer concentration), and 5 μ L of SensiFAST SYBR No-ROX mix (Bioline, London, UK). The run parameters are specified in Supplemental Table S1. The following primers were used: human mitochondrially-encoded NADH dehydrogenase 1 (MT-ND1): forward 5'-ATACCCATGGCCAACCTCCT-3', reverse 5'-GGGCCTTTGCGTAGTTGTAT-3'¹². Melting curve analysis and ethidium bromide-stained agarose gel electrophoresis were used to validate primer specificity. A plasmid encoding a human cDNA clone of MT-ND1 was purchased from ORIGENE (SC101172) and was used as a logarithmic mtDNA standard in 10-fold serial dilutions (1.93×10^6 copies – 1.93×10^0 copies). Data were processed according to Ruijter et al.²¹, fitted to the mtDNA standard, and normalized to plasma protein content.

2.5 Human plasma cytokine measurements

L-12p70, TNF, IL-10, IL-6, IL-1 β , and IL-8/CXCL8 concentrations were determined in serum samples using the Cytometric Bead Array (CBA) Human Inflammatory Cytokines Kit (BD Biosciences, Franklin, NJ) according to the manufacturer's instructions. The samples were analyzed in a blinded fashion and flow data were collected using a BD FACSCanto II (BD Biosciences). The results were analyzed with FCAP Array version 3.0 software (BD Biosciences). CCL2 plasma concentration was measured by ELISA (Duosets, R&D Systems, Minneapolis, MN). All reagents and solutions were prepared fresh each week according to the manufacturer's protocols and were sterile filtered using 0.2 μ M bottle-top vacuum filters (Corning, Corning, NY). Bovine serum albumin was of the highest available purity (cat. #A7030, Sigma-Aldrich, St. Louis, MO) and ELISAs were performed using clear 96-well flat bottom polystyrene microplates (#9018, Corning). All cytokine levels were normalized to plasma total protein content.

2.6 Mouse hepatic ischemia/reperfusion experiments

The animal experiments were approved by the institute's animal welfare committee and surgical procedures were as described¹³. MitoQ was dissolved to a concentration of 6 mg/mL MitoQ in sterile NaCl (Braun). After induction of anesthesia, 250 ng/kg – 3 mg/kg MitoQ or an equimolar amount of the inactive targeting moiety decyl-triphenylphosphonium (dTPP) in sterile NaCl was infused via the penile vein in a volume of 100 µL per 30 g body weight. After allowing MitoQ or dTPP to circulate for 10 min, partial (70%) liver ischemia was induced for 30 min¹³. As a control group, animals underwent sham surgery that entailed a laparotomy with mobilization of hilar structures, but without actual occlusion of the afferent vasculature. For every set of experiments, animals were randomly assigned to an experimental arm. For HMGB1 reconstitution experiments, 2.5 µg disulfide HMGB1 (IBL) in 100 µL sterile NaCl was administered intraperitoneally immediately after reperfusion was initiated. Disulfide HMGB1 was selected for the reconstitution experiments because (1) it is the predominant isoform released in mice subjected to hemorrhagic shock and resuscitation²² - a model that pathophysiologically resembles liver I/R - and (2) the disulfide isoform activates the hepatic I/R-pertinent TLR-4 signaling axis^{10,23,24}. Animals were sacrificed at 6 h or 24 h of reperfusion. Blood and liver samples were processed as described¹³. The number of animals per group per experiment is included in the figure legends. To account for variations in experimental conditions and animal batches, a new control group of vehicle-treated mice subjected to I/R was included in every new set of experiments.

2.7 Mouse liver histology

Mouse liver specimens were fixed in formalin, embedded in paraffin, and stained with hematoxylin and eosin as described¹³. The extent of confluent parenchymal necrosis was scored by a hepatopathologist (JV) according to the following grading system: 0=no necrosis, 1=<25% necrosis, 2=25-50% necrosis, 3=50-75% necrosis, and 4=>75% necrosis.

2.8 Western blot

Frozen liver (-80 °C) samples were homogenized with an Omni Tissue Master 125 (Omni International, Kennesaw, GA) in cell lysis buffer (50 mM HEPES, 150 mM NaCl, 1.5 mM MgCl₂, 1 mM EGTA, 10% glycerol, 0.1% Triton X-100 containing protease and phosphatase inhibitors). Cell debris was pelleted

(12,000 x g, 5 min), supernatant protein content determined (DC Protein Assay, Bio-Rad), and SDS-polyacrylamide gel electrophoresis (Bio-Rad Mini-PROTEAN) was performed with samples standardized to 30 µg protein/well. Proteins were separated using 7.5% gels, followed by electrophoretic elution onto PVDF membranes (Trans-Blot Turbo, Bio-Rad), as per manufacturer's instructions. Blots were run under reducing conditions. PVDF membranes were blocked (5% skim milk, 1 h), incubated with primary antibodies (Supplemental Table S1) for 16 h (4 °C) and stained with appropriate HRP-conjugated secondary antibodies (Santa Cruz). Immunoreactivity was detected using SuperSignal West Femto Substrate (Thermo Scientific) and digital chemiluminescence image capture (LAS-4000, FujiFilm, Tokyo, Japan). Densitometric analysis was performed with MultiGauge software (V3.0, FujiFilm, Tokyo, Japan), and all values were normalized to the expression of the housekeeping protein β-actin. All experiments were performed in triplicate.

2.9 Mouse plasma cytokine measurements

Mouse plasma samples were assayed for mouse GM-CSF, IFN-γ, IL-1β, IL-2, IL-4, IL-5, IL-6, IL12p70, IL-13, IL-18, and TNF-α using the ProcartaPlex Mouse Th1/Th2 extended 11-plex kit and mouse BAFF, IL-10, IL-22, RANTES/CCL5, TSLP, and VEGF-A using ProcartaPlex simplex kits on the Luminex platform (Affymetrix, Santa Clara, CA), according to the manufacturer's instructions. The relevance of these inflammatory messengers for hepatic I/R injury is summarized in Supplemental Table S3. In brief, samples were thawed on ice. The antibody-coated beads were mixed and washed, and incubated overnight at 4 °C with 1:1 diluted standards or samples. After washing, the beads were incubated with detection antibody mix for 30 min at room temperature. The beads were subsequently washed and incubated for 30 min at room temperature with streptavidin-PE. After washing, the beads were measured with a Luminex instrument (Bio-Plex 200, Bio-Rad) that was calibrated using Bio-Rad calibration beads. Standard curves were calculated using 5-parameter logistic regression in Bioplex 5.0 software. Heatmaps were generated using GENE-E software (<http://www.broadinstitute.org/cancer/software/GENE-E/>) and show the plasma cytokine levels of MitoQ-treated mice following 30 min of ischemia and 6 h or 24 h of reperfusion. Data per time point are expressed as fold-increase compared to the mean of the vehicle

control group, whereby blue indicates a decrease and red indicates an increase in the MitoQ group versus control animals subjected to I/R only.

2.10 Intravital imaging and spectroscopic quantification of reactive oxygen species production during hepatic I/R injury in mice

The oxidation-sensitive fluorogenic probe 5(6)-carboxy-dichlorodihydrofluorescein was prepared from 5(6)-carboxy-dichlorodihydrofluorescein diacetate and encapsulated in hepatocyte-targeted liposomes according to Reiniers et al²⁵. Liposomes (0.1 μ mol lipid/g body weight in 200 μ L 10 mM HEPES, 0.88% NaCl, 0.292 osmol/kg, pH = 7.4) were injected via the penile vein and circulated for 35 min to allow intrahepatic accumulation. Hepatic I/R was subsequently performed as described²⁵. To perform the surgical procedure with the mice positioned under the intravital imaging setup, ischemia was induced with a silicone sling placed around the hepatic pedicle instead of a microvascular clamp. During the first 10 min of reperfusion, hepatic probe conversion was quantified at 2-min intervals in real-time using a customized intravital fluorescence microscope (M165FC, Leica Microsystems, Wetzlar, Germany) equipped with a spectrometer (QE65000, Ocean Optics, Dunedin, FL). Spectroscopic data were integrated over the entire spectral width (λ = 250–1050 nm) and normalized to baseline.

2.11 Statistical analyses

Statistical analyses were performed using Graphpad Prism 6 (La Jolla, CA) and SPSS 21.0 (Chicago, IL), abiding by a significance level (α) of 0.05 unless otherwise indicated. Normal distribution of data sets with ≥ 8 values was assessed using a D'Agostino and Pearson omnibus test. Normally distributed data were tested for intragroup and intergroup differences using a student's t-test, a one-way ANOVA with Dunnett's post-hoc test, or a repeated measure ANOVA with Geisser-Greenhouse correction and Tukey's post-hoc correction. All continuous numerical variables that failed the normality test were log transformed and re-analyzed. Log-transformed data that followed a Gaussian distribution were analyzed parametrically as described. If the transformed data failed the normality test, non-parametric tests (Mann Whitney U, Kruskal-Wallis with Dunn's post-hoc test, or Friedman with Dunn's correction) were performed on the non-transformed data. Data sets with < 8 values group were tested parametrically. Categorical data were

analyzed using a Fisher's exact test (binary data) or a Chi-squared test (>2 variables) and correlations were tested using Spearman's rho.

3. Results

3.1 DAMP release after major liver resection in patients

To study DAMP release after clinical liver I/R, a total of 74 patients were enrolled in an observational study. Of the 74 study participants, 35 were excluded due to unresectable disease during surgical exploration (N=30), withdrawal of consent (N=1), an unanticipated change in primary surgeon (N=1), or because a minor instead of a major liver resection was performed (N=3). The relationship between hepatic I/R injury and DAMP release was therefore studied in 39 patients who underwent a major liver resection with (N=26, 'I/R') or without (N=13, 'CTRL') the intraoperative use of VIO. The study design is summarized in Supplemental Figure S1. The baseline patient characteristics are shown in Table 1 and the clinical outcomes are presented in Table 2.

The baseline patient characteristics were comparable between the two study arms. VIO use was associated with longer operating time, resection time, and hospital stay compared to the control group (Table 2). A trend towards more extensive liver resection was seen in the I/R group (Table 2). The severity of postoperative liver injury did not differ between the groups when judged by liver damage (i.e. the postoperative ALT peak) or liver function parameters such as INR and bilirubin (Table 2). There were also no differences in transfusion requirements, postoperative complications, or mortality between the control and I/R group (Table 2). As the aim of the study was to explore DAMP release and activation of sterile inflammation in I/R-subjected patients, it should be underscored that the study was neither designed nor powered to detect differences in patient outcomes between the control and I/R group.

Systemic DAMP levels were next determined in the full cohort at baseline and at 1 h and 6 h after surgery. HMGB1 and nucleosomes were assessed based on preclinical hepatic I/R work^{8,24}. Circulating mitochondrial DNA (mtDNA) was assayed because hepatic I/R injury is thought to originate in ROS-generating mitochondria⁵ and because mtDNA release has been documented in both animal and clinical studies on sterile liver injury^{11,12}. Figure 1A-B show that systemic HMGB1 and nucleosomes concentrations increased within 1 h after surgery in the combined cohort, which was accompanied by a rise in neutrophil activation (Fig. 1D). Systemic mtDNA levels remained unchanged during the first 6 h of

reperfusion (Fig. 1C). These data show that the DAMPs HMGB1 and nucleosomes are released into the circulation after major liver resection.

To determine whether DAMP release was caused by ischemia-mediated hepatocyte injury or by surgical trauma *per se*, which has been noted previously²⁶, the patient data were stratified into an I/R and a control group. Figure 2A-D show that, of the tested DAMPs, only HMGB1 levels increased significantly at 1 h of reperfusion in the I/R group but not in the control group. The release of the cytokines interleukin (IL)-1 β and IL-6 was also more pronounced in the I/R group than in the control group at 1 h of reperfusion (Fig. S2). The early intergroup differences in HMGB1 and cytokine release resolved 6 h after surgery (Fig. 2A, S2). Nucleosome release and neutrophil activation were comparable between groups at all time points (Fig. 2B-C). In line with the release of HMGB1 in only the I/R group, systemic HMGB1 levels after surgery correlated positively to the postoperative ALT peak (Fig. 2E) and the used duration of hepatic ischemia (Fig. 2F). Such a relationship was typically absent for cytokine levels or neutrophil activation (Fig. S3). Collectively, these results suggest that HMGB1 is the DAMP that is most pertinent to clinical hepatic I/R injury.

3.2 Neutralizing mitochondrial oxidative stress limits HMGB1 release after mouse liver I/R

After establishing that HMGB1 is released in patients after hepatic I/R, the therapeutic efficacy of inhibiting HMGB1 release was investigated in a validated mouse hepatic I/R model¹³.

Because mitochondrial oxidative injury is considered the most proximal trigger of I/R injury and therefore may cause the release of DAMPs, it was tested whether the mitochondria-targeted antioxidant MitoQ could limit HMGB1 release and, thereby, attenuate hepatic I/R injury in mice. The cytoprotective efficacy of MitoQ was established first. The intravenous administration of MitoQ reduced plasma ALT levels at 6 h and 24 h of reperfusion in mice over a 0.25-1 mg/kg dose range (Fig. 3A), whereas non-specific MitoQ toxicity was seen at higher dosages. Based on this pharmacodynamic profile, 1 mg/kg of MitoQ was used in all *in vivo* experiments.

In concordance with a previous report demonstrating the antioxidant efficacy of MitoQ in I/R-subjected mice²⁷, MitoQ reduced oxidation of the fluorogenic probe 5(6)-carboxy-dichlorofluorescein in hepatocytes during the first 10 min of reperfusion, as measured by intravital spectroscopy (Fig. 3B). The

fluorogenic probe was delivered specifically to hepatocytes using a hepatotargeted delivery system²⁵. MitoQ did not affect the number of leukocytes in the hepatic microcirculation during the first 90 min of reperfusion (Fig. S6, S7). The early reduction in oxidative stress (Fig. 3B) translated to a drop in hepatocellular necrosis and transaminase release at 24 h of reperfusion (Fig. 3C-D), indicating a reduction in hepatic I/R injury. Animals that received the inactive targeting moiety of MitoQ, dTPP, were not protected from I/R injury (Fig. 3C-D), reaffirming that the antioxidant properties of the ubiquinol moiety convey the hepatoprotective effects of MitoQ.

After demonstrating that MitoQ was able to reduce I/R injury, the effect of neutralizing mitochondrial oxidative stress on HMGB1 release after mouse liver I/R was explored. Figure 3E shows that MitoQ reduced plasma HMGB1 levels after I/R by approximately 50% at 6 h of reperfusion. Quantification of HMGB1 in liver biopsies by Western blot showed similar HMGB1 levels in MitoQ-treated and untreated mice subjected to I/R (Fig. 3F). This finding may relate to differences in resolving capacity between the techniques used for plasma and whole-liver HMGB1 quantification. To examine whether HMGB1 release was associated with the documented hepatoprotective effect of MitoQ, DAMP reconstitution experiments were performed. Infusing the pro-inflammatory disulfide isoform of HMGB1²⁸ at the start of reperfusion nullified the protective potential of MitoQ (Fig. 3G), which supports the hypothesis that I/R injury sequentially proceeds via mitochondrial oxidative injury and DAMP release.

Systemic HMGB1 alerts the immune system via the receptor for glycation end products (RAGE) and/or Toll-like receptor 4 (TLR-4)^{24,29}, which drive cytokine production by activating various pro-inflammatory transcription factors. After establishing that neutralizing mitochondrial oxidative stress with MitoQ decreased HMGB1 release and reduced hepatic I/R injury, it was determined whether MitoQ treatment also attenuated inflammatory signaling following mouse liver I/R. Levels of chemotactic and cytotoxic messengers such as tumor necrosis factor (TNF- α) and interleukin (IL-)1 β were lower in the MitoQ group at 6 h of reperfusion, whereas a stronger induction of anti-inflammatory IL-10 was noted at the 24 h time point (Fig. 3J). This favorable effect of MitoQ on cytokine profiles may have resulted in the downregulation of the leukocyte receptor VCAM-1, even though the expression of the principal sinusoidal neutrophil receptor ICAM-1 was unaffected (Fig. 3HI).

4. Discussion

This study shows that (i) the DAMP HMGB1 seems most pertinent in clinical liver I/R injury, (ii) that HMGB1 levels positively correlate with liver injury markers in I/R-subjected patients, and (iii) that treating mitochondrial oxidative injury with MitoQ prevents HMGB1 release and consequent sterile inflammation, ultimately attenuating I/R injury in mice.

Major liver resection remains associated with considerable mortality, exceeding 10% in patients with high-risk tumors³⁰. The ramifications of liver ischemia therefore still influence surgical practice on a daily basis. Part of the challenge is that supportive care is the only current treatment for hepatic I/R injury, and in that respect, several observations can be made based on the current work. It is the first report that shows DAMP release directly after major liver resection, and additionally identifies HMGB1 as the DAMP most pertinent to clinical I/R injury. Liver I/R in patients was characterized by an early rise in HMGB1 levels 1 h after surgery, whereas HMGB1 returned to baseline 6 h after surgery. The early release of HMGB1 fits previous reports showing that HMGB1 from hepatocytes is already propagated by ischemia, and persists throughout the reperfusion phase in mice subjected to I/R³¹. It is also consistent with the finding that HMGB1 is found in the caval effluent immediately after liver transplantation³². The notion that HMGB1 levels correlated to transaminase release and the duration of ischemia indicates that HMGB1 may hold prognostic or even therapeutic value, as HMGB1 is an active mediator of immune activation that could serve as an interventional target. Small-molecule inhibitors of the HMGB1 receptor RAGE are being clinically evaluated for ancillary indications³³, whereas inhibition of TLR receptors has been proposed to treat inflammatory disorders³⁴. Direct HMGB1 inhibition has also shown promise in treating drug-induced liver injury in mice³⁵. This starkly contrasts the liver injury markers such as ALT or bilirubin, which are 'passive' markers for hepatocellular injury that do not modulate immune responses. The latter also applies to other hepatic I/R biomarkers such as keratin 18³⁶. DAMP-targeted interventions could for instance be used on an on-demand basis to control I/R injury in patients with anticipated (or unexpected) extensive ischemia times. A similar rationale has driven the introduction of *in situ* liver cooling techniques^{37,38}.

HMGB1 could theoretically also derive from other cells or organs after liver I/R, such as the intestines³⁹. It is however most plausible that hepatocytes are the source of HMGB1, for several reasons.

First, the postoperative rise in HMGB1 is not seen in hepatocyte-specific HMGB1 knockout mice subjected to liver I/R⁴⁰. Similar results have been obtained with mice deficient in hepatocyte TLR-4, an innate immune receptor that mediates facilitates HMGB1 release after I/R^{24,41}. Second, HMGB1 levels were more prominent in caval than in portal blood after liver transplantation³², whereas no differences were noted between systemic and portal HMGB1 concentrations. The latter excludes the bowel as a source of HMGB1 after liver transplantation. Last, *in vitro* studies have shown that hepatocytes rendered hypoxic or exposed to the oxidant hydrogen peroxide release HMGB1 into the culture supernatant²⁴. An unanswered question is which HMGB1 isoform is released after liver I/R, as the biological effects of HMGB1 depend on the oxidation status of the protein²⁸. In addition, it should be elucidated how HMGB1 is inactivated and/or regulated at sites of inflammation. This is imperative given the transient nature of postoperative HMGB1 surges noted both after liver transplantation³² and in the current study (Fig. 2).

The finding that mtDNA levels were unaffected by liver I/R is unexpected, given that mtDNA release was seen in mice and patients with acetaminophen (APAP) hepatotoxicity, which pathophysiologically resembles I/R in terms of oxidative injury to hepatocyte mitochondria^{12,42,43}. The discrepancy may relate to several differences between I/R injury and APAP overdose. First, the mechanistic pathways culminating in mitochondrial damage are different. In case of APAP, cytoplasmic glutathione stores are depleted, leading to the accumulation of the toxic NAPQI that associates with mitochondrial proteins and leads to mitochondrial permeability transition (MPT) and necrotic cell death⁴³. Accordingly, APAP causes cytoplasmic redox stress that subsequently migrates to the mitochondria. In case of I/R, the depletion and subsequent repletion of the terminal substrate of the electron transport chain (ETC) - molecular oxygen - leads to an oxidative burst and ROS production that perturbs ETC proteins by redox modification and causes MPT and mainly necrotic cell death⁴⁴. Mitochondrial damage by I/R therefore has a mitochondrial origin, which could translate to differential mtDNA kinetics versus APAP-triggered mtDNA kinetics. Corroboratively, mtDNA release seems to be a tightly regulated process rather than a mere consequence of necrosis inasmuch as rendering livers necrotic with furosemide instead of APAP did not trigger mtDNA release¹². Second, hepatocellular injury in patients with APAP toxicity was considerably more severe than in our I/R cohort based on ALT levels¹². The proposition that mtDNA is released mainly in severe liver injury is also in line with a later report showing that mtDNA

release is more pronounced in patients with poor outcome after APAP overdose¹¹. One could further argue that ischemia by itself is the factor that differentiates APAP toxicity from I/R injury. Indeed, mtDNA release has been predominantly reported in patients with non-ischemic causes of sterile injury, which in addition to APAP hepatotoxicity includes inflammatory bowel disease⁴⁵ and trauma patients⁴⁶. This line of reasoning, however, does not align with the fact that we also did not find mtDNA release in patients who underwent a major hepatectomy without intraoperative VIO use (i.e., non-ischemic sterile liver injury).

The current data also highlight that mitochondrial oxidative stress may be an even more proximal target for intervention⁴⁷, as this may limit DAMP release. The finding that MitoQ was able to suppress HMGB1 release fits the earlier notion that the glutathione precursor n-acetyl-cysteine (NAC) reduced HMGB1 release after *in vitro* hepatocyte anoxia/reoxygenation²⁴. Antioxidants, including NAC, lack efficacy in various clinical scenarios, including hepatic I/R injury⁴⁸. MitoQ differs from these compounds in that it is designed to target the site of oxidant production after I/R (i.e., mitochondria) and also detoxifies the most relevant oxidant (i.e., superoxide)⁵. MitoQ has been used previously in mice to successfully treat hepatic I/R injury²⁷. In the latter report, MitoQ efficacy was assessed using surrogate markers for oxidative injury such as mitochondrial protein carbonylation and hepatic 3-nitrotyrosine content²⁷. Using a direct intravital fluorescence-based method²⁵ it was confirmed that MitoQ reduces hepatocyte oxidative stress early after I/R. In addition, MitoQ has already been employed in phase II studies where it curtailed transaminase levels in patients with hepatitis C⁴⁹, which is an encouraging follow-up to the preclinical notion that MitoQ is generally well-tolerated and not toxic⁵⁰. The clinical investigation and implementation of mitochondria-targeted antioxidants such as MitoQ therefore seems a realistic objective.

Several limitations of the current study should be considered when interpreting the results. The observational nature of the current study means that it is neither designed nor powered to detect differences in clinical outcomes. The similarity in post-operative liver injury parameters between the I/R and control group (Table 2) therefore does not mean that liver ischemia is innocuous, but that VIO in experienced hands is a safe salvage procedure when used to counteract the harms of excessive blood loss. The relatively favorable post-operative transaminase and bilirubin values recorded in the I/R group also relates to the fact that only patients with sufficient (future) remnant liver size and function are eligible for major liver resection. This is supported by the fact that the noted extent of liver injury (i.e., ALT

release) is comparable to previous clinical liver I/R cohorts^{51,52}. The interpretation of the clinical data is further hindered by the inability to separate the contribution of ischemic liver injury from the effects of surgical trauma on DAMP release. It has for instance been reported that the DAMP ATP is released from the resection plane after partial hepatectomy²⁶. In the latter study, patients were not exposed to ischemia during liver resection. Also, the duration of liver surgery and hepatic manipulation during surgery both influence the release of liver injury markers⁵³. The longer operating time and trend towards more extensive resections in the I/R group (Table 1) may therefore also add to the higher HMGB1 levels in the I/R group rather than VIO use only, although this does not per se disqualify the conclusions when contextualized to the mouse data. Last, it should be noted that, in line with available evidence⁵⁴, the majority of patients were operated using intermittent VIO (Table S4). This technique allows for brief periods of parenchymal (re)perfusion in between cycles of liver ischemia. In contrast, most animal models of hepatic I/R, including ours, employ continuous liver ischemia. As the anoxic period primes mitochondria for the post-ischemic burst of ROS production⁶, it is conceivable that intermittent VIO lessens the extent of mitochondrial oxidative injury after I/R. Accordingly, it also means that it remains to be shown whether I/R injury resulting from intermittent VIO is amenable to treatment with mitochondria-targeted antioxidants such as MitoQ.

In conclusion, it is shown that HMGB1 release is related to clinical liver I/R injury. The finding that the mitochondria-targeted antioxidant MitoQ limited HMGB1 release and reduced I/R injury in mice may pave the way for the clinical use of targeted antioxidants against early-onset radicals and oxidants to attenuate hepatic I/R injury.

5. Acknowledgements

Readers wishing to receive raw study data should contact the corresponding author. The authors are grateful to Wouter van Riel, Noor Hagemeijer, Marieke Smit, and Annemiek Dekker for assisting with the collection of patient samples and to Albert van Wijk for analytical support. Lori Zbytnuik and Michelle Wilson from the Kubes lab (Calgary) are acknowledged for technical and infrastructural support. Katarzyna Stevens and Pina Colarusso from the Live Cell Imaging Facility (Snyder Institute, Calgary) are acknowledged for assistance with intravital imaging and image analysis. The authors thank Edward Chouchani, Tracy Prime, and Sebastian Rogatti from the MRC Mitochondrial Biology Unit in Cambridge for technical and infrastructural help with the MitoQ experiments.

RVG was supported by a PhD Scholarship and The Young Talent Fund, both from the Academic Medical Center in Amsterdam. MH was supported by grants from the Dutch Anti-Cancer Foundation (Stichting Nationaal Fonds Tegen Kanker) in Amsterdam, the Phospholipid Research Center in Heidelberg, the Nijbakker-Morra Foundation in Leiden, and Stichting Technologische Wetenschap (STW). MH is currently supported by the Dutch Cancer Society (project # 10666). This work was also supported by the Live Cell Imaging Facility (Snyder Institute, Calgary) funded by an equipment and infrastructure grant from the Canadian Foundation Innovation (CFI), the Alberta Science and Research Authority, and the Mouse Phenomics Resources Laboratory funded by the Snyder Institute for Chronic Diseases at the University of Calgary.

6. References

1. Pringle JH. V. Notes on the arrest of hepatic hemorrhage due to trauma. *Ann Surg* 1908; **48**: 541-9.
2. van Golen RF, van Gulik TM, Heger M. The sterile immune response during hepatic ischemia/reperfusion. *Cytokine Growth Factor Rev* 2012; **23**: 69 - 84.
3. van Riel WG, van Golen RF, Reiniers MJ, Heger M, van Gulik TM. How much ischemia can the liver tolerate during resection? *Hepatobiliary Surg Nutr* 2016; **1**: 58-71.
4. van Golen RF, van Gulik TM, Heger M. Mechanistic overview of reactive species-induced degradation of the endothelial glycocalyx during hepatic ischemia/reperfusion injury. *Free Radic Biol Med* 2012; **52**: 1382-402.
5. Chouchani ET, Pell VR, James AM, Work LM, Saeb-Parsy K, Frezza C, et al. A unifying mechanism for mitochondrial superoxide production during ischemia-reperfusion injury. *Cell Metab* 2016; **23**: 254-63.
6. Chouchani ET, Pell VR, Gaude E, Aksentijević D, Sundier SY, Robb EL, et al. Ischaemic accumulation of succinate controls reperfusion injury through mitochondrial ROS. *Nature* 2014; **515**: 431-5.
7. Reiniers MJ, van Golen RF, van Gulik TM, Heger M. Reactive oxygen and nitrogen species in steatotic hepatocytes: A molecular perspective on the pathophysiology of ischemia-reperfusion injury in the fatty liver. *Antioxid Redox Signal* 2013; **21**: 1119-42.
8. Huang H, Evankovich J, Yan W, Nace G, Zhang L, Ross M, et al. Endogenous histones function as alarmins in sterile inflammatory liver injury through toll-like receptor 9. *Hepatology* 2011; **54**: 999-1008.
9. Bamboat ZM, Ocuin LM, Balachandran VP, Obaid H, Plitas G, Dematteo RP. Conventional dcs reduce liver ischemia/reperfusion injury in mice via IL-10 secretion. *J Clin Invest* 2010; **120**: 559-69.
10. Tsung A, Sahai R, Tanaka H, Nakao A, Fink MP, Lotze MT, et al. The nuclear factor HMGB1 mediates hepatic injury after murine liver ischemia-reperfusion. *J Exp Med* 2005; **201**: 1135-43.
11. McGill MR, Staggs VS, Sharpe MR, Lee WM, Jaeschke H, Acute Liver Failure Study Group. Serum mitochondrial biomarkers and damage-associated molecular patterns are higher in acetaminophen overdose patients with poor outcome. *Hepatology* 2014; **60**: 1336-45.
12. McGill MR, Sharpe MR, Williams CD, Taha M, Curry SC, Jaeschke H. The mechanism underlying acetaminophen-induced hepatotoxicity in humans and mice involves mitochondrial damage and nuclear DNA fragmentation. *J Clin Invest* 2012; **122**: 1574-83.

13. van Golen RF, Reiniers MJ, Heger M, Verheij J. Solutions to the discrepancies in the extent of liver damage following ischemia/reperfusion in standard mouse models. *J Hepatol* 2014; **62**: 975-7.
14. Dindo D, Demartines N, Clavien PA. Classification of surgical complications: A new proposal with evaluation in a cohort of 6336 patients and results of a survey. *Ann Surg* 2004; **240**: 205-13.
15. Rehm M, Bruegger D, Christ F, Conzen P, Thiel M, Jacob M, et al. Shedding of the endothelial glycocalyx in patients undergoing major vascular surgery with global and regional ischemia. *Circulation* 2007; **116**: 1896-906.
16. Zeerleder S, Zwart B, te Velthuis H, Manoe R, Bulder I, Rensink I, Aarden LA. A plasma nucleosome releasing factor (NRF) with serine protease activity is instrumental in removal of nucleosomes from secondary necrotic cells. *FEBS Lett* 2007; **581**: 5382-8.
17. van Nieuwenhuijze AE, van Lopik T, Smeenk RJ, Aarden LA. Time between onset of apoptosis and release of nucleosomes from apoptotic cells: Putative implications for systemic lupus erythematosus. *Ann Rheum Dis* 2003; **62**: 10-4.
18. van Montfoort ML, Stephan F, Lauw MN, Hutten BA, Van Mierlo GJ, Solati S, et al. Circulating nucleosomes and neutrophil activation as risk factors for deep vein thrombosis. *Arterioscler Thromb Vasc Biol* 2013; **33**: 147-51.
19. Nuijens JH, Abbink JJ, Wachtfogel YT, Colman RW, Eerenberg AJ, Dors D, et al. Plasma elastase alpha 1-antitrypsin and lactoferrin in sepsis: Evidence for neutrophils as mediators in fatal sepsis. *J Lab Clin Med* 1992; **119**: 159-68.
20. Nakahira K, Kyung SY, Rogers AJ, Gazourian L, Youn S, Massaro AF, et al. Circulating mitochondrial DNA in patients in the ICU as a marker of mortality: Derivation and validation. *PLoS Med* 2013; **10**: e1001577; discussion e1001577.
21. Ruijter JM, Ramakers C, Hoogaars WM, Karlen Y, Bakker O, van den Hoff MJ, Moorman AF. Amplification efficiency: Linking baseline and bias in the analysis of quantitative PCR data. *Nucleic Acids Res* 2009; **37**:e45.
22. Sun Q, Loughran P, Shapiro R, Shrivastava IH, Antoine DJ, Li T, et al. Redox-dependent regulation of hepatocyte absent in melanoma 2 inflammasome activation in sterile liver injury in mice. *Hepatology* 2017; **65**: 253-68.

23. Yang H, Wang H, Ju Z, Ragab AA, Lundbäck P, Long W, et al. MD-2 is required for disulfide hmgb1-dependent TLR4 signaling. *J Exp Med* 2015; **212**: 5-14.
24. Tsung A, Klune JR, Zhang X, Jeyabalan G, Cao Z, Peng X, et al. HMGB1 release induced by liver ischemia involves toll-like receptor 4 dependent reactive oxygen species production and calcium-mediated signaling. *J Exp Med* 2007; **204**: 2913-23.
25. Reiniers MJ, van Golen RF, Bonnet S, Broekgaarden M, van Gulik TM, Egmond MR, Heger M. Preparation and practical applications of 2',7'-dichlorodihydrofluorescein in redox assays. *Anal Chem* 2017; **89**: 3853-7.
26. Gonzales E, Julien B, Serrière-Lanneau V, Nicou A, Doignon I, Lagoudakis L, et al. ATP release after partial hepatectomy regulates liver regeneration in the rat. *J Hepatol* 2010; **52**: 54-62.
27. Mukhopadhyay P, Horváth B, Zsengellér Z, Bátkai S, Cao Z, Kechrid M, et al. Mitochondrial reactive oxygen species generation triggers inflammatory response and tissue injury associated with hepatic ischemia-reperfusion: Therapeutic potential of mitochondrially targeted antioxidants. *Free Radic Biol Med* 2012; **53**: 1123-38.
28. Venereau E, Casalgrandi M, Schiraldi M, Antoine DJ, Cattaneo A, De Marchis F, et al. Mutually exclusive redox forms of HMGB1 promote cell recruitment or proinflammatory cytokine release. *J Exp Med* 2012; **209**: 1519-28.
29. Huebener P, Pradere JP, Hernandez C, Gwak GY, Caviglia JM, Mu X, et al. The HMGB1/RAGE axis triggers neutrophil-mediated injury amplification following necrosis. *J Clin Invest* 2015; **125**: 539-50.
30. Wiggers JK, Koerkamp BG, Cieslak KP, Doussot A, van Klaveren D, Allen PJ, et al. Postoperative mortality after liver resection for perihilar cholangiocarcinoma: Development of a risk score and importance of biliary drainage of the future liver remnant. *J Am Coll Surg* 2016; **223**: 321-331.e1.
31. Evankovich J, Cho SW, Zhang R, Cardinal J, Dhupar R, Zhang L, et al. High mobility group box 1 release from hepatocytes during ischemia and reperfusion injury is mediated by decreased histone deacetylase activity. *J Biol Chem* 2010; **285**: 39888-97.
32. Ilmakunnas M, Tukiainen EM, Rouhiainen A, Rauvala H, Arola J, Nordin A, et al. High mobility group box 1 protein as a marker of hepatocellular injury in human liver transplantation. *Liver Transpl* 2008; **14**: 1517-25.

33. Burstein AH, Grimes I, Galasko DR, Aisen PS, Sabbagh M, Mjalli AM. Effect of TTP488 in patients with mild to moderate alzheimer's disease. *BMC Neurol* 2014; **14**:12.
34. Hennessy EJ, Parker AE, O'Neill LA. Targeting toll-like receptors: Emerging therapeutics? *Nat Rev Drug Discov* 2010; **9**: 293-307.
35. Lundbäck P, Lea JD, Sowinska A, Ottosson L, Fürst CM, Steen J, et al. A novel high mobility group box 1 neutralizing chimeric antibody attenuates drug-induced liver injury and postinjury inflammation in mice. *Hepatology* 2016; **64**: 1699-710.
36. Yang M, Antoine DJ, Weemhoff JL, Jenkins RE, Farhood A, Park BK, Jaeschke H. Biomarkers distinguish apoptotic and necrotic cell death during hepatic ischemia/reperfusion injury in mice. *Liver Transpl* 2014; **20**: 1372-82.
37. Reiniers MJ, van Golen RF, Heger M, Mearadji B, Bennink RJ, Verheij J, van Gulik TM. In situ hypothermic perfusion with retrograde outflow during right hemihepatectomy: First experiences with a new technique. *J Am Coll Surg* 2013; **218**: e7-16.
38. Reiniers MJ, Olthof PB, van Golen RF, Heger M, van Beek AA, Meijer B, et al. Hypothermic perfusion with retrograde outflow during right hepatectomy is safe and feasible. *Surgery* 2017; **162**: 48-58.
39. Kojima M, Tanabe M, Shinoda M, Yamada S, Miyasho T, Suda K, et al. Role of high mobility group box chromosomal protein 1 in ischemia-reperfusion injury in the rat small intestine. *J Surg Res* 2012; **178**: 466-71.
40. Huang H, Nace GW, McDonald KA, Tai S, Klune JR, Rosborough BR, et al. Hepatocyte specific HMGB1 deletion worsens the injury in liver ischemia/reperfusion: A role for intracellular HMGB1 in cellular protection. *Hepatology* 2013; **59**: 1984-97.
41. Nace GW, Huang H, Klune JR, Eid RE, Rosborough BR, Korff S, et al. Cellular specific role of toll-like receptor 4 in hepatic ischemia-reperfusion injury. *Hepatology* 2013; **58**: 374-87.
42. He Y, Feng D, Li M, Gao Y, Ramirez T, Cao H, et al. Hepatic mitochondrial DNA/toll-like receptor 9/microrna-223 forms a negative feedback loop to limit neutrophil overactivation and acetaminophen hepatotoxicity in mice. *Hepatology* 2017; **66**: 220-34.
43. Ramachandran A, Duan L, Akakpo JY, Jaeschke H. Mitochondrial dysfunction as a mechanism of drug-induced hepatotoxicity: Current understanding and future perspectives. *J Clin Transl Res* 2018; **4**.

44. Jaeschke H, Lemasters JJ. Apoptosis versus oncotic necrosis in hepatic ischemia/reperfusion injury. *Gastroenterology* 2003; **125**: 1246-57.
45. Boyapati RK, Dorward DA, Tamborska A, Kalla R, Venthram NT, Doherty MK, et al. Mitochondrial DNA is a pro-inflammatory damage-associated molecular pattern released during active IBD. *Inflamm Bowel Dis* 2018; **24**: 2113-22.
46. Zhang Q, Raouf M, Chen Y, Sumi Y, Sursal T, Junger W, et al. Circulating mitochondrial DAMPs cause inflammatory responses to injury. *Nature* 2010; **464**: 104-7.
47. Heger M, Reiniers MJ, van Golen RF. Mitochondrial metabolomics unravel the primordial trigger of ischemia/reperfusion injury. *Gastroenterology* 2015; **148**: 1071-3.
48. Bahde R, Spiegel HU. Hepatic ischaemia-reperfusion injury from bench to bedside. *Br J Surg* 2010; **97**: 1461-75.
49. Gane EJ, Weilert F, Orr DW, Keogh GF, Gibson M, Lockhart MM, et al. The mitochondria-targeted anti-oxidant mitoquinone decreases liver damage in a phase II study of hepatitis C patients. *Liver Int* 2010; **30**: 1019-26.
50. Rodriguez-Cuenca S, Cochemé HM, Logan A, Abakumova I, Prime TA, Rose C, et al. Consequences of long-term oral administration of the mitochondria-targeted antioxidant mitoq to wild-type mice. *Free Radic Biol Med* 2010; **48**: 161-72.
51. van den Broek MA, Bloemen JG, Dello SA, van de Poll MC, Olde Damink SW, Dejong CH. Randomized controlled trial analyzing the effect of 15 or 30 min intermittent pringle maneuver on hepatocellular damage during liver surgery. *J Hepatol* 2011; **55**: 337-45.
52. Beck-Schimmer B, Breitenstein S, Bonvini JM, Lesurtel M, Ganter M, Weber A, et al. Protection of pharmacological preconditioning in liver surgery: Results of a prospective randomized controlled trial. *Ann Surg* 2012; **256**: 837-45.
53. van de Poll MC, Derikx JP, Buurman WA, Peters WH, Roelofs HM, Wigmore SJ, Dejong CH. Liver manipulation causes hepatocyte injury and precedes systemic inflammation in patients undergoing liver resection. *World J Surg* 2007; **31**: 2033-8.
54. Belghiti J, Noun R, Malafosse R, Jagot P, Sauvanet A, Pierangeli F, et al. Continuous versus intermittent portal triad clamping for liver resection: A controlled study. *Ann Surg* 1999; **229**: 369-75.

7. Figure legends

Figure 1. DAMP release and neutrophil activation after clinical liver I/R

A-D show plasma levels (median±IQR) of the DAMPs HMGB1, nucleosomes, and mtDNA, and the marker for neutrophil activity E-AT at 1 h and 6 h after liver surgery in patients. Note that the y-axes are scaled logarithmically. E-AT=elastase- α 1-antitrypsin complex; HMGB1=high mobility group box 1; mtDNA=mitochondrial DNA. # indicates $p<0.05$ versus $t=0$.

Figure 2. HMGB1 release correlates to postoperative liver injury after major liver resection

A-D show systemic DAMP levels (median±IQR) for patients operated with VIO (I/R, red) or without VIO (control, blue). **E-F** display the correlation between circulating HMGB1 and liver ischemia time and the post-operative hepatocellular injury peak. The dashed lines indicate the 95% confidence interval of the regression line. Additional correlation data are presented in Supplemental Figures S3. # indicates $p < 0.05$ versus $t=0$ in the I/R group, \$ indicates $p < 0.05$ versus $t=0$ in the control group, and * indicates $p < 0.05$ between the groups indicated by the solid line. ALT=aspartate alanine aminotransferase; E-AT=elastase- α 1-antitrypsin complex; HMGB1=high mobility group box 1; I/R=ischemia/reperfusion; IQR=interquartile range; mtDNA=mitochondrial DNA; VIO=vascular inflow occlusion.

Figure 3. MitoQ attenuates hepatic I/R injury in mice by suppressing HMGB1 release

A shows the dose-response relationship between MitoQ and hepatocellular injury. The 1 mg/kg MitoQ dosage was used in all subsequent experiments (solid line). **B** demonstrates that MitoQ mitigated hepatic oxidative stress during early reperfusion as measured by real-time *in vivo* microscopy/spectroscopy. **C-D** show that MitoQ decreased ALT release and hepatocellular necrosis at 24 h reperfusion whereas redox-inactive MitoQ (dTPP) was not protective (also see Fig. S4). **E-F** indicate that MitoQ attenuated HMGB1 release but did not affect intracellular HMGB1 levels. **G** demonstrates that reconstitution of disulfide HMGB1 reverses the protective effects of MitoQ. **H-I** show that MitoQ decreased expression of the leukocyte receptor VCAM-1 but did not affect ICAM-1 expression. The heat map (**J**) depicts a decrease (blue) or increase (red) in plasma cytokine concentration in MitoQ-treated animals subjected to I/R versus vehicle-treated animals subjected to I/R. The dots indicate a statistically significant difference between the MitoQ and control group. Full hepatocellular damage and cytokine results are included in Supplemental Figure S5 and Supplemental Table S6 and a functional description of measured cytokines is included in Supplemental Table S3. Results are shown as mean±SEM, except for **D** (median±range). Western blot results are presented as densitometric analysis. One representative blot per group is included per graph. Group sizes are ≥6 animals/group, except for **B** (3-4 mice/group). Area under the curve analysis was used to assess differences in ROS production (**B**). * indicates $p < 0.05$ in the MitoQ versus the I/R group. au=arbitrary unit; ALT=aspartate alanine aminotransferase; CDCF=5(6)-carboxy-dichlorofluorescein; dTPP= decyl-triphenylphosphonium; ROS=reactive oxygen species; HMGB1=high mobility group box 1; ICAM-1=intercellular adhesion molecule 1; VCAM-1=vascular cell adhesion molecule 1.

		CTRL (N=13)	I/R (N=26)	p-value
Age (years, median ± IQR)		62 (45 – 73)	66 (53 – 70)	0.670
Gender, male (n, %)		8 (62)	18 (69)	0.725
BMI (median ± IQR)		25.2 (22.9 – 26.3)	23.9 (20.9 – 26.8)	0.418
ASA score (n, %)	I II III	3 (23) 10 (77) 0 (0)	6 (23) 14 (54) 6 (23)	0.153
Diagnosis (n, %)	CRC metastasis PHCC IHCC HCC Benign Other	1 (9) 3 (23) 2 (15) 2 (15) 3 (23) 2 (15)	4 (15) 13 (50) 2 (8) 3 (12) 3 (12) 1 (3)	0.132
Preoperative chemotherapy, yes (n, %)		2 (15)	4 (15)	1.000
Biliary drainage, yes (n, %)		3 (23)	9 (35)	0.714
PVE, yes (n, %)		1 (8)	1 (4)	1.000
ALT baseline, U/L (median ± IQR)		30 (25 – 52)	53 (24 – 71)	0.294
AST baseline, U/L (median ± IQR)		32 (28 – 52)	45 (28 – 73)	0.178
Total bilirubin baseline, uM/L (median ± IQR)		9 (6 – 14)	7 (5 – 14)	0.471
INR baseline (median ± IQR)		1.0 (1.0 – 1.1)	1.0 (1.0 – 1.1)	0.676

Table 1. Baseline characteristics

Shown are the baseline characteristics of the control (CTRL) and ischemia/reperfusion (I/R) groups.

ALT=alanine aminotransferase; ASA=American Society of Anesthesiologists; AST=aspartate aminotransferase; BMI=body mass index; CRC=colorectal cancer metastases; HCC=hepatocellular carcinoma; IHCC=intrahepatic cholangiocarcinoma; INR=international normalized ratio; IQR=interquartile range; PHCC=perihilar cholangiocarcinoma; PVE=portal vein embolization Categorical data were analyzed using Fisher's exact test (binary data) and Chi-square test (>2 variables). Differences between numerical variables were assessed using student's t-tests.

	CTRL (N=13)	I/R (N=26)	p-value
Resected segments [#] (%)			0.131
3	6 (46.2%)	5 (19.2%)	
≥4	7 (53.8%)	21 (80.8%)	
Resection time, min (median±IQR)	59 (41.5 – 71.5)	82 (60 – 130)	0.006
Duration of ischemia ^{&} min (median±IQR)	N/A	48 (31 – 68)	
Duration of surgery, min (median±IQR)	306 (261 – 373.5)	460 (380 – 503)	0.001
Transfusion requirement, units (%)			0.455
0	9 (62.9)	12 (48)	
1-2	2 (15.4)	6 (24)	
≥3	2 (15.4)	7 (28)	
Hospital stay, days (median±IQR)	9 (7.5 – 11)	11.5 (8 – 22)	0.036
Grade III-V complications [@] (%)	7 (53.8)	13 (52)	1.000
ICU admission (%)	3 (23.1)	7 (26.9)	1.000
In-hospital mortality (%)	1 (7.7)	2 (8.0)	1.000
Peak ALT, U/L (median±IQR)	273 (142.5 – 641.5)	456 (289 – 784)	0.152
Peak INR (median±IQR)	1.19 (1.12 – 1.31)	1.30 (1.17 – 1.41)	0.411
Peak total bilirubin, μmol/L (median±IQR)	17 (14 – 34)	32 (19 – 47)	0.129

Table 2. Clinical outcomes.

Designates the number of resected Couinaud liver segments. & Patients were subjected to continuous or intermittent vascular inflow occlusion as specified in Supplemental Table S4. Details on the resected liver segments can be found in Supplemental Tables S4 and S5. @ Complications were scored according to the Clavien-Dindo classification¹⁴. A histopathological assessment of the resection specimens is included in Supplemental Table S4. CTRL=control group; I/R=ischemia/reperfusion group; ALT=aspartate alanine aminotransferase; ICU=intensive care unit; INR=international normalized ratio; IQR=interquartile range; min=minutes. Categorical data were analyzed using Fisher's exact test (binary data) and Chi-square test (>2 variables). Differences between numerical variables were assessed using student's t-tests.

The damage-associated molecular pattern HMGB1 is released early after clinical hepatic ischemia/reperfusion

Formatted: English (United States)

Rowan F. van Golen¹, Megan J. Reiniers¹, Gerben Marsman², Lindy K. Alles¹, Derrick M. van Rooyen³, Björn Petri^{4,5,6}, Vincent A. Van der Mark^{1,7}, Adriaan A. van Beek⁸, Ben Meijer⁸, Martinus A. Maas¹, Sacha Zeerleder^{2,10}, Joanne Verheij⁹, Geoffrey C. Farrell³, Brenda M. Luken², Narci C. Teoh³, Thomas M. van Gulik¹, Michael P. Murphy¹¹, Michal Heger^{1*}

1 Department of Surgery (Experimental Laboratory), Academic Medical Center, University of Amsterdam, Amsterdam, the Netherlands

2 Department of Immunopathology, Sanquin Research and Landsteiner Laboratory, Academic Medical Center, University of Amsterdam, Amsterdam, the Netherlands

3 Liver Research Group, Australian National University at The Canberra Hospital, Canberra, Australia

4 Department of Microbiology, Immunology, and Infectious Diseases, Cumming School of Medicine, University of Calgary, Calgary AB T2N 1N4, Alberta, Canada

5 Department of Physiology and Pharmacology, Cumming School of Medicine, University of Calgary, Calgary AB T2N 1N4, Alberta, Canada

6 Snyder Institute for Chronic diseases, University of Calgary, Calgary, Canada

7 Tytgat Institute for Gastrointestinal and Liver Research, Academic Medical Center, University of Amsterdam, Amsterdam, the Netherlands

8 Department of Cell Biology and Immunology, Wageningen University, Wageningen, the Netherlands

9 Department of Pathology, Academic Medical Center, University of Amsterdam, Amsterdam, the Netherlands

10 Department of Hematology, Academic Medical Center, University of Amsterdam, Amsterdam, the Netherlands

11 Medical Research Council Mitochondrial Biology Unit, Cambridge, United Kingdom

***Correspondence:** Michal Heger, Department of Surgery (Experimental Laboratory), Academic Medical Center, University of Amsterdam, Meibergdreef 9, 1105 AZ Amsterdam, the Netherlands

Tel: +31 20 5665573. Fax: +31 20 6976621. Email: m.heger@amc.uva.nl.

Financial support: ~~MH is~~RVG was supported by a PhD Scholarship and The Young Talent Fund, both from the Academic Medical Center in Amsterdam. MH was supported by grants from the Dutch Anti-Cancer Foundation (Stichting Nationaal Fonds Tegen Kanker) in Amsterdam, the Phospholipid Research Center in Heidelberg, the Nijbakker-Morra Foundation in Leiden, and Stichting Technologische Wetenschap (STW). ~~RFvGMH is currently supported by a PhD Scholarship and the Young Talent Fund, both from the Academic Medical Center, University of Amsterdam.~~Dutch Cancer Society (project # 10666).

Formatted: English (United States)

Abstract

Objective and background. Activation of sterile inflammation after hepatic I/R culminates in liver injury. The route to liver damage starts with mitochondrial oxidative stress and cell death during early reperfusion. The link between mitochondrial oxidative stress, damage-associated molecular pattern (DAMP) release, and sterile immune signalling is incompletely understood and lacks clinical validation. The aim of the study was to ~~investigate~~validate this relation in a clinical liver I/R cohort and to limit DAMP release using a mitochondria-targeted antioxidant in I/R-subjected mice.

Formatted: English (United States)

Methods. Plasma levels of the DAMPs high-mobility group box 1 (HMGB1), mitochondrial DNA, and nucleosomes were measured in 39 patients enrolled in an observational study who underwent a major liver resection with (N=29) or without (N=13) intraoperative liver ischemia. Circulating cytokine and neutrophil activation markers were also determined. In mice, the mitochondria-targeted antioxidant MitoQ was intravenously infused in attempt to limit DAMP release, reduce sterile inflammation, and suppress I/R injury.

Results. In patients, HMGB1 was elevated following liver resection with I/R compared to liver resection without I/R. HMGB1 correlated positively with ischemia duration and peak post-operative transaminase (ALT) levels. There were no differences in mitochondrial DNA, nucleosome, or cytokine release. In mice, MitoQ neutralized hepatic oxidative stress and decreased HMGB1 release by $\pm 50\%$. MitoQ suppressed transaminase release, hepatocellular necrosis, and cytokine production. Reconstituting disulfide HMGB1 during reperfusion reversed these protective effects.

Conclusion. HMGB1 seems the most pertinent DAMP ~~to~~in clinical hepatic I/R injury. Neutralizing mitochondrial oxidative stress may limit DAMP release after hepatic I/R and reduce liver damage.

Formatted: English (United States)

Keywords:

Damage-associated molecular patterns

Antioxidants

Intravital microscopy

Liver resection

Sterile inflammation

~~Mitochondria~~

Mitochondrial DNA

Formatted: English (United States)

Abbreviations:

ALT = alanine aminotransferase

ASA = American Society of Anesthesiologists

AST = aspartate aminotransferase

BMI = body mass index

CTRL = control (group)

CRC = colorectal cancer metastasis

DAMP = damage-associated molecular pattern

dTPP = decyl-triphenylphosphonium

HCC = hepatocellular carcinoma

HMGB1 = high-mobility group box 1

I/R = ischemia/reperfusion

ICAM = intercellular adhesion molecule

IHC = intrahepatic cholangiocarcinoma

IL = interleukin

INR = international normalized ratio

IQR = interquartile range

mtDNA = mitochondrial DNA

PHCC = perihilar cholangiocarcinoma

PVE = portal vein embolization

RAGE = receptor for advanced glycation end products

ROS = reactive oxygen species

TLR = toll-like receptor

NAC = N-acetylcysteine

VIO = vascular inflow occlusion

VCAM = vascular cell adhesion protein

Formatted: English (United States)

1. Introduction

During major liver resection, the induction of liver ischemia by surgical clamping of the afferent hepatic vasculature is used to counter the risks of excessive blood loss. This surgical technique is known as vascular inflow occlusion (VIO) or the Pringle maneuver¹. When employed within predefined time limits and in selected patients, this manoeuvre is considered safe. ~~The~~However, the transient lack of organ perfusion and oxygenation ~~however,~~ also inadvertently causes ischemia/reperfusion (I/R) injury²⁻⁴ and the severity of hepatic I/R injury impacts the recovery of patients after major liver surgery.

Formatted: English (United States)

Formatted: English (United States)

Formatted: English (United States)

Activation of sterile inflammation is a key feature of hepatic I/R injury. During ischemia, the lack of oxygen halts oxidative phosphorylation and leads to the build-up of citric acid cycle metabolites such as succinate^{5,6}. Once the oxygen supply is restored, the consumption of accumulated succinate during the first minutes of reperfusion fuels a burst of reactive oxygen species (ROS) production by the mitochondrial electron transport chain^{5,6}. The consequent wave of ROS-induced cell death triggers the release of damage-associated molecular patterns (DAMPs) by hepatocytes. DAMPs are innocuous intracellular constituents that become potent triggers of the innate immune system once released into the circulation^{2,7}. Effector cells of the innate immune system such as neutrophils in turn confer the bulk of hepatic tissue injury. Based on this sequence of events, DAMPs occupy a crucial role in the onset of I/R injury as signal transducers and amplifiers of the sterile immune response.

Formatted: English (United States)

Several DAMPs, including histones⁸, DNA⁹, and high-mobility group box 1 (HMGB1)¹⁰ have been causally linked to hepatic I/R injury in animal studies. DAMP release has also been measured in clinical accounts of sterile liver injury^{11,12}. However, the link between mitochondrial oxidative stress and DAMP release has not been clinically elaborated in the context of hepatic I/R injury to date, and was therefore investigated in this study. To that end, DAMP release was studied in patients undergoing liver resection with or without being subjected to I/R.

Formatted: English (United States)

It is shown that patients who underwent major liver surgery rapidly exhibit DAMP release after resection. Of the tested DAMPs, only HMGB1 levels increased specifically in I/R-subjected patients and not in the control group operated without I/R. HMGB1 release correlated positively with ischemia time and postoperative hepatocellular injury markers. The results were back-translated to a validated mouse model¹³ to allow experimental confirmation and further elaboration. Decreasing mitochondrial oxidative

Formatted: English (United States)

damage during early reperfusion with the mitochondria-targeted antioxidant MitoQ in mice prevented HMGB1 release and attenuated the I/R immune response. Decreasing mitochondrial oxidative damage therefore may potentially improve outcomes in patients undergoing major liver surgery.

2. Materials and methods

References to the supplemental information are indicated with the prefix 'S'.

2.1 Study participants and study design

The effect of liver surgery performed with or without intraoperative liver ischemia on DAMP release was investigated in a single-~~center~~center, observational trial registered at <https://ClinicalTrials.gov> under identifier NCT01700660. Eligible for participation were all patients scheduled for a major liver resection (removal of ≥ 3 Couinaud segments) that were ≥ 18 years old and had an American Society of ~~Anaesthesiology~~Anesthesiology, physical status score of ≤ 3 . Patients were excluded from the study when considered unresectable during surgical exploration, when the employed ischemia time was < 20 min, when they underwent an emergency operation, or when the patient was pregnant or breast-feeding. Because the decision whether or not to use vascular inflow occlusion (VIO) and thereby subject patients to I/R was made at the discretion of the performing surgeon based on the actual or anticipated amount of blood loss, participants were non-randomly assigned to either the I/R group (N=26) or the control group (N=13). Intermittent VIO was typically performed in cycles comprising 20 min of ischemia followed by 10 min of reperfusion. In a minor fraction of patients, the operative cause necessitated the use of continuous VIO (see Supplemental Table S4). All patients were operated by the same primary surgeon (~~FvG~~TVG).

Blood samples were drawn from a central venous catheter after the induction of general ~~anaesthesia~~anesthesia (i.e., at baseline) and 1 and 6 h after the start of reperfusion (I/R group) or completion of parenchymal transection (CTRL group). Plasma liver injury (ALT) and liver function (international normalized ratio (INR), total bilirubin) were determined as part of routine patient care. Post-operative complications were categorized according to the Clavien-Dindo grading ~~system~~¹³ ~~system~~¹⁴. All experimental results were normalized to plasma protein content (Pierce BCA Protein Assay Kit, Life Technologies, Carlsbad, CA) to correct for hemodilution, as ~~described~~¹⁴ ~~described~~¹⁵. All study protocols were approved by the Institutional Review Board and written informed consent was obtained from all participants before undergoing any study-related procedures. The study design is summarized in Supplemental Figure S1.

Formatted: English (United States)

2.2 Circulating HMGB1

Plasma HMGB1 levels were determined in 10 μ L of EDTA-anticoagulated plasma samples by ELISA (IBL International, Hamburg, Germany) according to manufacturer's instructions. All samples were measured in duplicate in regular sensitivity mode on a Synergy HT microplate reader (BioTek Instruments, Winooski, VT).

2.3 Circulating nucleosomes and elastase- α 1-antitrypsin complexes

Nucleosome levels were assessed by ELISA as previously ~~described~~¹⁵ ~~described~~¹⁶. Briefly, monoclonal antibody CLB-ANA/60 (Sanquin, Amsterdam, the Netherlands) that recognizes histone 3 was used as capture antibody. Biotinylated F(ab)2 fragments of monoclonal antibody CLB-ANA/58 (Sanquin), which recognizes an epitope exposed on complexes of dsDNA histone 2A and histone 2B in combination with poly-horseradish peroxidase-~~labelled~~^{labeled} streptavidin (Sanquin) were used for detection. As a standard, we used culture supernatant of Jurkat cells (1×10^6 cells/mL), cultured for an additional week without refreshing the medium, to obtain 100% apoptotic cells. One unit is the amount of nucleosomes released by ≈ 100 Jurkat cells. The lower detection limit of the assay was 2.5 U/~~ml~~⁴⁶ ~~ml~~¹⁷. The reference range for circulating nucleosomes in healthy individuals is 0-10.3 U/mL.

Elastase- α 1-antitrypsin complexes (E-AT) were measured by ELISA as ~~described~~¹⁷ ~~described~~¹⁸. This assay was adapted from a previously described ~~radioimmunoassay~~¹⁸ ~~radioimmunoassay~~¹⁹. Briefly, plates were coated with a polyclonal rabbit anti-human neutrophil elastase antibody (1.5 μ g/mL; Sanquin). Standard and samples were diluted in high-performance ELISA buffer (HPE; Sanquin) + 40 μ g/mL bovine IgG. Bound complexes were detected with a biotinylated monoclonal anti- α 1-antitrypsin antibody (1 μ g/mL; Sanquin) in combination with poly-horseradish peroxidase-~~labelled~~^{labeled} streptavidin. Results are expressed in ng/mL by reference to a standard curve of normal human citrated plasma in which EA-T were generated by incubation with porcine elastase (final concentration 2 μ g/mL; Sigma, Zwijndrecht, the Netherlands) for 15 min at room temperature. The detection limit of the assay was 2 ng/mL. The reference range for EA-T in healthy individuals is 8.5 to 55.7 ng/mL.

2.4 Circulating mitochondrial DNA

Plasma mitochondrial DNA levels were determined according to Nakahira et al.¹⁹²⁰, with minor modifications. Total DNA was isolated from 190 μ L of heparin-anticoagulated plasma using the QIAamp DNA Blood Mini Kit (cat. #51106, Qiagen) according to the manufacturer's instructions. DNA was eluted in 100 μ L of elution buffer. Levels of mitochondrial DNA (mtDNA) were analyzed in duplicate by real-time quantitative PCR on a Lightcycler 480 (Roche) using a reaction volume of 10 μ L consisting of 2 μ L of DNA, 2 μ L of nuclease-free water (Qiagen), 1 μ L of primer mix (0.5 μ M final primer concentration), and 5 μ L of SensiFAST SYBR No-ROX mix (Bioline, London, UK). The run parameters are specified in Supplemental Table S1. The following primers were used: human mitochondrially-encoded NADH dehydrogenase 1 (MT-ND1): forward 5'-ATACCCATGGCCAACCTCCT-3', reverse 5'-GGGCCTTTGCGTAGTTGTAT-3'¹². Melting curve analysis and ethidium bromide-stained agarose gel electrophoresis were used to validate primer specificity. A plasmid encoding a human cDNA clone of MT-ND1 was purchased from ORIGENE (SC101172) and was used as a logarithmic mtDNA standard in 10-fold serial dilutions (1.93×10^6 copies – 1.93×10^0 copies). Data ~~was~~ were processed according to Ruijter et al.²⁰²¹, fitted to the mtDNA standard, and normalized to plasma protein content.

2.5 Human plasma cytokine measurements

L-12p70, TNF, IL-10, IL-6, IL-1 β , and IL-8/CXCL8 concentrations were determined in serum samples using the Cytometric Bead Array (CBA) Human Inflammatory Cytokines Kit (BD Biosciences, Franklin, NJ) according to the manufacturer's instructions. The samples were analyzed in a blinded fashion and flow data were collected using a BD FACSCanto II (BD Biosciences). The results were analyzed with FCAP Array version 3.0 software (BD Biosciences). CCL2 plasma concentration was measured by ELISA (Duosets, R&D Systems, Minneapolis, MN). All reagents and solutions were prepared fresh each week according to the manufacturer's protocols and were sterile filtered using 0.2 μ M bottle-top vacuum filters (Corning, Corning, NY). Bovine serum albumin was of the highest available purity (cat. #A7030, Sigma-Aldrich, St. Louis, MO) and ELISAs were performed using clear 96-well flat bottom polystyrene microplates (#9018, Corning). All cytokine levels were normalized to plasma total protein content.

2.6 Mouse hepatic ischemia/reperfusion experiments

The animal experiments were approved by the institute's animal welfare committee and surgical procedures were as ~~described~~²⁴ ~~described~~¹³. MitoQ was dissolved to a concentration of 6 mg/mL MitoQ in sterile NaCl (Braun). After induction of anesthesia, 250 ng/kg – 3 mg/kg MitoQ or an equimolar amount of the inactive targeting moiety decyl-triphenylphosphonium (dTTP) in sterile NaCl was infused via the penile vein in a volume of 100 µL per 30 g body weight. After allowing MitoQ or dTTP to circulate for 10 min, partial (70%) liver ischemia was induced for 30 ~~min~~²⁴ ~~min~~¹³. As a control group, animals underwent sham surgery that entailed a laparotomy with mobilization of hilar structures, but without actual occlusion of the afferent vasculature. For every set of experiments, animals were randomly assigned to an experimental arm. For HMGB1 reconstitution experiments, 2.5 µg disulfide HMGB1 (IBL) in 100 µL sterile NaCl was administered intraperitoneally immediately after reperfusion was initiated. Disulfide HMGB1 was selected for the reconstitution experiments because (1) it is the predominant isoform released in mice subjected to hemorrhagic shock and resuscitation²² - a model that pathophysiologically resembles liver I/R - and (2) the disulfide isoform activates the hepatic I/R-pertinent TLR-4 signaling axis^{10,23,24}. Animals were sacrificed at 6 h or 24 h of reperfusion. Blood and liver samples were processed as ~~described~~²⁴ ~~To account for slight~~ ~~described~~¹³. The number of animals per group per experiment is included in the figure legends. To account for variations in experimental conditions and animal batches, a new control group of vehicle-treated mice subjected to I/R was included in every new set of experiments. ~~Clinical chemistry results of the mouse experiments are therefore expressed as a percentage of this reference group.~~

Formatted: Font: Bold

2.7 Mouse liver histology

Mouse liver specimens were fixed in formalin, embedded in paraffin, and stained with hematoxylin and eosin as ~~described~~²⁴ ~~described~~¹³. The extent of confluent parenchymal necrosis was scored by a hepatopathologist (JV) according to the following grading system: 0=no necrosis, 1=<25% necrosis, 2=25-50% necrosis, 3=50-75% necrosis, and 4=>75% necrosis.

2.8 Western blot

Frozen liver (-80 °C) samples were homogenized with an Omni Tissue Master 125 (Omni International, Kennesaw, GA) in cell lysis buffer (50 mM HEPES, 150 mM NaCl, 1.5 mM MgCl₂, 1 mM EGTA, 10% glycerol, 0.1% ~~triton~~ Triton X-100 containing protease and phosphatase inhibitors). Cell debris was pelleted (12,000 x g, 5 min), supernatant protein content determined (DC Protein Assay, Bio-Rad), and SDS-polyacrylamide gel electrophoresis (Bio-Rad Mini-PROTEAN) was performed with samples standardized to 30 µg protein/well. Proteins were separated using 7.5% gels, followed by electrophoretic elution onto PVDF membranes (Trans-Blot Turbo, Bio-Rad), as per manufacturer's instructions. Blots were run under reducing conditions. PVDF membranes were blocked (5% skim-milk, 1 h), incubated with primary antibodies (Supplemental Table S1) for 16 h (4 °C) and stained with appropriate HRP-conjugated secondary antibodies (Santa Cruz). Immunoreactivity was detected using SuperSignal West Femto Substrate (Thermo Scientific) and digital chemiluminescence image capture (LAS-4000, FujiFilm, Tokyo, Japan). ~~Densitometry was quantified using~~ Densitometric analysis was performed with MultiGauge software (V3.0, FujiFilm, Tokyo, Japan), and all values were normalized to the expression of the housekeeping protein β-actin. All experiments were performed in triplicate.

2.9 Mouse plasma cytokine measurements

Mouse plasma samples were assayed for mouse GM-CSF, IFN-γ, IL-1β, IL-2, IL-4, IL-5, IL-6, IL12p70, IL-13, IL-18, and TNF-α using the ProcartaPlex Mouse Th1/Th2 extended 11-plex kit and mouse BAFF, IL-10, IL-22, RANTES/CCL5, TSLP, and VEGF-A using ProcartaPlex simplex kits on the Luminex platform (Affymetrix, Santa Clara, CA), according to the manufacturer's instructions. The relevance of these inflammatory messengers for hepatic I/R injury is summarized in Supplemental Table S3. In brief, samples were thawed on ice. The antibody-coated beads were mixed and washed, and ~~subsequently~~ incubated overnight at 4 °C with 1:1 diluted standards or samples. After washing, the beads were incubated with detection antibody mix for 30 min at room temperature. The beads were subsequently washed and incubated for 30 min at room temperature with streptavidin-PE. After washing, the beads were measured with a Luminex instrument (Bio-Plex 200, Bio-Rad) that was calibrated using Bio-Rad calibration beads. Standard curves were calculated using 5-parameter logistic regression in Bioplex 5.0 software. Heatmaps were generated using GENE-E software

(<http://www.broadinstitute.org/cancer/software/GENE-E/>) and show the plasma cytokine levels of MitoQ-treated mice following 30 min of ischemia and 6 h or 24 h of reperfusion. Data per time point are expressed as fold-increase compared to the mean of the vehicle control group, whereby blue indicates a decrease and red indicates an increase in the MitoQ group versus control animals subjected to I/R only.

Formatted: No underline

Formatted: No underline

2.10 Intravital imaging and spectroscopic quantification of reactive oxygen species production during hepatic I/R injury in mice

The oxidation-sensitive fluorogenic probe 5(6)-carboxy-dichlorodihydrofluorescein was prepared from 5(6)-carboxy-dichlorodihydrofluorescein diacetate and encapsulated in hepatocyte-targeted liposomes according to Reiniers et al²⁵. Liposomes (0.1 μ mol lipid/g body weight in 200 μ L 10 mM HEPES, 0.88% NaCl, 0.292 osmol/kg, pH = 7.4) were injected via the penile vein and circulated for 35 min to allow intrahepatic accumulation. Hepatic I/R was subsequently performed as described²⁵. To perform the surgical procedure with the mice positioned under the intravital imaging setup, ischemia was induced with a silicone sling placed around the hepatic pedicle instead of a microvascular clamp. During the first 10 min of reperfusion, hepatic probe conversion was quantified at 2-min intervals in real-time using a customized intravital fluorescence microscope (M165FC, Leica Microsystems, Wetzlar, Germany) equipped with a spectrometer (QE65000, Ocean Optics, Dunedin, FL). Spectroscopic data were integrated over the entire spectral width (λ = 250–1050 nm) and normalized to baseline.

Formatted: English (United States)

2.11 Statistical analyses

Statistical analyses were performed using Graphpad Prism 6 (La Jolla, CA) and SPSS 21.0 (Chicago, IL), abiding by a significance level (α) of 0.05 unless otherwise indicated. Normal distribution of data sets with ≥ 8 values was assessed using a D'Agostino and Pearson omnibus test. Normally distributed data were tested for intragroup and intergroup differences using a student's t-test, a one-way ANOVA with Dunnet's post-hoc test, or a repeated measure ANOVA with Geisser-Greenhouse correction and Tukey's post-hoc correction. All continuous numerical variables that failed the normality test were log transformed and re-analyzed. Log-transformed data that followed a Gaussian distribution were analyzed parametrically as described. If the transformed data failed the normality test, non-parametric tests (Mann Whitney U,

Formatted: English (United States)

Formatted: No underline, Font color: Auto, English (United States)

Formatted: English (United States)

Formatted: No underline, Font color: Auto, English (United States)

Formatted: No underline, Font color: Auto, English (United States)

Formatted: No underline, Font color: Auto, English (United States)

Kruskall-Wallis with Dunn's post-hoc test, or Friedman with Dunn's correction) were performed on the non-transformed data. Data sets with <8 values group were tested parametrically. Categorical data were analyzed using a Fisher's exact test (binary data) or a Chi-squared test (>2 variables) and correlations were tested using Spearman's rho.

Formatted: English (United States)

3. Results

3.1 DAMP release after major liver resection in patients

To study DAMP release after clinical liver I/R, a total of 74 patients were enrolled in an observational study. Of the 74 study participants, 35 were excluded due to unresectable disease during surgical exploration (N=30), withdrawal of consent (N=1), an unanticipated change in primary surgeon (N=1), or because a minor instead of a major liver resection was performed (N=3). The relationship between hepatic I/R injury and DAMP release was therefore studied in 39 patients who underwent a major liver resection with (N=26, 'I/R') or without (N=13, 'CTRL') the intraoperative use of VIO. The study design is summarized in Supplemental Figure S1. The baseline patient characteristics are shown in Table 1 and the clinical outcomes are presented in Table 2.

The baseline patient characteristics were comparable between the two study arms. VIO use was associated with longer operating time, resection time, and hospital stay compared to the control group (Table 2). A trend towards more extensive liver resection was seen in the I/R group (Table 2). The severity of postoperative liver injury did not differ between the groups when judged by liver damage (i.e. the postoperative ALT peak) or liver function parameters such as INR ~~or~~and bilirubin (Table 2). There were also no differences in transfusion requirements, postoperative complications, or mortality between the control and I/R group (Table 2). As the aim of the study was to explore DAMP release and activation of sterile inflammation in I/R-subjected patients, it should be underscored that the study was neither designed nor powered to detect differences in patient outcomes between the control and I/R group.

Systemic DAMP levels were next determined in the full cohort at baseline and at 1 h and 6 h after surgery. HMGB1 and nucleosomes were assessed based on preclinical hepatic I/R work^{8,24}. Circulating mitochondrial DNA (mtDNA) was assayed because hepatic I/R injury is thought to originate in ROS-generating mitochondria⁵ and because mtDNA release has been documented in both animal and clinical studies on sterile liver injury^{11,12}. Figure 1A-B show that systemic HMGB1 and nucleosomes concentrations increased within 1 h after surgery in the combined cohort, which was accompanied by a rise in neutrophil activation (Fig. 1D). Systemic mtDNA levels remained unchanged during the first 6 h of

Formatted: No underline, Font color: Auto, English (United States)

Formatted: English (United States)

Formatted: No underline, Font color: Auto, English (United States)

Formatted: English (United States)

Formatted: No underline, Font color: Auto, English (United States)

Formatted: English (United States)

Formatted: No underline, Font color: Auto, English (United States)

Formatted: No underline, Font color: Auto, English (United States)

Formatted: English (United States)

Formatted: No underline, Font color: Auto, English (United States)

reperfusion (Fig. 1C). These data show that the DAMPs HMGB1 and nucleosomes are released into the circulation after major liver resection.

To determine whether DAMP release was caused by ischemia-mediated hepatocyte injury or by surgical trauma *per se*, which has been noted previously²⁶, the patient data were next stratified into an I/R and a control group. Figure 2A-D show that, of the tested DAMPs, only HMGB1 levels increased significantly at 1 h of reperfusion in the I/R group but not in the control group. The release of the cytokines interleukin (IL)-1 β and IL-6 was also more pronounced in the I/R group than in the control group at 1 h of reperfusion (Fig. S2). The early intergroup differences in HMGB1 and cytokine release resolved 6 h after surgery (Fig. 2A, S2). Nucleosome release and neutrophil activation were comparable between groups at all time points (Fig. 2B-C). In line with the release of HMGB1 in only the I/R group, systemic HMGB1 levels after surgery correlated positively to the postoperative ALT peak (Fig. 2E) and the used duration of hepatic ischemia (Fig. 2F). Such a relationship was typically absent for cytokine levels or neutrophil activation (Fig. S3). Collectively, these results suggest that HMGB1 is the DAMP that is most pertinent to clinical hepatic I/R injury.

3.2 Neutralizing mitochondrial oxidative stress limits HMGB1 release after mouse liver I/R

After establishing that HMGB1 is released in patients after hepatic I/R, the therapeutic efficacy of inhibiting HMGB1 release was investigated in a validated mouse hepatic I/R model²⁴ model¹³. Because mitochondrial oxidative injury is considered the most proximal trigger of I/R injury and therefore may cause the release of DAMPs, it was tested whether the mitochondria-targeted antioxidant MitoQ could limit HMGB1 release and, thereby, attenuate hepatic I/R injury in mice. The cytoprotective efficacy of MitoQ was established first. The intravenous administration of MitoQ reduced plasma ALT levels at 6 h and 24 h of reperfusion in mice over a 0.25-1 mg/kg dose range (Fig. 3A), whereas non-specific MitoQ toxicity was seen at higher dosages. Based on this pharmacodynamic profile, 1 mg/kg of MitoQ was used in all *in vivo* experiments.

In concordance with a previous report demonstrating the antioxidant efficacy of MitoQ in I/R-subjected mice²⁷, MitoQ reduced oxidation of the fluorogenic probe 5(6)-carboxy-dichlorofluorescein in hepatocytes during the first 10 min of reperfusion, as measured by intravital spectroscopy (Fig. 3B). The

Formatted: English (United States)

Formatted: No underline, Font color: Auto, English (United States)

Formatted: No underline, Font color: Auto, English (United States)

Formatted: No underline, Font color: Auto, English (United States)

Formatted: No underline, Font color: Auto, English (United States)

Formatted: English (United States)

Formatted: No underline, Font color: Auto, English (United States)

Formatted: English (United States)

Formatted: No underline, Font color: Auto, English (United States)

Formatted: No underline, Font color: Auto, English (United States)

Formatted: English (United States)

Formatted: No underline, Font color: Auto, English (United States)

Formatted: English (United States)

Formatted: No underline, Font color: Auto, English (United States)

fluorogenic probe was delivered specifically to hepatocytes using a hepatotargeted delivery system²⁵. MitoQ did not affect the number of leukocytes in the hepatic microcirculation during the first 90 min of reperfusion (Fig. ~~S8, S9~~S6, S7). The early reduction in oxidative stress (Fig. 3B) ~~however did~~ ~~translate~~translated to a drop in hepatocellular necrosis and transaminase release at 24 h of reperfusion (Fig. 3C-D), indicating a reduction in hepatic I/R injury. Animals that received the inactive targeting moiety of MitoQ, dTPP, were not protected from I/R injury (Fig. 3C-D), reaffirming that the antioxidant properties of the ubiquinol moiety convey the hepatoprotective effects of MitoQ.

After demonstrating that MitoQ was able to reduce I/R injury, the effect of neutralizing mitochondrial oxidative stress on HMGB1 release after mouse liver I/R was explored ~~next~~. Figure 3E shows that MitoQ reduced plasma HMGB1 levels after I/R by approximately 50% at 6 h of reperfusion. Quantification of HMGB1 in liver biopsies by Western blot showed similar HMGB1 levels in MitoQ-treated and untreated mice subjected to I/R (Fig. 3F). This finding may relate to differences in resolving capacity between the techniques used for plasma and whole-liver HMGB1 quantification. To examine whether HMGB1 release was associated with the documented hepatoprotective effect of MitoQ, DAMP reconstitution experiments were performed ~~next~~. Infusing the pro-inflammatory disulfide isoform of HMGB1²⁸ at the start of reperfusion nullified the protective potential of MitoQ (Fig. 3G), which supports the hypothesis that I/R injury sequentially proceeds via mitochondrial oxidative injury and DAMP release.

Systemic HMGB1 alerts the immune system via the receptor for glycation end products (RAGE) and/or Toll-like receptor 4 (TLR-4)^{24,29}, which drive cytokine production by activating various pro-inflammatory transcription factors. After establishing that neutralizing mitochondrial oxidative stress with MitoQ decreased HMGB1 release and reduced hepatic I/R injury, it was ~~next investigated~~determined whether MitoQ treatment also attenuated inflammatory ~~signalling~~signaling following mouse liver I/R. Levels of chemotactic and cytotoxic messengers such as ~~tumour~~tumor necrosis factor (TNF- α) and interleukin (IL-) 1β were lower in the MitoQ group at 6 h of reperfusion, whereas a stronger induction of anti-inflammatory IL-10 was noted at the 24 h time point (Fig. 3J). This ~~favourable~~favorable effect of MitoQ on cytokine profiles may have resulted in the downregulation of the leukocyte receptor VCAM-1, even though the expression of the principal sinusoidal neutrophil receptor ICAM-1 was unaffected (Fig. 3H).

Formatted: No underline, Font color: Auto, English (United States)

Formatted: Font color: Auto, English (United States)

Formatted: No underline, Font color: Auto, English (United States)

Formatted: English (United States)

Formatted: No underline, Font color: Auto, English (United States)

Formatted: No underline, Font color: Auto, English (United States)

Formatted: No underline, Font color: Auto, English (United States)

Formatted: English (United States)

Formatted: No underline, Font color: Auto, English (United States)

Formatted: No underline, Font color: Auto, English (United States)

Formatted: No underline, Font color: Auto, English (United States)

Formatted: No underline, Font color: Auto, English (United States)

Formatted: No underline, Font color: Auto, English (United States)

Formatted: No underline, Font color: Auto, English (United States)

Formatted: No underline, Font color: Auto, English (United States)

Formatted: No underline, Font color: Auto, English (United States)

Formatted: No underline, Font color: Auto, English (United States)

Formatted: English (United States)

| ▲

▲

Formatted: No underline, Font color: Auto, English (United States)

Formatted: English (United States)

4. Discussion

This study shows that (i) the DAMP HMGB1 seems most pertinent ~~to~~ clinical liver I/R injury, (ii) that HMGB1 levels positively correlate with ~~liver~~ injury markers in I/R-subjected patients, and (iii) that treating mitochondrial oxidative injury with MitoQ prevents HMGB1 release and consequent sterile inflammation, ultimately attenuating I/R injury in mice.

~~Hepatic I/R injury remains a clinical challenge. Although a downward trend in VIO use has been reported³⁰, this may relate to the advent of laparoscopic liver surgery, the tendency to undertake parenchyma-sparing resections, and demographic differences between regions. Even if routine VIO use were on the decline, it can be necessary to curtail excessive blood loss during complex resections. Moreover, patients can be excluded from surgery based on the preoperative assessment of future remnant liver volume and function, a decision that also considers potential effects of I/R on the liver remnant. Nevertheless, major Major liver resection remains associated with considerable mortality, exceeding 10% in patients with high-risk tumors³⁴. These data indicate that the tumors³⁰. The ramifications of liver ischemia therefore still influence surgical practice on a daily basis.~~

~~Part of the challenge is that supportive care is the only current treatment for hepatic I/R injury, and in that respect, several observations can be made based on the current work. It is the first report that shows DAMP release directly after major liver resection, and additionally identifies HMGB1 as the DAMP most pertinent to clinical I/R injury. The finding that mtDNA levels were unaffected by liver I/R is surprising, given that mtDNA release was seen in patients with acetaminophen intoxication, which pathophysiologically resembles I/R in terms of oxidative liver injury⁴². It should be noted, however, that the primary site of oxidative stress differs between hepatic I/R injury (mitochondria) and acetaminophen overdose (cytosol). How the subcellular site of (initial) hepatocyte injury affects the release of specific DAMPs remains to be experimentally pursued.~~

~~Liver I/R in patients was characterized by an early rise in HMGB1 levels 1 h after surgery, whereas HMGB1 returned to baseline 6 h after surgery. The early release of HMGB1 fits previous reports showing that HMGB1 from hepatocytes is already propagated by ischemia, and persists throughout the reperfusion phase in mice subjected to I/R³¹. It is also consistent with the finding that HMGB1 is found in the caval effluent immediately after liver transplantation³². The notion that HMGB1 levels correlated to~~

Formatted: No underline, Font color: Auto, English (United States)

Formatted: English (United States)

Formatted: No underline, Font color: Auto, English (United States)

Formatted: No underline, Font color: Auto, English (United States)

Formatted: No underline, Font color: Auto, English (United States)

Formatted: English (United States)

Formatted: No underline, Font color: Auto, English (United States)

Formatted: No underline, Font color: Auto, English (United States)

Formatted: No underline, Font color: Auto, English (United States)

Formatted: No underline, Font color: Auto, English (United States)

Formatted: No underline, Font color: Auto, English (United States)

transaminase release and the duration of ischemia indicates that HMGB1 may hold prognostic or even therapeutic value, as HMGB1 is an active mediator of immune activation that could serve as an interventional target. Small-molecule inhibitors of the HMGB1 receptor RAGE are being clinically evaluated for ancillary ~~indications~~³² indications³³, whereas inhibition of TLR receptors has been proposed to treat inflammatory ~~disorders~~³³ disorders³⁴. Direct HMGB1 inhibition has also shown promise in treating drug-induced liver injury in ~~mice~~³⁴ mice³⁵. This starkly contrasts the liver injury markers such as ALT or bilirubin, which are 'passive' markers for hepatocellular injury that do not modulate immune responses. The latter also applies to other hepatic I/R biomarkers such as keratin ~~18~~³⁵ 18³⁶. DAMP-targeted interventions could for instance be used on an on-demand basis to control I/R injury in patients with anticipated (or unexpected) extensive ischemia times. A similar rationale has driven the introduction of *in situ* liver cooling ~~techniques~~^{36,37} techniques^{37,38}.

~~Although HMGB1 after liver I/R could theoretically also derive from other cells or organs after liver I/R, such as the intestines~~³⁸ literature suggests intestines³⁹. It is however most plausible that hepatocytes are the source of HMGB1, for several reasons. First, the postoperative rise in HMGB1 is not seen in hepatocyte-specific HMGB1 knockout mice subjected to liver I/R^{39,40}. Similar results have been obtained with mice deficient in hepatocyte TLR-4, an innate immune receptor that mediates facilitates HMGB1 release after I/R^{24,40,41}. Second, HMGB1 levels were more prominent in caval than in portal blood after liver ~~transplantation~~⁴⁴ transplantation³², whereas no differences were noted between systemic and portal HMGB1 concentrations. The latter excludes the bowel as a source of HMGB1 after liver transplantation. Last, *in vitro* studies have shown that hepatocytes rendered hypoxic or exposed to the oxidant hydrogen peroxide release HMGB1 into the culture supernatant²⁴. ~~Current An~~ unanswered questions are question is which HMGB1 isoform is released after liver I/R, as the biological effects of HMGB1 depend on the oxidation status of the protein²⁸. In addition, it should be elucidated how HMGB1 ~~levels are~~ is inactivated and/or regulated at sites of inflammation. This is imperative given the transient nature of postoperative HMGB1 surges noted both after liver ~~transplantation~~⁴⁴ transplantation³² and in the current study (Fig. 2).

~~The presented data also highlight that detoxifying mitochondrial oxidative stress may be an even more proximal target for intervention. The finding that mtDNA levels were unaffected by liver I/R is unexpected, given that mtDNA release was seen in mice and patients with acetaminophen (APAP)~~

Formatted: No underline, Font color: Auto, English (United)

Formatted: English (United States)

Formatted: No underline, Font color: Auto, English (United)

hepatotoxicity, which pathophysiologically resembles I/R in terms of oxidative injury to hepatocyte mitochondria^{12,42,43}. The discrepancy may relate to several differences between I/R injury and APAP overdose. First, the mechanistic pathways culminating in mitochondrial damage are different. In case of APAP, cytoplasmic glutathione stores are depleted, leading to the accumulation of the toxic NAPQI that associates with mitochondrial proteins and leads to mitochondrial permeability transition (MPT) and necrotic cell death⁴³. Accordingly, APAP causes cytoplasmic redox stress that subsequently migrates to the mitochondria. In case of I/R, the depletion and subsequent repletion of the terminal substrate of the electron transport chain (ETC) - molecular oxygen - leads to an oxidative burst and ROS production that perturbs ETC proteins by redox modification and causes MPT and mainly necrotic cell death⁴⁴. Mitochondrial damage by I/R therefore has a mitochondrial origin, which could translate to differential mtDNA kinetics versus APAP-triggered mtDNA kinetics. Corroboratively, mtDNA release seems to be a tightly regulated process rather than a mere consequence of necrosis inasmuch as rendering livers necrotic with furosemide instead of APAP did not trigger mtDNA release¹². Second, hepatocellular injury in patients with APAP toxicity was considerably more severe than in our I/R cohort based on ALT levels¹². The proposition that mtDNA is released mainly in severe liver injury is also in line with a later report showing that mtDNA release is more pronounced in patients with poor outcome after APAP overdose¹¹. One could further argue that ischemia by itself is the factor that differentiates APAP toxicity from I/R injury. Indeed, mtDNA release has been predominantly reported in patients with non-ischemic causes of sterile injury, which in addition to APAP hepatotoxicity includes inflammatory bowel disease⁴⁵ and trauma patients⁴⁶. This line of reasoning, however, does not align with the fact that we also did not find mtDNA release in patients who underwent a major hepatectomy without intraoperative VIO use (i.e., non-ischemic sterile liver injury).

The current data also highlight that mitochondrial oxidative stress may be an even more proximal target for intervention⁴⁷, as this may limit DAMP release. The finding that MitoQ was able to suppress HMGB1 release fits the earlier notion that the glutathione precursor n-acetyl-cysteine (NAC) reduced HMGB1 release after *in vitro* hepatocyte anoxia/reoxygenation²⁴. Antioxidants, including NAC, lack efficacy in various clinical scenarios, including hepatic I/R⁴² R injury⁴⁸. MitoQ differs from these compounds in that it is designed to target the site of oxidant production after I/R (i.e., mitochondria) and

Formatted: No underline, Font color: Auto, English (United)

Formatted: No underline, Font color: Auto, English (United)

also detoxifies the most relevant oxidant (i.e., superoxide)⁵. ~~Moreover~~ MitoQ has been used previously in mice to successfully treat hepatic I/R injury²⁷. In the latter report, MitoQ efficacy was assessed using surrogate markers for oxidative injury such as mitochondrial protein carbonylation and hepatic 3-nitrotyrosine content²⁷. Using a direct intravital fluorescence-based method²⁵ it was confirmed that MitoQ reduces hepatocyte oxidative stress early after I/R. In addition, MitoQ has already been ~~used~~ employed in phase II studies ~~and has for instance reduced~~ where it curtailed transaminase levels in patients with hepatitis ~~C⁴³C⁴⁹~~, which is an encouraging follow-up to the preclinical notion that MitoQ is generally well-tolerated and not ~~toxic⁴⁴~~ toxic⁵⁰. The clinical investigation and implementation of mitochondria-targeted antioxidants such as MitoQ therefore ~~is an attainable~~ seems a realistic objective.

~~Several limitations of the current study should be considered when interpreting the results.~~ The observational nature of the current study means that it is neither designed nor powered to detect differences in clinical outcomes. The similarity in post-operative ~~hepatocellular~~ liver injury parameters between the I/R and control group (Table 2) therefore does not mean that liver ischemia is innocuous, but that VIO in experienced hands is a safe salvage procedure when used to counteract the harms of excessive blood loss. The relatively ~~favourable~~ favorable post-operative transaminase and bilirubin values recorded in the I/R group also relates to the fact that only patients with sufficient (future) remnant liver size and function are eligible for major liver resection. ~~This is supported by the fact that the noted extent of liver injury (i.e., ALT release) is comparable to previous clinical liver I/R cohorts^{51,52}.~~ The interpretation of the clinical data is further hindered by the inability to separate the contribution of ischemic liver injury from the effects of surgical trauma on ~~postoperative~~ DAMP release. It has for instance been reported that the DAMP ATP is released from the resection plane after partial hepatectomy²⁶. ~~In the latter study, patients were not exposed to ischemia during liver resection.~~ Also, the duration of liver surgery and hepatic manipulation during surgery both influence the release of liver injury ~~markers⁴⁵~~ markers⁵³. The longer operating time and trend towards more extensive resections in the I/R group (Table 1) may therefore also add to the higher HMGB1 levels in the I/R group rather than VIO use only. ~~although this does not per se disqualify the conclusions when contextualized to the mouse data. Last, it should be noted that, in line with available evidence⁵⁴, the majority of patients were operated using intermittent VIO (Table S4). This technique allows for brief periods of parenchymal (re)perfusion in between cycles of liver~~

Formatted: No underline, Font color: Auto, English (United)

Formatted: English (United States)

Formatted: No underline, Font color: Auto, English (United)

ischemia. In contrast, most animal models of hepatic I/R, including ours, employ continuous liver ischemia. As the anoxic period primes mitochondria for the post-ischemic burst of ROS production⁶, it is conceivable that intermittent VIO lessens the extent of mitochondrial oxidative injury after I/R. Accordingly, it also means that it remains to be shown whether I/R injury resulting from intermittent VIO is amenable to treatment with mitochondria-targeted antioxidants such as MitoQ.

▲ In conclusion, it is shown that HMGB1 release is related to clinical liver I/R injury. The finding that the mitochondria-targeted antioxidant MitoQ limited HMGB1 release and reduced I/R injury in mice may pave the way for the clinical use of targeted antioxidants against early-onset radicals and oxidants to attenuate hepatic I/R injury.

Formatted: No underline, Font color: Auto, English (United States)

Formatted: English (United States)

Formatted: No underline, Font color: Auto, English (United States)

Formatted: English (United States)

5. Acknowledgements

Readers wishing to receive raw study data should contact the corresponding author. The authors are grateful to Wouter van Riel, Noor Hagemeijer, Marieke Smit, and Annemiek Dekker for assisting with the collection of patient samples and to Albert van Wijk for analytical support. Lori Zbytniuk and Michelle Wilson from the Kubes lab (Calgary) are acknowledged for technical and infrastructural support. Katarzyna Stevens and Pina Colarusso from the Live Cell Imaging Facility (Snyder Institute, Calgary) are acknowledged for assistance with intravital imaging and image analysis. The authors thank Edward Chouchani, Tracy Prime, and Sebastian Rogatti from the MRC Mitochondrial Biology Unit in Cambridge for technical and infrastructural help with the MitoQ experiments.

RVG ~~is was~~ supported by a PhD Scholarship and The Young Talent Fund, both from the Academic Medical Center in Amsterdam. MH ~~is was~~ supported by grants from the Dutch Anti-Cancer Foundation (Stichting Nationaal Fonds Tegen Kanker) in Amsterdam, the Phospholipid Research Center in Heidelberg, the Nijbakker-Morra Foundation in Leiden, and Stichting Technologische Wetenschap (STW). ~~MH is currently supported by the Dutch Cancer Society (project # 10666).~~ This work was also supported by the Live Cell Imaging Facility (Snyder Institute, Calgary) funded by an equipment and infrastructure grant from the Canadian Foundation Innovation (CFI), the Alberta Science and Research Authority, and the Mouse Phenomics Resources Laboratory funded by the Snyder Institute for Chronic Diseases at the University of Calgary.

Formatted: No underline, Font color: Auto, English (United States)

Formatted: English (United States)

Formatted: No underline, Font color: Auto, English (United States)

Formatted: English (United States)

Formatted: No underline, Font color: Auto, English (United States)

Formatted: No underline, Font color: Auto, English (United States)

Formatted: No underline, Font color: Auto, English (United States)

Formatted: No underline, Font color: Auto, English (United States)

Formatted: English (United States)

Formatted: No underline, Font color: Auto, English (United States)

Formatted: English (United States)

6. References

1. Pringle JH. V. Notes on the arrest of hepatic hemorrhage due to trauma. *Ann Surg* 1908; **48**: 541-9.
2. van Golen RF, van Gulik TM, Heger M. The sterile immune response during hepatic ischemia/reperfusion. *Cytokine Growth Factor Rev* 2012; **23**: 69 - 84.
3. van Riel WG, van Golen RF, Reiniers MJ, Heger M, van Gulik TM. How much ischemia can the liver tolerate during resection? *Hepatobiliary Surg Nutr* ~~2015~~; **2016**; **1**: 58-71.
4. van Golen RF, van Gulik TM, Heger M. Mechanistic overview of reactive species-induced degradation of the endothelial glycocalyx during hepatic ischemia/reperfusion injury. *Free Radic Biol Med* 2012; **52**: 1382-402.
5. Chouchani ET, Pell VR, James AM, Work LM, Saeb-Parsy K, Frezza C, et al. A unifying mechanism for mitochondrial superoxide production during ischemia-reperfusion injury. *Cell Metab* 2016; **23**: 254-63.
6. Chouchani ET, Pell VR, Gaude E, Aksentijević D, Sundier SY, Robb EL, et al. Ischaemic accumulation of succinate controls reperfusion injury through mitochondrial ROS. *Nature* 2014; **515**: 431-5.
7. Reiniers MJ, van Golen RF, van Gulik TM, Heger M. Reactive oxygen and nitrogen species in steatotic hepatocytes: A molecular perspective on the pathophysiology of ischemia-reperfusion injury in the fatty liver. *Antioxid Redox Signal* 2013; **21**: 1119-42.
8. Huang H, Evankovich J, Yan W, Nace G, Zhang L, Ross M, et al. Endogenous histones function as alarmins in sterile inflammatory liver injury through toll-like receptor 9. *Hepatology* 2011; **54**: 999-1008.
9. Bamboat ZM, Ocun LM, Balachandran VP, Obaid H, Plitas G, Dematteo RP. Conventional dcs reduce liver ischemia/reperfusion injury in mice via IL-10 secretion. *J Clin Invest* 2010; **120**: 559-69.
10. Tsung A, Sahai R, Tanaka H, Nakao A, Fink MP, Lotze MT, et al. The nuclear factor HMGB1 mediates hepatic injury after murine liver ischemia-reperfusion. *J Exp Med* 2005; **201**: 1135-43.
11. McGill MR, Staggs VS, Sharpe MR, Lee WM, Jaeschke H, Acute Liver Failure Study Group. Serum mitochondrial biomarkers and damage-associated molecular patterns are higher in acetaminophen overdose patients with poor outcome. *Hepatology* 2014; **60**: 1336-45.
12. McGill MR, Sharpe MR, Williams CD, Taha M, Curry SC, Jaeschke H. The mechanism underlying acetaminophen-induced hepatotoxicity in humans and mice involves mitochondrial damage and nuclear DNA fragmentation. *J Clin Invest* 2012; **122**: 1574-83.

Formatted: No underline, Font color: Auto, English (United

States)

Formatted: No underline, Font color: Auto, English (United

States)

Formatted: No underline, Font color: Auto, English (United

States)

Formatted: No underline, Font color: Auto, English (United

States)

Formatted: No underline, Font color: Auto, English (United

States)

Formatted: No underline, Font color: Auto, English (United

States)

Formatted: No underline, Font color: Auto, English (United

States)

Formatted: No underline, Font color: Auto, English (United

States)

Formatted: No underline, Font color: Auto, English (United

States)

Formatted: No underline, Font color: Auto, English (United

States)

Formatted: No underline, Font color: Auto, English (United

States)

Formatted ...

Formatted ...

Formatted ...

Formatted ...

Formatted ...

~~13.~~ ~~van Golen RF, Reiniers MJ, Heger M, Verheij J. Solutions to the discrepancies in the extent of liver damage following ischemia/reperfusion in standard mouse models. *J Hepatol* 2014; **62**: 975-7.~~ ~~Dindo D, Demartines N, Clavien PA. Classification of surgical complications: A new proposal with evaluation in a cohort of 6336 patients and results of a survey. *Ann Surg* 2004; **240**: 205-13.~~

Formatted: No underline, Font color: Auto, English (United States)

14. Dindo D, Demartines N, Clavien PA. Classification of surgical complications: A new proposal with evaluation in a cohort of 6336 patients and results of a survey. *Ann Surg* 2004; **240**: 205-13.

Formatted: English (United States)

Formatted: No underline, Font color: Auto, English (United States)

15. Rehm M, Bruegger D, Christ F, Conzen P, Thiel M, Jacob M, et al. Shedding of the endothelial glycocalyx in patients undergoing major vascular surgery with global and regional ischemia. *Circulation* 2007; **116**: 1896-906.

Formatted: No underline, Font color: Auto, English (United States)

4516. Zeerleder S, Zwart B, te Velthuis H, Manoe R, Bulder I, Rensink I, Aarden LA. A plasma nucleosome releasing factor (NRF) with serine protease activity is instrumental in removal of nucleosomes from secondary necrotic cells. *FEBS Lett* 2007; **581**: 5382-8.

Formatted: English (United States)

Formatted: No underline, Font color: Auto, English (United States)

4617. van Nieuwenhuijze AE, van Lopik T, Smeenk RJ, Aarden LA. Time between onset of apoptosis and release of nucleosomes from apoptotic cells: Putative implications for systemic lupus erythematosus. *Ann Rheum Dis* 2003; **62**: 10-4.

Formatted: English (United States)

Formatted: No underline, Font color: Auto, English (United States)

4718. van Montfoort ML, Stephan F, Lauw MN, Hutten BA, Van Mierlo GJ, Solati S, et al. Circulating nucleosomes and neutrophil activation as risk factors for deep vein thrombosis. *Arterioscler Thromb Vasc Biol* 2013; **33**: 147-51.

Formatted: English (United States)

Formatted: No underline, Font color: Auto, English (United States)

4819. Nuijens JH, Abbink JJ, Wachtfogel YT, Colman RW, Eerenberg AJ, Dors D, et al. Plasma elastase alpha 1-antitrypsin and lactoferrin in sepsis: Evidence for neutrophils as mediators in fatal sepsis. *J Lab Clin Med* 1992; **119**: 159-68.

Formatted: English (United States)

Formatted: No underline, Font color: Auto, English (United States)

4920. Nakahira K, Kyung SY, Rogers AJ, Gazourian L, Youn S, Massaro AF, et al. Circulating mitochondrial DNA in patients in the ICU as a marker of mortality: Derivation and validation. *PLoS Med* 2013; **10**: e1001577; discussion e1001577.

Formatted: English (United States)

Formatted: No underline, Font color: Auto, English (United States)

2021. Ruijter JM, Ramakers C, Hoogaars WM, Karlen Y, Bakker O, van den Hoff MJ, Moorman AF. Amplification efficiency: Linking baseline and bias in the analysis of quantitative PCR data. *Nucleic Acids Res* 2009; **37**: e45.

Formatted: English (United States)

Formatted: No underline, Font color: Auto, English (United States)

Formatted: English (United States)

21. ~~van Golzen RF, Reiniers MJ, Heger M, Vorheij J. Solutions to the discrepancies in the extent of liver damage following ischemia/reperfusion in standard mouse models. *J Hepatol* 2014; **62**: 975-7.~~

Formatted: No underline, Font color: Auto, English (United States)

22. Sun Q, Loughran P, Shapiro R, Shrivastava IH, Antoine DJ, Li T, et al. Redox-dependent regulation of hepatocyte absent in melanoma 2 inflammasome activation in sterile liver injury in mice. *Hepatology* 2017; **65**: 253-68.

Formatted: No underline, Font color: Auto, English (United States)

23. Yang H, Wang H, Ju Z, Ragab AA, Lundbäck P, Long W, et al. MD-2 is required for disulfide hmgb1-dependent TLR4 signaling. *J Exp Med* 2015; **212**: 5-14.

Formatted: English (United States)

Formatted: No underline, Font color: Auto, English (United States)

24. Tsung A, Klune JR, Zhang X, Jeyabalan G, Cao Z, Peng X, et al. HMGB1 release induced by liver ischemia involves toll-like receptor 4 dependent reactive oxygen species production and calcium-mediated signaling. *J Exp Med* 2007; **204**: 2913-23.

Formatted: English (United States)

Formatted: No underline, Font color: Auto, English (United States)

25. Reiniers MJ, van Golzen RF, Bonnet S, Broekgaarden M, van Gulik TM, Egmond MR, Heger M. Preparation and practical applications of 2',7'-dichlorodihydrofluorescein in redox assays. *Anal Chem* 2017; **89**: 3853-7.

Formatted: English (United States)

Formatted: No underline, Font color: Auto, English (United States)

26. Gonzales E, Julien B, Serrière-Lanneau V, Nicou A, Doignon I, Lagoudakis L, et al. ATP release after partial hepatectomy regulates liver regeneration in the rat. *J Hepatol* 2010; **52**: 54-62.

Formatted: English (United States)

Formatted: No underline, Font color: Auto, English (United States)

27. Mukhopadhyay P, Horváth B, Zsengellér Z, Bátkai S, Cao Z, Kechrid M, et al. Mitochondrial reactive oxygen species generation triggers inflammatory response and tissue injury associated with hepatic ischemia-reperfusion: Therapeutic potential of mitochondrially targeted antioxidants. *Free Radic Biol Med* 2012; **53**: 1123-38.

Formatted: English (United States)

Formatted: No underline, Font color: Auto, English (United States)

28. Venereau E, Casalgrandi M, Schiraldi M, Antoine DJ, Cattaneo A, De Marchis F, et al. Mutually exclusive redox forms of HMGB1 promote cell recruitment or proinflammatory cytokine release. *J Exp Med* 2012; **209**: 1519-28.

Formatted: English (United States)

Formatted: No underline, Font color: Auto, English (United States)

29. Huebener P, Pradere JP, Hernandez C, Gwak GY, Caviglia JM, Mu X, et al. The HMGB1/RAGE axis triggers neutrophil-mediated injury amplification following necrosis. *J Clin Invest* 2015; **125**: 539-50.

Formatted: English (United States)

Formatted: No underline, Font color: Auto, English (United States)

30. ~~Fan ST, Lo CM, Poon RT, Young C, Liu CL, Yuen WK, et al. Continuous improvement of survival outcomes of resection of hepatocellular carcinoma: A 20-year experience. *Ann Surg* 2011; **253**: 745-58.~~

Formatted: English (United States)

Formatted: No underline, Font color: Auto, English (United States)

~~31~~ Wiggers JK, Koerkamp BG, Cieslak KP, Doussot A, van Klaveren D, Allen PJ, et al. Postoperative mortality after liver resection for perihilar cholangiocarcinoma: Development of a risk score and importance of biliary drainage of the future liver remnant. *J Am Coll Surg* 2016; **223**: 321-331.e1.

Formatted: No underline, Font color: Auto, English (United States)

~~31~~, ~~32~~ Evankovich J, Cho SW, Zhang R, Cardinal J, Dhupar R, Zhang L, et al. High mobility group box 1 release from hepatocytes during ischemia and reperfusion injury is mediated by decreased histone deacetylase activity. *J Biol Chem* 2010; **285**: 39888-97.

Formatted: English (United States)

Formatted: No underline, Font color: Auto, English (United States)

~~32~~, Ilmakunnas M, Tukiainen EM, Rouhiainen A, Rauvala H, Arola J, Nordin A, et al. High mobility group box 1 protein as a marker of hepatocellular injury in human liver transplantation. *Liver Transpl* 2008; **14**: 1517-25.

Formatted: No underline, Font color: Auto, English (United States)

Formatted: English (United States)

~~33~~, Burstein AH, Grimes I, Galasko DR, Aisen PS, Sabbagh M, Mjalli AM. Effect of TTP488 in patients with mild to moderate alzheimer's disease. *BMC Neurol* 2014; **14**:12.

Formatted: No underline, Font color: Auto, English (United States)

Formatted: English (United States)

~~3334~~, Hennessy EJ, Parker AE, O'Neill LA. Targeting toll-like receptors: Emerging therapeutics? *Nat Rev Drug Discov* 2010; **9**: 293-307.

Formatted: No underline, Font color: Auto, English (United States)

Formatted: English (United States)

~~3435~~, Lundbäck P, Lea JD, Sowinska A, Ottosson L, Fürst CM, Steen J, et al. A novel high mobility group box 1 neutralizing chimeric antibody attenuates drug-induced liver injury and postinjury inflammation in mice. *Hepatology* 2016; **64**: 1699-710.

Formatted: No underline, Font color: Auto, English (United States)

Formatted: English (United States)

~~3536~~, Yang M, Antoine DJ, Weemhoff JL, Jenkins RE, Farhood A, Park BK, Jaeschke H. Biomarkers distinguish apoptotic and necrotic cell death during hepatic ischemia/reperfusion injury in mice. *Liver Transpl* 2014; **20**: 1372-82.

Formatted: No underline, Font color: Auto, English (United States)

Formatted: English (United States)

~~3637~~, Reiniers MJ, van Golen RF, Heger M, Mearadji B, Bennink RJ, Verheij J, van Gulik TM. In situ hypothermic perfusion with retrograde outflow during right hemihepatectomy: First experiences with a new technique. *J Am Coll Surg* 2013; **218**: e7-16.

Formatted: English (United States)

Formatted: No underline, Font color: Auto, English (United States)

~~3738~~, Reiniers MJ, Olthof PB, van Golen RF, Heger M, van Beek AA, Meijer B, et al. Hypothermic perfusion with retrograde outflow during right hepatectomy is safe and feasible. *Surgery* 2017; **162**: 48-58.

Formatted: English (United States)

Formatted: No underline, Font color: Auto, English (United States)

~~3839~~, Kojima M, Tanabe M, Shinoda M, Yamada S, Miyasho T, Suda K, et al. Role of high mobility group box chromosomal protein 1 in ischemia-reperfusion injury in the rat small intestine. *J Surg Res* 2012; **178**: 466-71.

Formatted: English (United States)

Formatted: No underline, Font color: Auto, English (United States)

Formatted: English (United States)

~~3940~~, Huang H, Nace GW, McDonald KA, Tai S, Klune JR, Rosborough BR, et al. Hepatocyte specific HMGB1 deletion worsens the injury in liver ischemia/reperfusion: A role for intracellular HMGB1 in cellular protection. *Hepatology* 2013; **59**: 1984-97.

Formatted: No underline, Font color: Auto, English (United States)

~~4041~~, Nace GW, Huang H, Klune JR, Eid RE, Rosborough BR, Korff S, et al. Cellular specific role of toll-like receptor 4 in hepatic ischemia-reperfusion injury. *Hepatology* 2013; **58**: 374-87.

Formatted: English (United States)

Formatted: No underline, Font color: Auto, English (United States)

~~44-42~~. He Y, Feng D, Li M, Gao Y, Ramirez T, Cao H, et al. Hepatic mitochondrial DNA/toll-like receptor 9/microrna-223 forms a negative feedback loop to limit neutrophil overactivation and acetaminophen hepatotoxicity in mice. *Hepatology* 2017; **66**: 220-34.

Formatted: English (United States)

~~43~~. Ramachandran A, Duan L, Akakpo JY, Jaeschke H. Mitochondrial dysfunction as a mechanism of drug-induced hepatotoxicity: Current understanding and future perspectives. *J Clin Transl Res* 2018; **4**.

~~44~~. Jaeschke H, Lemasters JJ. Apoptosis versus oncotic necrosis in hepatic ischemia/reperfusion injury. *Gastroenterology* 2003; **125**: 1246-57.

~~45~~. Boyapati RK, Dorward DA, Tamborska A, Kalla R, Ventham NT, Doherty MK, et al. Mitochondrial DNA is a pro-inflammatory damage-associated molecular pattern released during active IBD. *Inflamm Bowel Dis* 2018; **24**: 2113-22.

~~46~~. Zhang Q, Raoof M, Chen Y, Sumi Y, Sursal T, Junger W, et al. Circulating mitochondrial DAMPs cause inflammatory responses to injury. *Nature* 2010; **464**: 104-7.

~~47~~. Heger M, Reiniers MJ, van Golen RF. Mitochondrial metabolomics unravel the primordial trigger of ischemia/reperfusion injury. *Gastroenterology* 2015; **148**: 1071-3.

~~48~~, Ilmakunnas M, Tukiaainen EM, Rouhiainen A, Rauvala H, Arola J, Nordin A, et al. High mobility group box 1 protein as a marker of hepatocellular injury in human liver transplantation. *Liver Transpl* 2008; **14**: 4517-25.

Formatted: No underline, Font color: Auto, English (United States)

~~42~~, Bahde R, Spiegel HU. Hepatic ischaemia-reperfusion injury from bench to bedside. *Br J Surg* 2010; **97**: 1461-75.

Formatted: English (United States)

Formatted: No underline, Font color: Auto, English (United States)

~~4349~~, Gane EJ, Weilert F, Orr DW, Keogh GF, Gibson M, Lockhart MM, et al. The mitochondria-targeted anti-oxidant mitoquinone decreases liver damage in a phase II study of hepatitis C patients. *Liver Int* 2010; **30**: 1019-26.

Formatted: English (United States)

Formatted: No underline, Font color: Auto, English (United States)

Formatted: English (United States)

4450. Rodriguez-Cuenca S, Cochemé HM, Logan A, Abakumova I, Prime TA, Rose C, et al.

Consequences of long-term oral administration of the mitochondria-targeted antioxidant mitoq to wild-type mice. *Free Radic Biol Med* 2010; **48**: 161-72.

45-51. van den Broek MA, Bloemen JG, Dello SA, van de Poll MC, Olde Damink SW, Dejong CH. Randomized controlled trial analyzing the effect of 15 or 30 min intermittent pringle maneuver on hepatocellular damage during liver surgery. *J Hepatol* 2011; **55**: 337-45.

52. Beck-Schimmer B, Breitenstein S, Bonvini JM, Lesurtel M, Ganter M, Weber A, et al. Protection of pharmacological preconditioning in liver surgery: Results of a prospective randomized controlled trial. *Ann Surg* 2012; **256**: 837-45.

53. van de Poll MC, Derikx JP, Buurman WA, Peters WH, Roelofs HM, Wigmore SJ, Dejong CH. Liver manipulation causes hepatocyte injury and precedes systemic inflammation in patients undergoing liver resection. *World J Surg* 2007; **31**: 2033-8.

54. Belghiti J, Noun R, Malafosse R, Jagot P, Sauvanet A, Pierangeli F, et al. Continuous versus intermittent portal triad clamping for liver resection: A controlled study. *Ann Surg* 1999; **229**: 369-75.

Formatted: No underline, Font color: Auto, English (United States)

Formatted: English (United States)

Formatted: No underline, Font color: Auto, English (United States)

Formatted: English (United States)

Formatted: No underline, Font color: Auto, English (United States)

Formatted: English (United States)

7. Figure legends

Figure 1. DAMP release and neutrophil activation after clinical liver I/R

A-D show plasma levels (median±IQR) of the DAMPs HMGB1, nucleosomes, and mtDNA, and the marker for neutrophil activity E-AT at 1 h and 6 h after liver surgery in patients. Note that the y-axes are scaled logarithmically. E-AT=elastase- α 1-antitrypsin complex; HMGB1=high mobility group box 1; mtDNA=mitochondrial DNA. # indicates $p < 0.05$ versus $t=0$.

Formatted: No underline, Font color: Auto, English (United States)

Formatted: English (United States)

Formatted: No underline, Font color: Auto, English (United States)

Formatted: English (United States)

Formatted: No underline, Font color: Auto, English (United States)

Formatted: No underline, Font color: Auto, English (United States)

Formatted: No underline, Font color: Auto, English (United States)

Formatted: English (United States)

Formatted: No underline, Font color: Auto, English (United States)

Formatted: English (United States)

Figure 2. HMGB1 release correlates to postoperative liver injury after major liver resection

A-D show systemic DAMP levels (median±IQR) for patients operated with VIO (I/R, red) or without VIO (control, blue). **E-F** display the correlation between circulating HMGB1 and liver ischemia time and the post-operative hepatocellular injury peak. The dashed lines indicate the 95% confidence interval of the regression line. Additional correlation data are presented in Supplemental Figures S3. # indicates p<0.05 versus t=0 in the I/R group, \$ indicates p<0.05 versus t=0 in the control group, and * indicates p<0.05 between the groups indicated by the solid line. ALT=aspartate alanine aminotransferase; E-AT=elastase- α 1-antitrypsin complex; HMGB1=high mobility group box 1; I/R=ischemia/reperfusion; IQR=interquartile range; mtDNA=mitochondrial DNA; VIO=vascular inflow occlusion.

Formatted: No underline, Font color: Auto, English (United States)

Formatted: English (United States)

Formatted: No underline, Font color: Auto, English (United States)

Formatted: No underline, Font color: Auto, English (United States)

Formatted: No underline, Font color: Auto, English (United States)

Formatted: English (United States)

Formatted: No underline, Font color: Auto, English (United States)

Formatted: English (United States)

Figure 3. MitoQ attenuates hepatic I/R injury in mice by suppressing HMGB1 release

A shows the dose-response relationship between MitoQ and hepatocellular injury. The 1 mg/kg MitoQ dosage was used in all subsequent experiments (solid line). **B** demonstrates that MitoQ mitigated hepatic oxidative stress during early reperfusion as measured by real-time *in vivo* microscopy/spectroscopy. **C-D** show that MitoQ decreased ALT release and hepatocellular necrosis at 24 h reperfusion whereas redox-inactive MitoQ (dTPP) was not protective (also see Fig. S4). **E-F** indicate that MitoQ attenuated HMGB1 release but did not affect intracellular HMGB1 levels. **G** demonstrates that reconstitution of disulfide HMGB1 reverses the protective effects of MitoQ. **H-I** show that MitoQ decreased expression of the leukocyte receptor VCAM-1 but did not affect ICAM-1 expression. The heat map (**J**) depicts a decrease (blue) or increase (red) in plasma cytokine concentration in MitoQ-treated animals subjected to I/R versus vehicle-treated animals subjected to I/R. The dots indicate a statistically significant difference between the MitoQ and control group. Full hepatocellular damage and cytokine results are included in Supplemental [Figure S5-7](#) and [Supplemental Table S6](#), and a functional description of measured cytokines is included in Supplemental Table S3. Results are shown as mean±SEM, except for **D** (median±range). Western blot results are presented as densitometric analysis. One representative blot per group is included per graph. Group sizes are ≥6 animals/group, except for **B** (3-4 mice/group). Area under the curve analysis was used to assess differences in ROS production (**B**). * indicates p<0.05 in the MitoQ versus the I/R group. au=arbitrary unit; ALT=aspartate alanine aminotransferase; CDCF=5(6)-carboxy-dichlorofluorescein; dTPP= decyl-triphenylphosphonium; ROS=reactive oxygen species; HMGB1=high mobility group box 1; ICAM-1=intercellular adhesion molecule 1; VCAM-1=vascular cell adhesion molecule 1.

Formatted: No underline, Font color: Auto, English (United States)

Formatted: English (United States)

Formatted: No underline, Font color: Auto, English (United States)

Formatted: No underline, Font color: Auto, English (United States)

Formatted: No underline, Font color: Auto, English (United States)

Formatted: English (United States)

Formatted: No underline, Font color: Auto, English (United States)

Formatted: English (United States)

	CTRL (N=13)	I/R (N=26)	p-value
Resected segments [#] (%)			0.131
3	6 (46.2%)	5 (19.2%)	
≥4	7 (53.8%)	21 (80.8%)	
Resection time, min (median±IQR)	59 (41.5 – 71.5)	82 (60 – 130)	0.006
Duration of ischemia ^{&} min (median±IQR)	N/A	48 (31 – 68)	
Duration of surgery, min (median±IQR)	306 (261 – 373.5)	460 (380 – 503)	0.001
Transfusion requirement, units (%)			0.455
0	9 (62.9)	12 (48)	
1-2	2 (15.4)	6 (24)	
≥3	2 (15.4)	7 (28)	
Hospital stay, days (median±IQR)	9 (7.5 – 11)	11.5 (8 – 22)	0.036
Grade III-V complications [@] (%)	7 (53.8)	13 (52)	1.000
ICU admission (%)	3 (23.1)	7 (26.9)	1.000
In-hospital mortality (%)	1 (7.7)	2 (8.0)	1.000
Peak ALT, U/L (median±IQR)	273 (142.5 – 641.5)	456 (289 – 784)	0.152
Peak INR (median±IQR)	1.19 (1.12 – 1.31)	1.30 (1.17 – 1.41)	0.411
Peak total bilirubin, μmol/L (median±IQR)	17 (14 – 34)	32 (19 – 47)	0.129

Formatted: No underline, Font color: Auto, English (United States)

Formatted: No underline, Font color: Auto, English (United States)

Formatted: English (United States)

Table 2. Clinical outcomes.

Designates the number of resected Couinaud liver segments. & Patients were subjected to continuous or intermittent vascular inflow occlusion as specified in Supplemental Table S4. [Details on the resected liver segments can be found in Supplemental Tables S4 and S5.](#) @ Complications were scored according to the Clavien-Dindo classification^{43,44}. A histopathological assessment of the resection specimens is included in Supplemental Table S4. CTRL=control group; I/R=ischemia/reperfusion group; ALT=aspartate alanine aminotransferase; ICU=intensive care unit; INR=international normalized ratio; IQR=interquartile range; min=minutes. Categorical data were analyzed using Fisher's exact test (binary data) and Chi-square test (>2 variables). Differences between numerical variables were assessed using student's t-tests.

Figure 1
[Click here to download high resolution image](#)

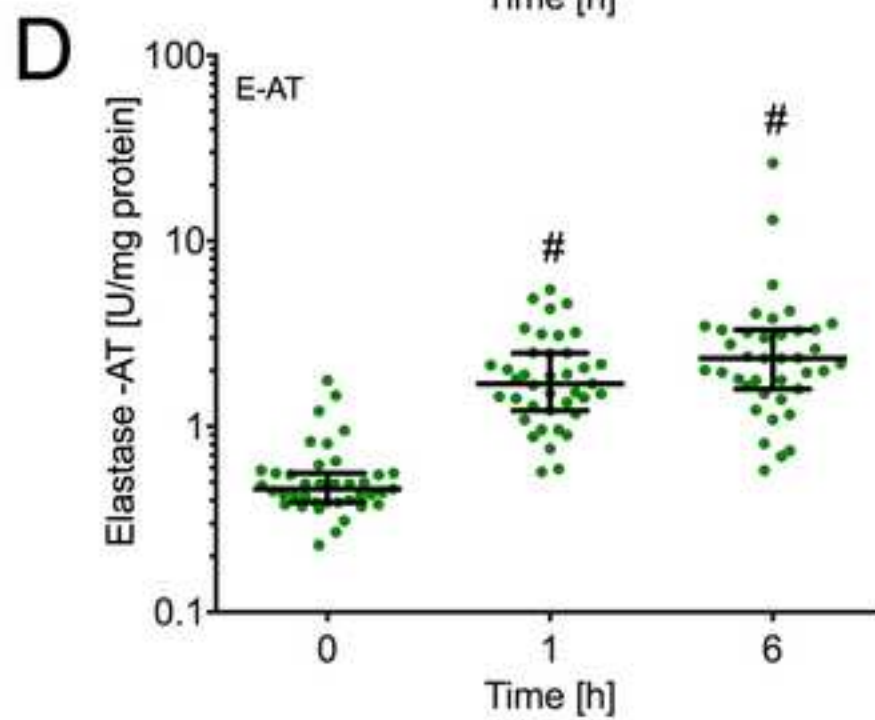
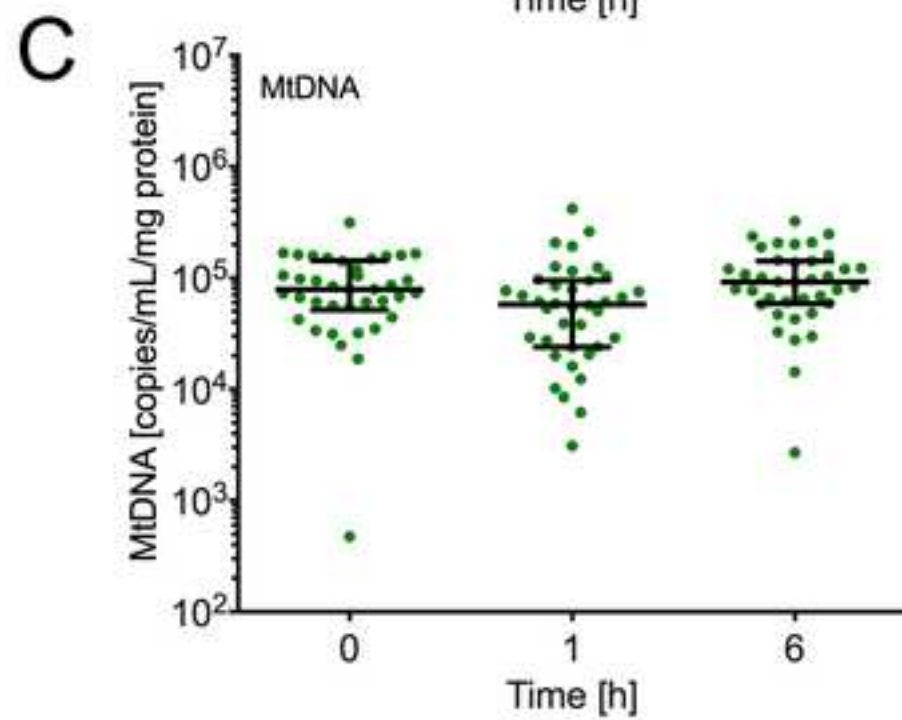
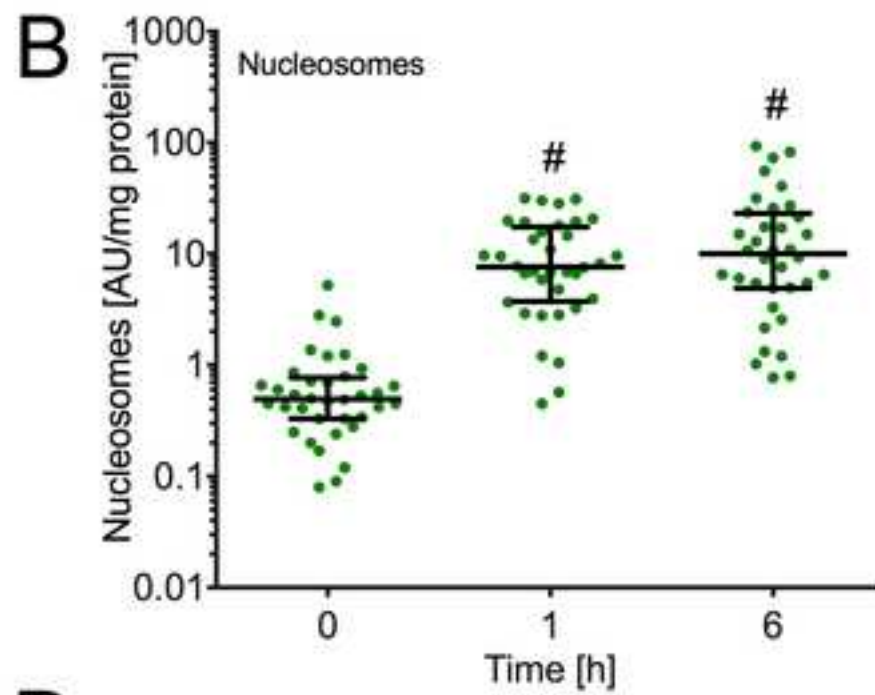
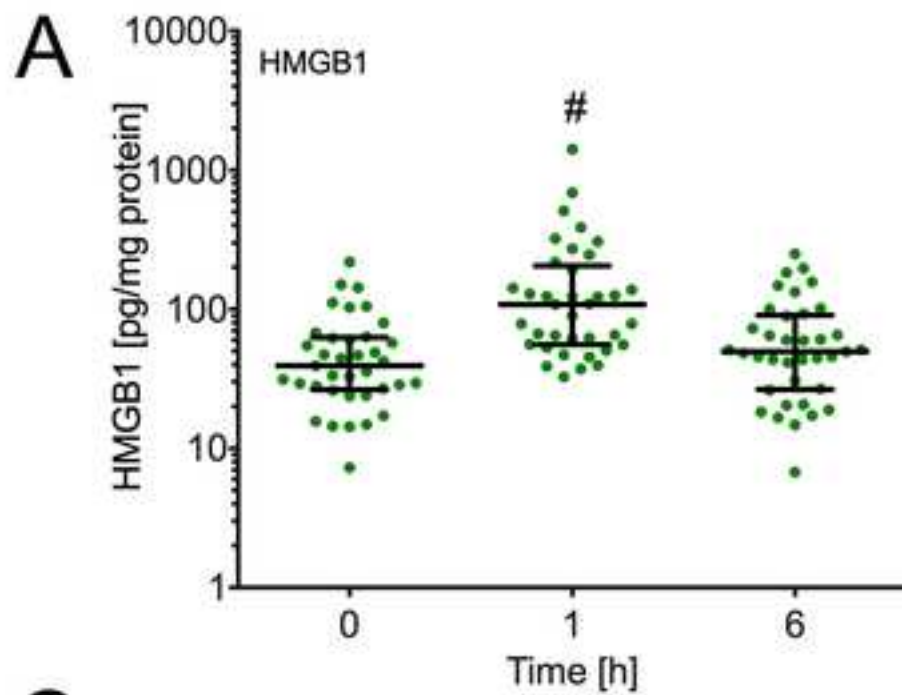


Figure 2
[Click here to download high resolution image](#)

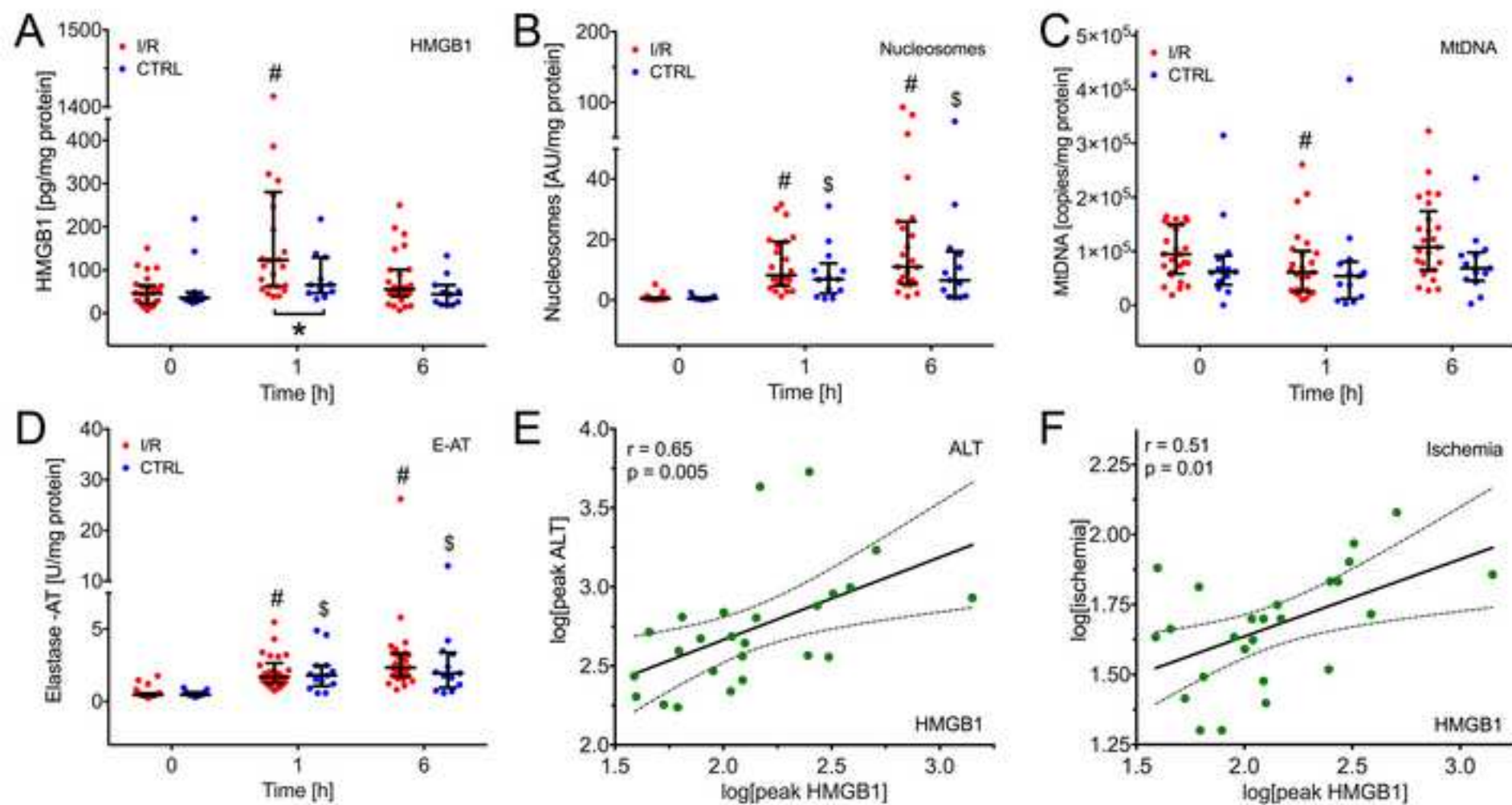


Figure 3
[Click here to download high resolution image](#)

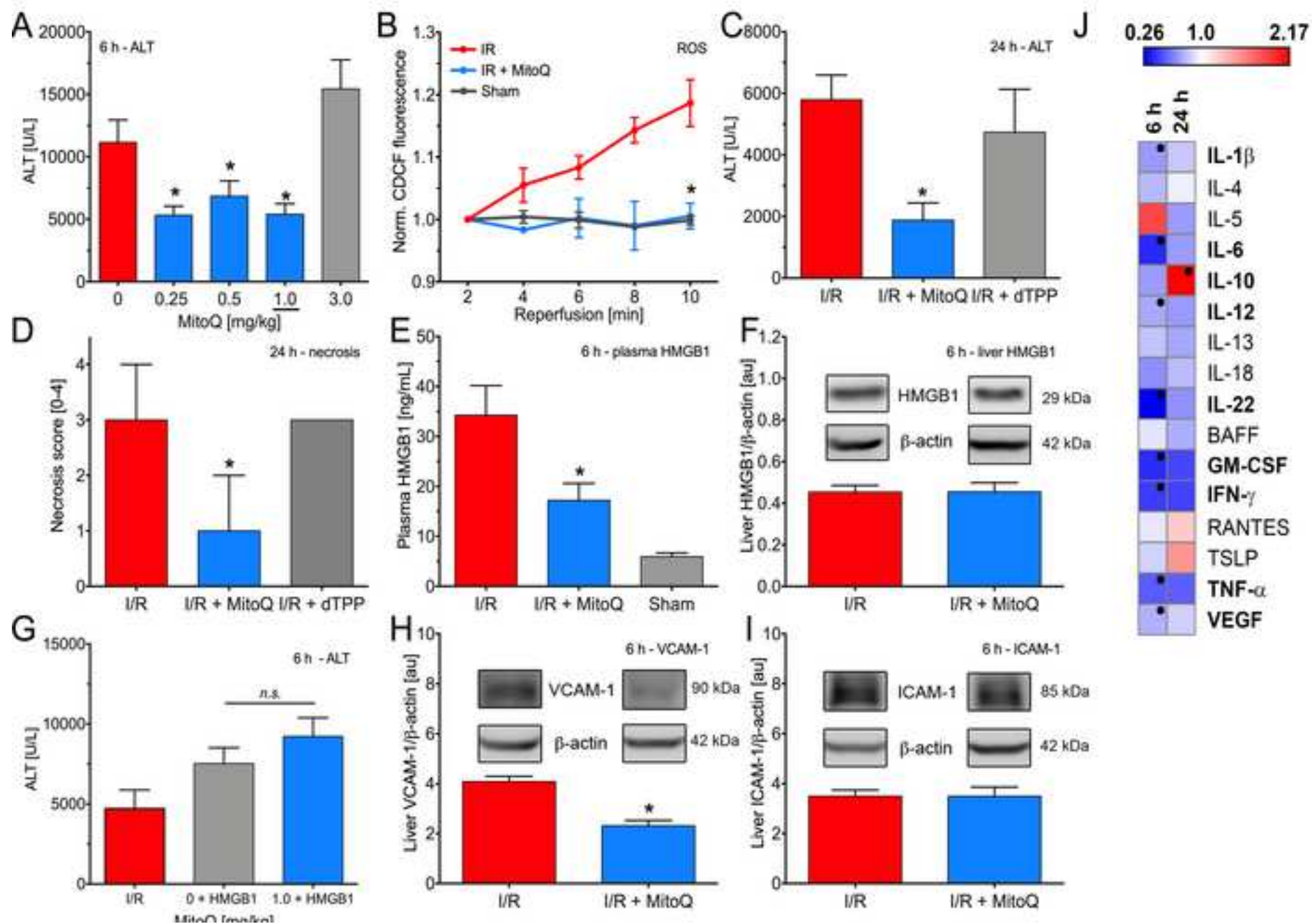


Figure S1

[Click here to download high resolution image](#)

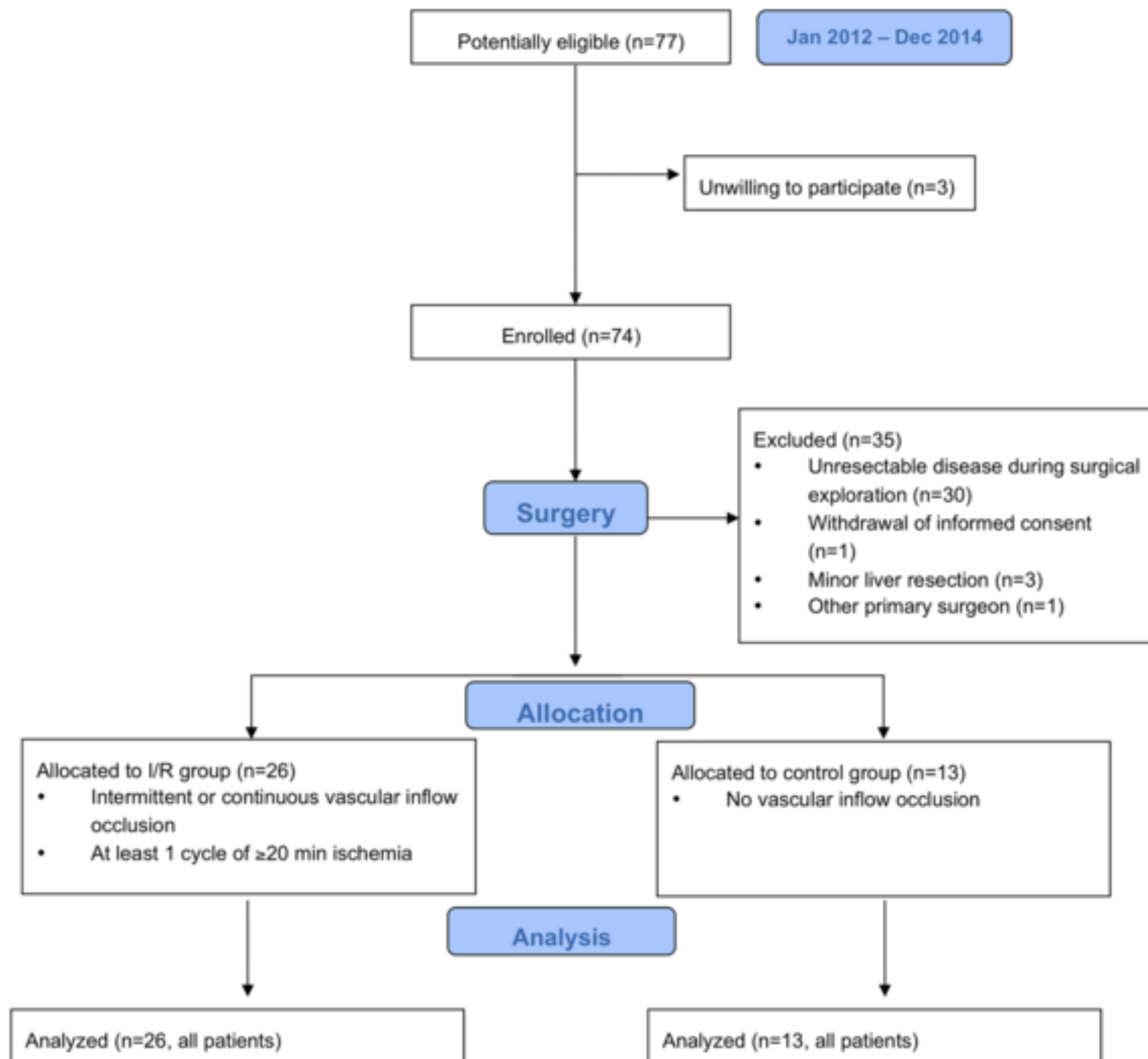


Figure S2

[Click here to download high resolution image](#)

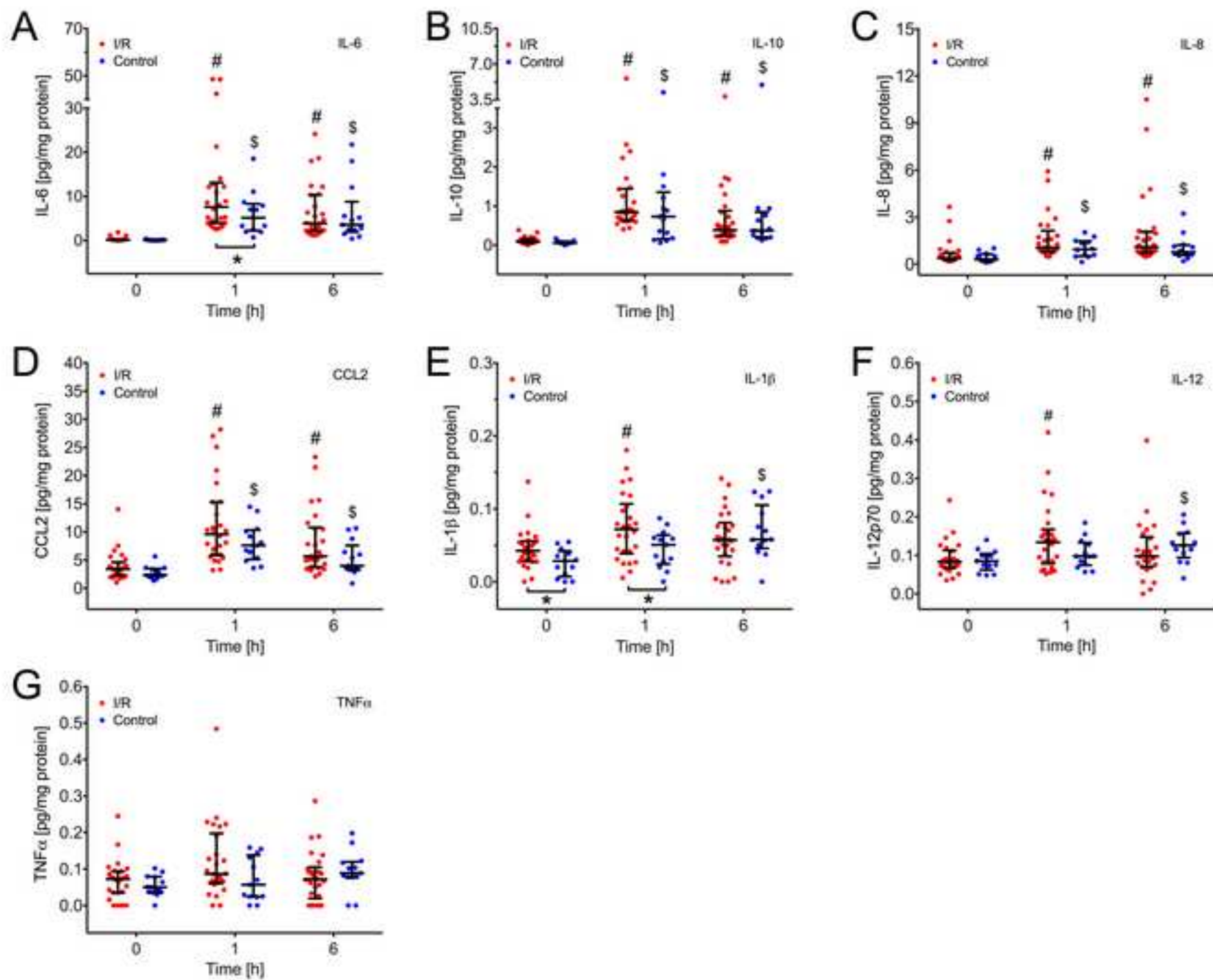


Figure S3
[Click here to download high resolution image](#)

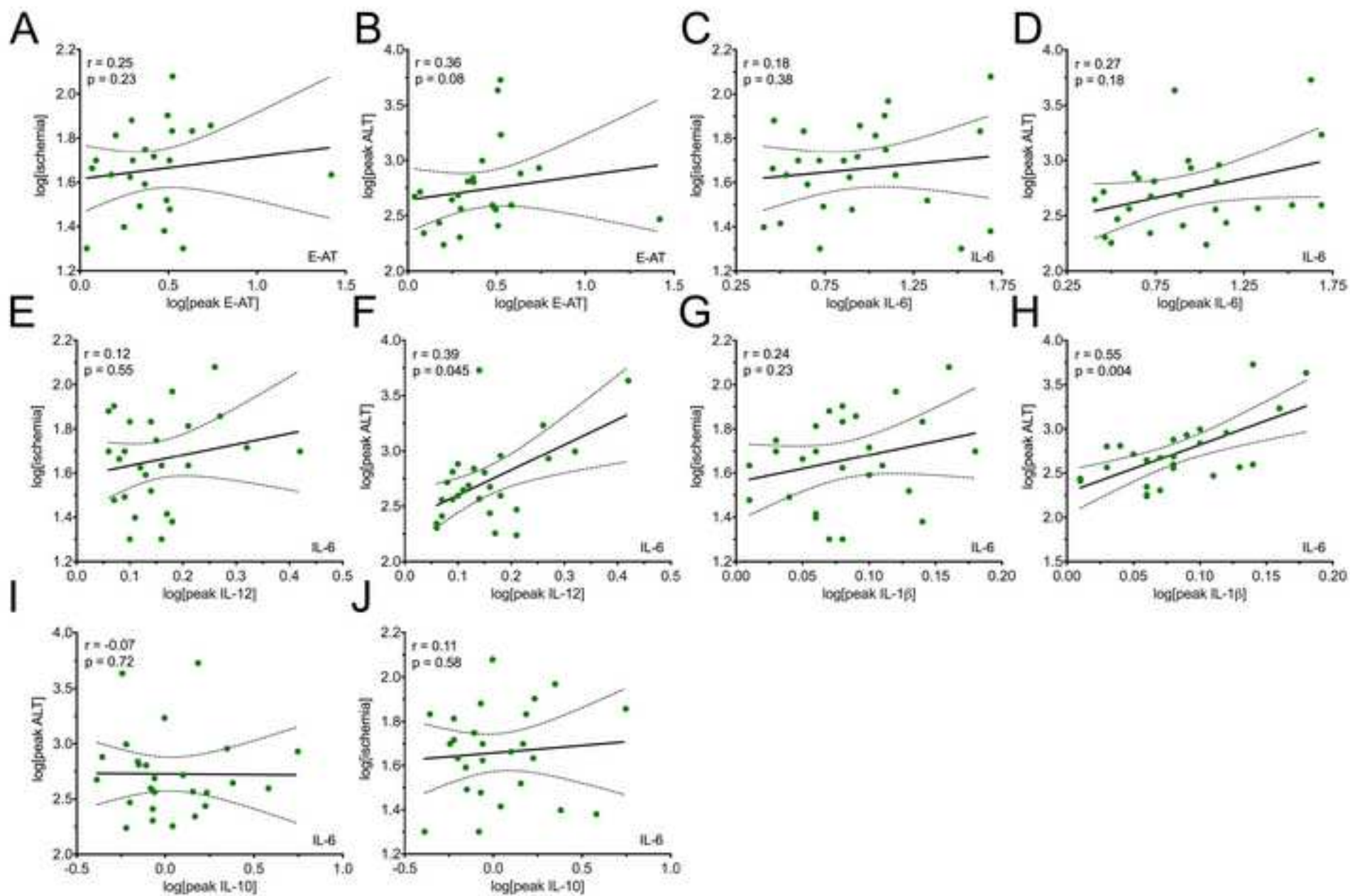


Figure S4
[Click here to download high resolution image](#)

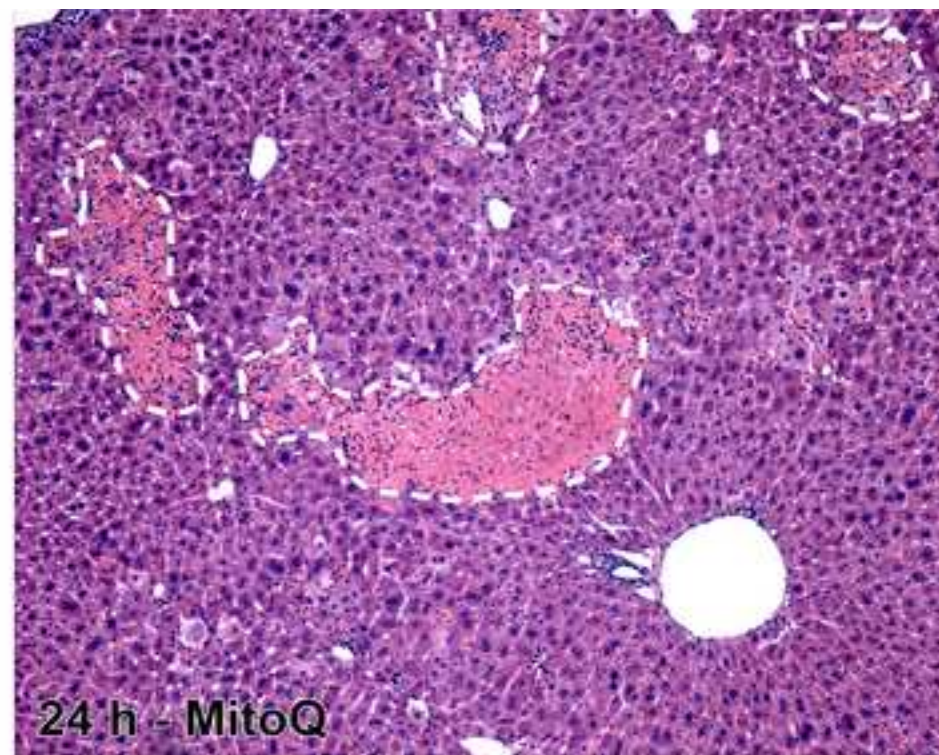


Figure S5
[Click here to download high resolution image](#)

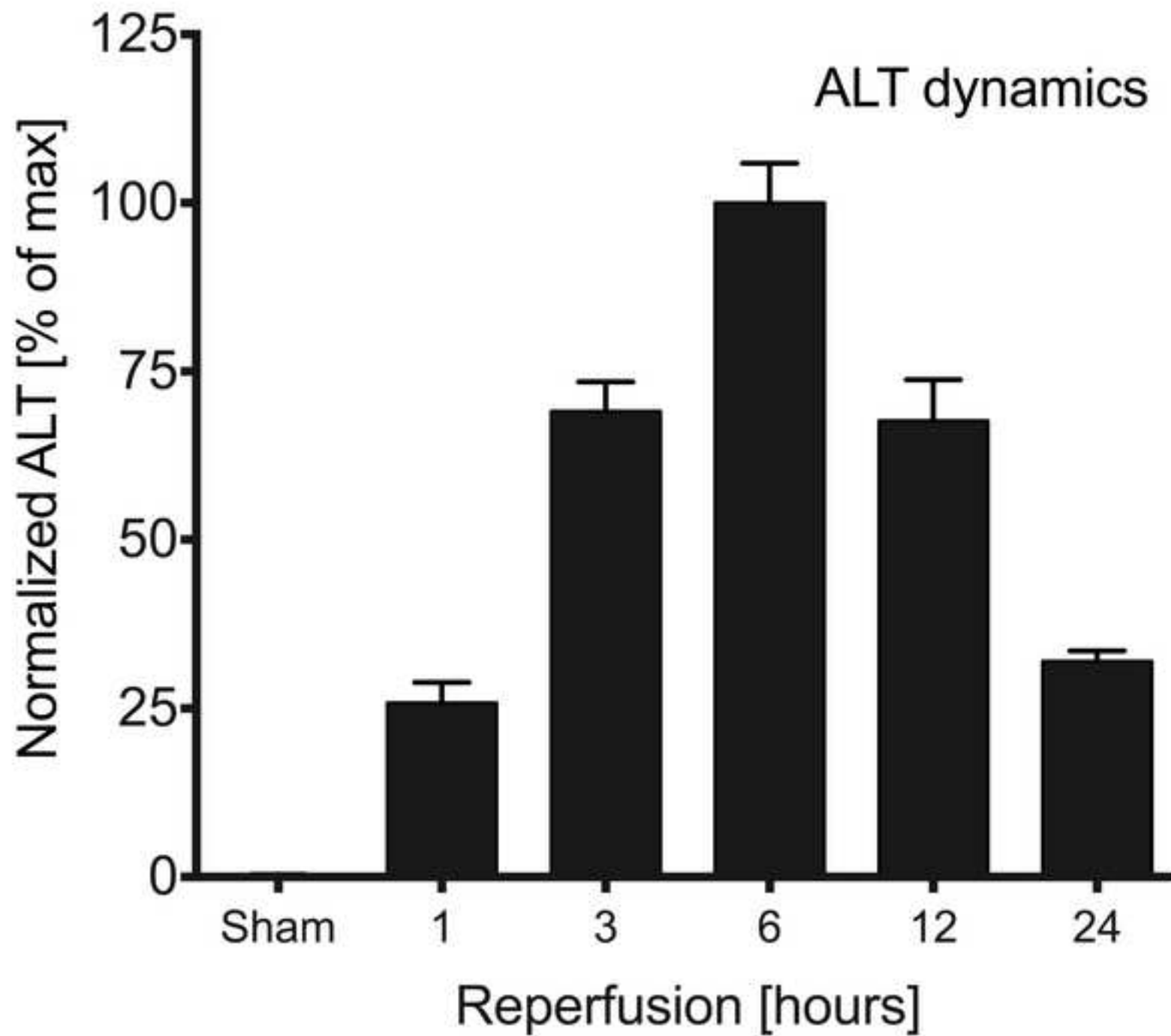


Figure S6

[Click here to download high resolution image](#)

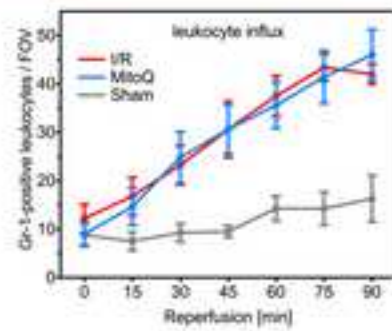
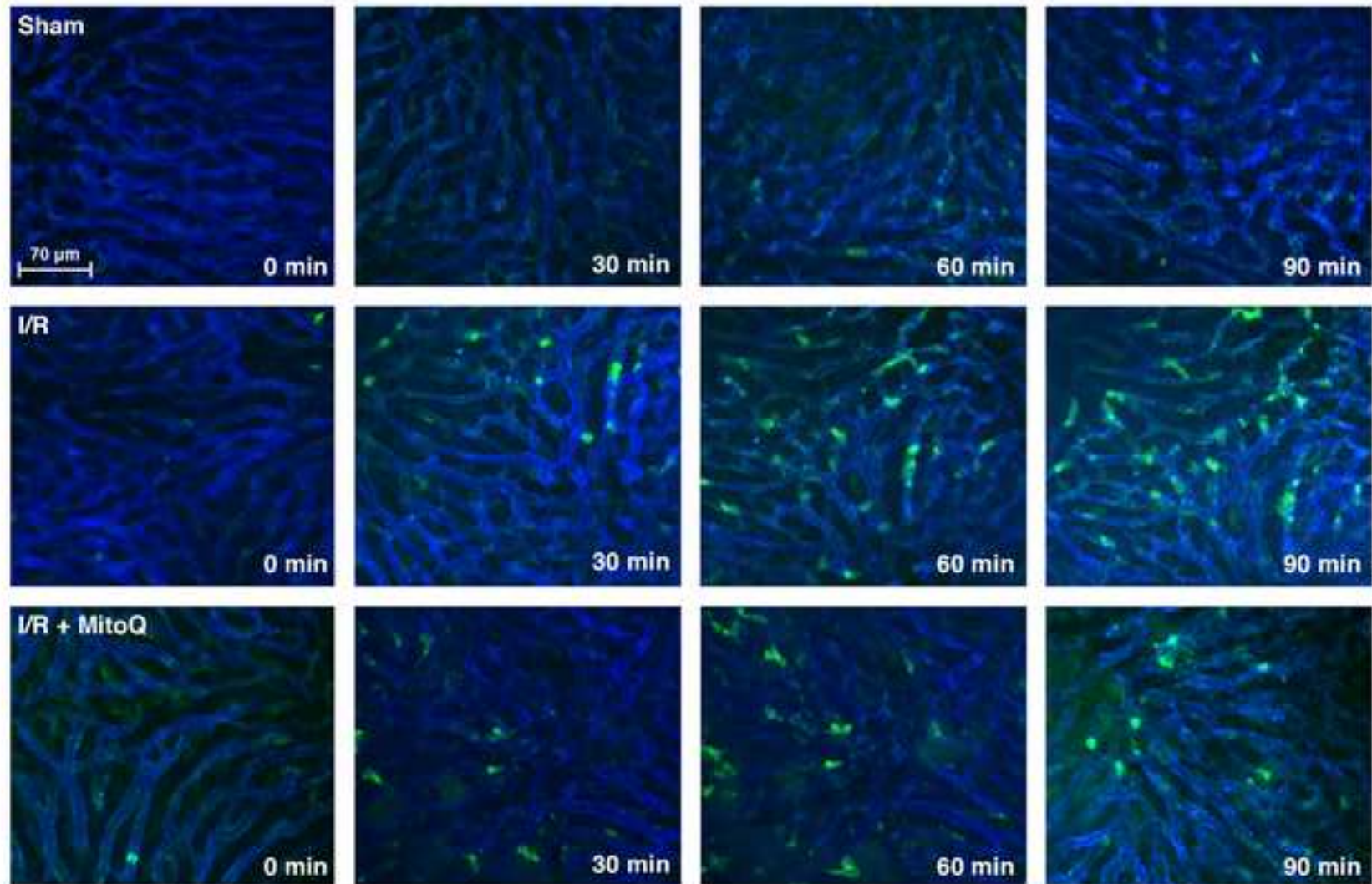


Figure S7

[Click here to download high resolution image](#)

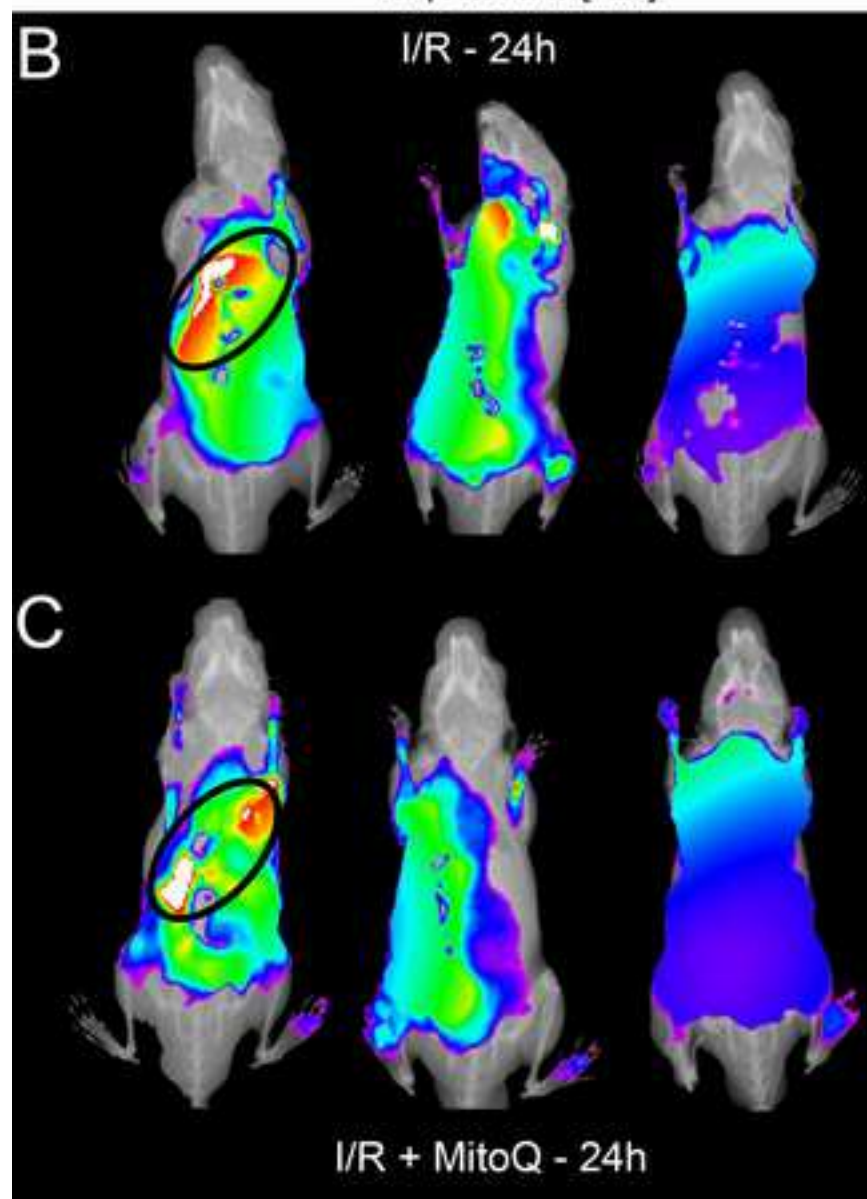
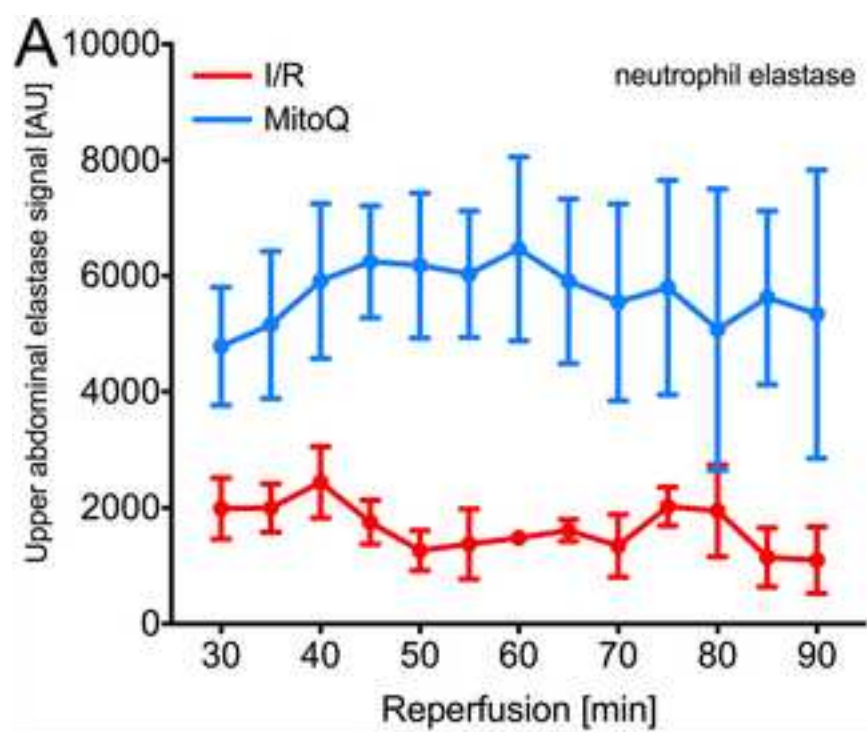


Table 1

		CTRL (N=13)	I/R (N=26)	p-value
Age (years, median ± IQR)		62 (45 – 73)	66 (53 – 70)	0.670
Gender, male (n, %)		8 (62)	18 (69)	0.725
BMI (median ± IQR)		25.2 (22.9 – 26.3)	23.9 (20.9 – 26.8)	0.418
ASA score (n, %)	I	3 (23)	6 (23)	0.153
	II	10 (77)	14 (54)	
	III	0 (0)	6 (23)	
Diagnosis (n, %)	CRC metastasis	1 (9)	4 (15)	0.132
	PHCC	3 (23)	13 (50)	
	IHCC	2 (15)	2 (8)	
	HCC	2 (15)	3 (12)	
	Benign	3 (23)	3 (12)	
	Other	2 (15)	1 (3)	
Preoperative chemotherapy, yes (n, %)		2 (15)	4 (15)	1.000
Biliary drainage, yes (n, %)		3 (23)	9 (35)	0.714
PVE, yes (n, %)		1 (8)	1 (4)	1.000
ALT baseline, U/L (median ± IQR)		30 (25 – 52)	53 (24 – 71)	0.294
AST baseline, U/L (median ± IQR)		32 (28 – 52)	45 (28 – 73)	0.178
Total bilirubin baseline, uM/L (median ± IQR)		9 (6 – 14)	7 (5 – 14)	0.471
INR baseline (median ± IQR)		1.0 (1.0 – 1.1)	1.0 (1.0 – 1.1)	0.676

Table 1. Baseline characteristics

Shown are the baseline characteristics of the control (CTRL) and ischemia/reperfusion (I/R) groups.

ALT=alanine aminotransferase; ASA=American Society of Anesthesiologists; AST=aspartate aminotransferase; BMI=body mass index; CRC=colorectal cancer metastases; HCC=hepatocellular carcinoma; IHCC=intrahepatic cholangiocarcinoma; INR=international normalized ratio;

IQR=interquartile range; PHCC=perihilar cholangiocarcinoma; PVE=portal vein

embolization Categorical data were analyzed using Fisher's exact test (binary data) and Chi-square test (>2 variables). Differences between numerical variables were assessed using student's t-tests.

Table 2

	CTRL (N=13)	I/R (N=26)	p-value
Resected segments [#] (%)			0.131
3	6 (46.2%)	5 (19.2%)	
≥4	7 (53.8%)	21 (80.8%)	
Resection time, min (median±IQR)	59 (41.5 – 71.5)	82 (60 – 130)	0.006
Duration of ischemia ^{&} min (median±IQR)	N/A	48 (31 – 68)	
Duration of surgery, min (median±IQR)	306 (261 – 373.5)	460 (380 – 503)	0.001
Transfusion requirement, units (%)			0.455
0	9 (62.9)	12 (48)	
1-2	2 (15.4)	6 (24)	
≥3	2 (15.4)	7 (28)	
Hospital stay, days (median±IQR)	9 (7.5 – 11)	11.5 (8 – 22)	0.036
Grade III-V complications [@] (%)	7 (53.8)	13 (52)	1.000
ICU admission (%)	3 (23.1)	7 (26.9)	1.000
In-hospital mortality (%)	1 (7.7)	2 (8.0)	1.000
Peak ALT, U/L (median±IQR)	273 (142.5 – 641.5)	456 (289 – 784)	0.152
Peak INR (median±IQR)	1.19 (1.12 – 1.31)	1.30 (1.17 – 1.41)	0.411
Peak total bilirubin, μmol/L (median±IQR)	17 (14 – 34)	32 (19 – 47)	0.129

Table 2. Clinical outcomes.

Designates the number of resected Couinaud liver segments. & Patients were subjected to continuous or intermittent vascular inflow occlusion as specified in Supplemental Table S1.

@ Complications were scored according to the Clavien-Dindo classification [Dindo 2004]. A histopathological assessment of the resection specimens is included in Supplemental Table

S4. CTRL=control group; I/R=ischemia/reperfusion group; ALT=aspartate alanine

aminotransferase; ICU=intensive care unit; INR=international normalized ratio;

IQR=interquartile range; min=minutes. Categorical data were analyzed using Fisher's exact

test (binary data) and Chi-square test (>2 variables). Differences between numerical variables were assessed using student's t-tests.

SUPPLEMENTAL INFORMATION

The damage-associated molecular pattern HMGB1 is released early after clinical hepatic ischemia/reperfusion

Rowan F. van Golen¹. Megan J. Reiniers¹. Gerben Marsman². Lindy K. Alles¹. Derrick M. van Rooyen³. Björn Petri^{4,5,6}. Vincent A. Van der Mark^{1,7}. Adriaan A. van Beek⁸. Ben Meijer⁸. Martinus A. Maas¹. Sacha Zeerleder^{2,10}. Joanne Verheij⁹. Geoffrey C. Farrell³. Brenda M. Luken². Narci C. Teoh³. Thomas M. van Gulik¹. Michael P. Murphy¹¹. Michal Heger^{1*}

1 Department of Experimental Surgery. Academic Medical Center. University of Amsterdam. Amsterdam. the Netherlands

2 Department of Immunopathology. Sanquin Research and Landsteiner Laboratory. Academic Medical Center. University of Amsterdam. Amsterdam. the Netherlands

3 Liver Research Group. Australian National University at The Canberra Hospital. Canberra. Australia

4 Department of Microbiology, Immunology, and Infectious Diseases. Cumming School of Medicine. University of Calgary. Calgary AB T2N 1N4. Alberta. Canada

5 Department of Physiology and Pharmacology. Cumming School of Medicine. University of Calgary. Calgary AB T2N 1N4. Alberta. Canada

6 Snyder Institute for Chronic diseases. University of Calgary. Calgary. Canada

7 Tytgat Institute for Gastrointestinal and Liver Research. Academic Medical Center. University of Amsterdam. Amsterdam. the Netherlands

8 Department of Cell Biology and Immunology. Wageningen University. Wageningen. the Netherlands

9 Department of Pathology. Academic Medical Center. University of Amsterdam. Amsterdam. the Netherlands

10 Department of Hematology. Academic Medical Center. University of Amsterdam. Amsterdam. the Netherlands

11 Medical Research Council Mitochondrial Biology Unit. Cambridge. United Kingdom

*Corresponding author:

Michal Heger

Department of Experimental Surgery

Academic Medical Center

University of Amsterdam

Meibergdreef 9

1105 AZ Amsterdam. the Netherlands

(T) +31 20 5665573

(F) +31-20-6976621

(E) m.heger@amc.uva.nl

SUPPLEMENTARY MATERIALS AND METHODS

S1.1 Histological assessment of surgical resection specimens

Liver tissue from the surgical resection specimen was harvested at a distance of the tumor site and processed for histological analysis as part of routine clinical care. Histological analysis was performed by a hepatopathologist (JV). Due to the known heterogeneity in parenchymal status between the resected liver and the remnant liver, in particular in patients with hilar cholangiocarcinoma, the results of the histopathological analysis are presented in a descriptive manner in Supplemental Table S2.

S1.2 Intravital spinning disc confocal microscopy of neutrophil dynamics after mouse liver I/R

Experiments were approved by the animal ethics committee of the University of Calgary (protocol #AC12-0162) and all animals were treated in accordance with¹. Male C57BL/6J mice (N = 14, Charles River, Montreal, Quebec, Canada) weighing between 20-26 g were housed under standard laboratory conditions with unrestricted access to chow and water. The animals were acclimated for at least 2 d before entering the experiment. Surgical and intravital imaging procedures were as described². Antibodies and MitoQ were added to sterile 0.9% NaCl (B. Braun Melsungen, Melsungen, Germany) to a final infusion volume of 100 μ L. The used antibodies and antibody concentrations were: sinusoidal endothelial cells: rat anti-mouse CD31-PE, 10 μ L of 200 μ g/mL (cat. # 12-0311-83, clone 390, eBioscience, San Diego, CA); neutrophils: rat anti-mouse Ly-6G (Gr-1)-Alexa Fluor 647, 10 μ L of 500 μ g/mL (cat. # 127610, clone 1A8, BioLegend). The mixture was infused into the penile vein immediately before surgery. Hepatic I/R was subsequently induced as described in the Materials and Methods section of the main text. Intravital spinning disc confocal microscopy was performed with a Quorum Wave FX-X1 spinning disk confocal system as described in². The following emission filters were used for the antibody-conjugated fluorophores: 593 \pm 40 (CD31-PE) and 692 \pm 40 (Gr1-Alexa Fluor 647), respectively. Imaging was performed with an Olympus UPlanFL-N, 10 \times , NA = 0.2 objective. The hardware settings were kept constant during all experiments (PE channel: laser power 71, exposure time 120 ms, camera gain 1, camera sensitivity 224; Alexa Fluor 647 channel: laser power 100, exposure time 120 ms, camera gain 1, camera sensitivity 174). Image acquisition was performed under Volocity software control (Version 6.3.1.

Perkin Elmer, Waltham, MA). Image acquisition was performed for 1 min at a frame rate of 13 Hz per fluorescence channel after the start of reperfusion (the time interval between clip removal and image acquisition was on average 4 min) and at $t = 4 + 15, 30, 45, 60, 75,$ and 90 min reperfusion. The number of neutrophils per field of view was manually counted using ImageJ/FIJI (NIH, Bethesda, MD) software.

S1.3 Non-invasive whole body imaging of intrahepatic neutrophil elastase activity

Non-invasive whole body imaging was performed using an InVivoXtreme 4MP (BRUKER, formerly Carestream, USA). Mice were shaved and depilated 24 h prior to imaging. Neutrophils were labelled 4 h prior to imaging via tail vein injection using Neutrophil Elastase 680 FAST (Perkin Elmer) according to the manufacturer's protocol (4 nmol dye/mouse in 100 μ l of saline) and visualized using 650 nm excitation and 700 nm emission wavelength filters. Mice were imaged ventrally from 30 min until 90 min post I/R with or without MitoQ treatment in 5-min intervals. In addition, animals were imaged 24 h post-I/R. During the whole imaging procedure the mice were anesthetized with isoflurane and kept at 37 °C in a ventilated imaging chamber. The imaging protocol for each time point contained three steps: 1. reflectance imaging (2 s exposure time), 2. fluorescence imaging at 650/700 nm (4 s exposure time), and 3. X-ray imaging (10 s exposure time). The imaging protocol for each 25-degree angle of the 360-degree spin contained two steps: 1. Fluorescence imaging at 650/700 nm (2 s exposure time) and 2. X-ray imaging (10 s exposure time). Images were quantified with Bruker molecular imaging software (version 7.1.3.20550) using a constant ventral region of interest for all animals that covered the upper ventral abdominal area in the anatomical region of the murine liver.

SUPPLEMENTARY FIGURES AND RESULTS

Figure S1 – CONSORT study flow chart

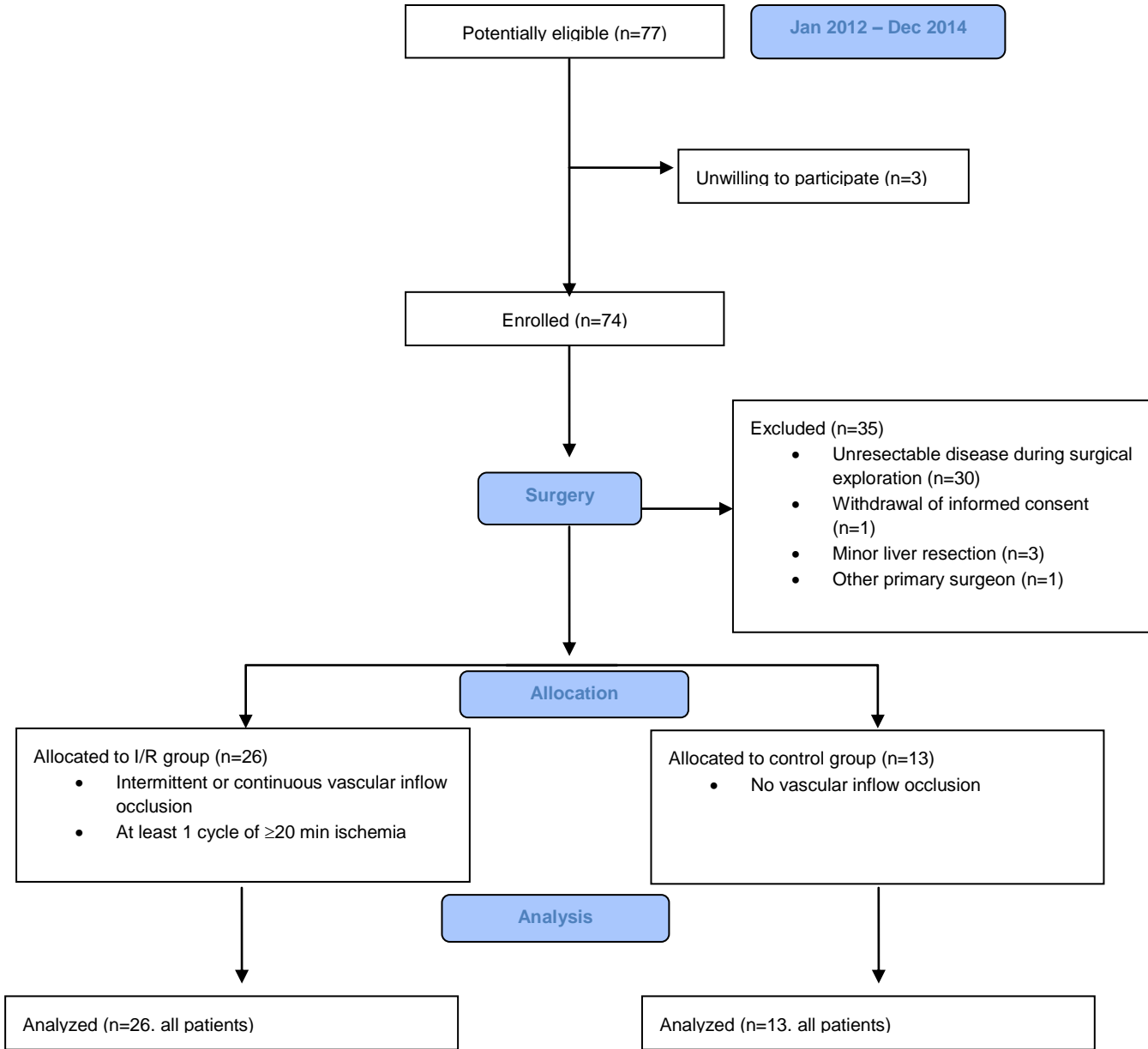
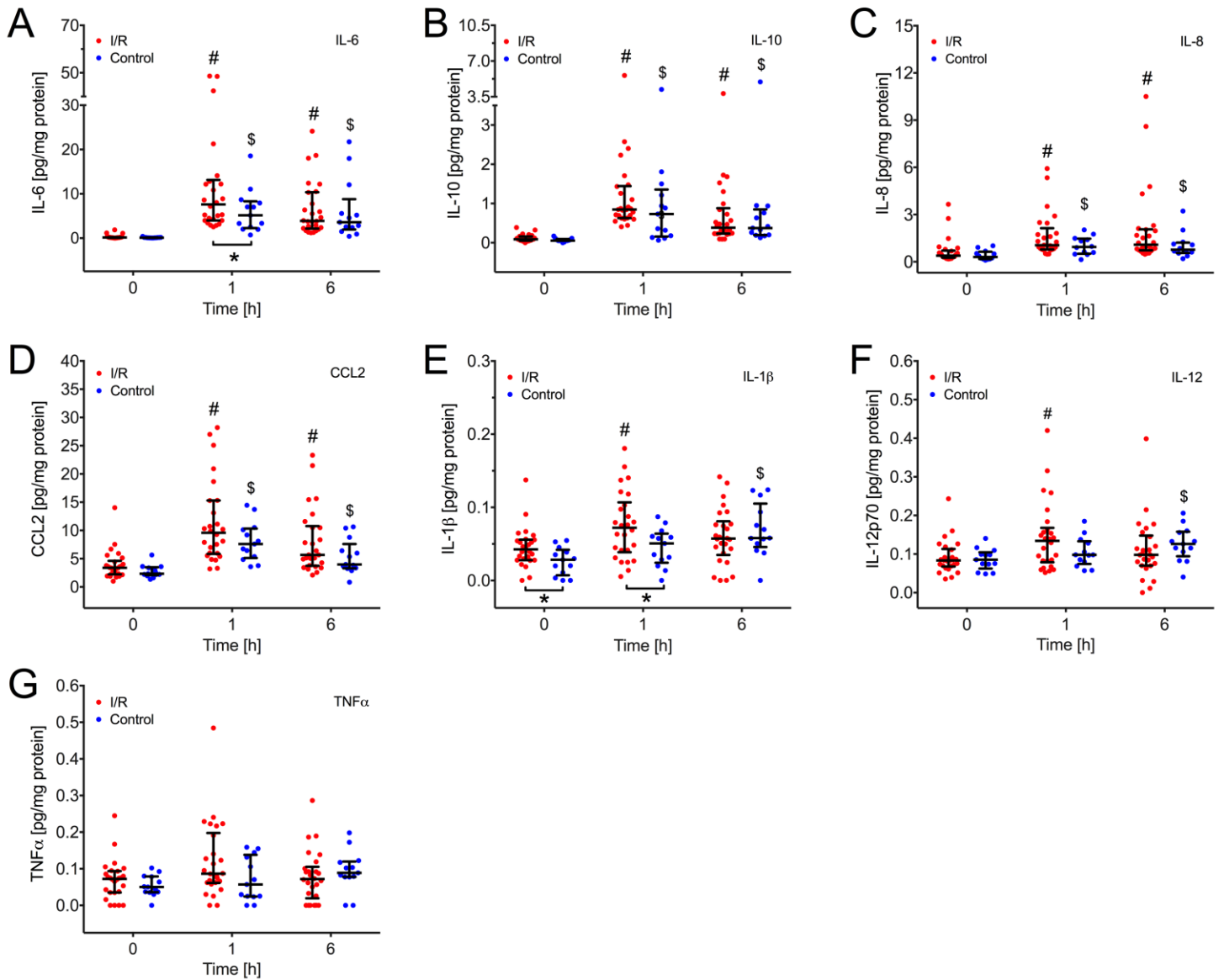


Figure S2. Plasma cytokine and chemokine levels after clinical liver I/R

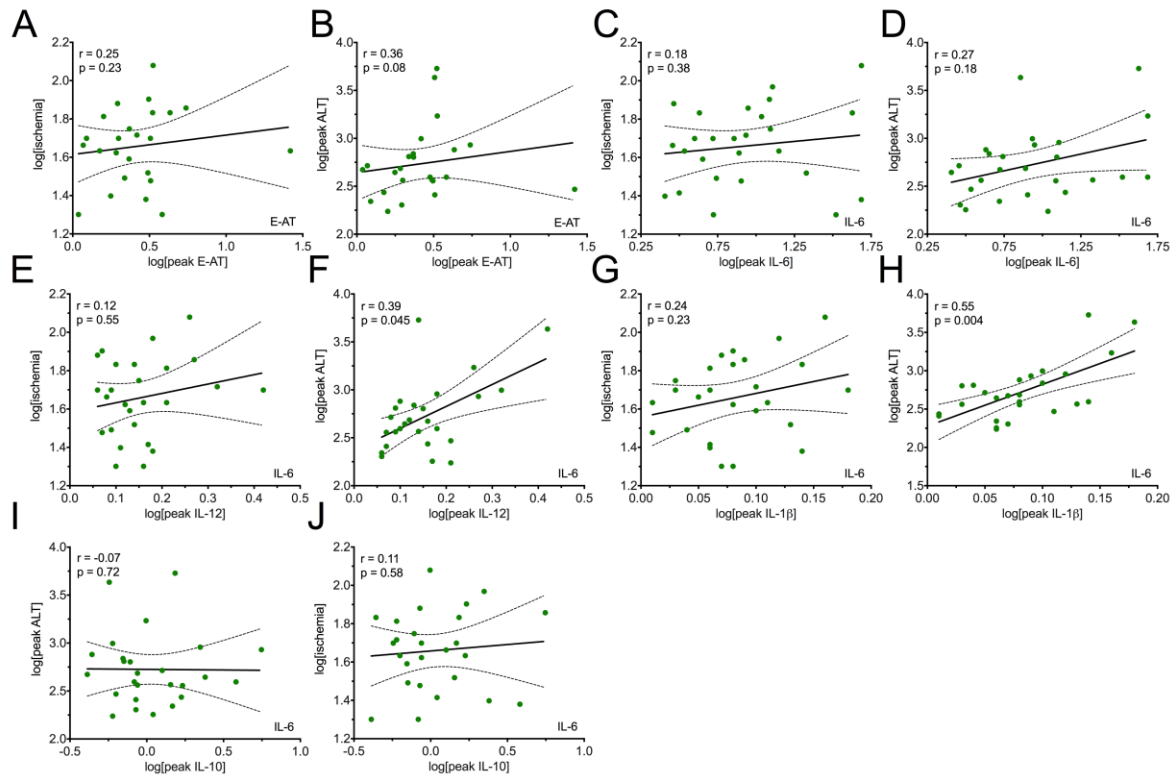


Cytokine and chemokine signalling has been extensively studied in pre-clinical liver I/R models³ but data on the (early) release of pro-inflammatory mediators following clinical liver I/R are scarce.

A shows that the increase in the cytokine interleukin (IL)-6 was more pronounced in the I/R group at 1 h of reperfusion than in the control group. This difference was not detectable at 6 h of reperfusion. **B** indicates that the anti-inflammatory cytokine IL-10 increased in both study groups during the first 6 h of reperfusion, without intergroup differences. **C** and **D** indicate that the monocyte chemoattractant CCL2 and neutrophil chemoattractant IL-8 are released into the circulation immediately following major liver resection, irrespective of the intraoperative use of liver I/R. In contrast, an early (i.e., at 1 h of reperfusion) but transient rise in plasma IL-12 and IL-1 β levels was only noted in the I/R group, whereas this response

was delayed until 6 h after surgery in the control group (**E-F**). Last, **G** shows that plasma levels of $\text{TNF}\alpha$ remained at baseline in both study arms during the entire study period, which not only contradicts a large body of pre-clinical I/R literature, but is also surprising given the importance of $\text{TNF}\alpha$ in stimulating liver regeneration following partial hepatectomy^{4,5}. The functional relevance of these differences in the release of cytokines between patients subjected to major hepatectomy with and without VIO remains to be elucidated experimentally. Plasma cytokine levels were measured as described in the main text and normalized to plasma total protein content to correct for perioperative hemodilution⁶. Intragroup differences between the three time points were analysed using a repeated measurements ANOVA (normally distributed data) or a Friedman test (non-normal data). Differences between the VIO and control group at a given time point (intergroup differences) were assessed using a student's t-test (normally distributed data) or Mann Whitney U-test (non-normal data). See the main text for additional details. # indicates $p < 0.05$ versus $t=0$ in the VIO group. \$ indicates $p < 0.05$ versus $t=0$ in the control group, and * indicates $p < 0.05$ between the study groups indicated by the solid line. CCL2 = chemokine (C-C motif) ligand 2; IL-1 β = interleukin 1 beta; IL-8 = interleukin 8; IL-12 = interleukin 12; $\text{TNF}\alpha$ = tumour necrosis factor alpha; VIO = vascular inflow occlusion

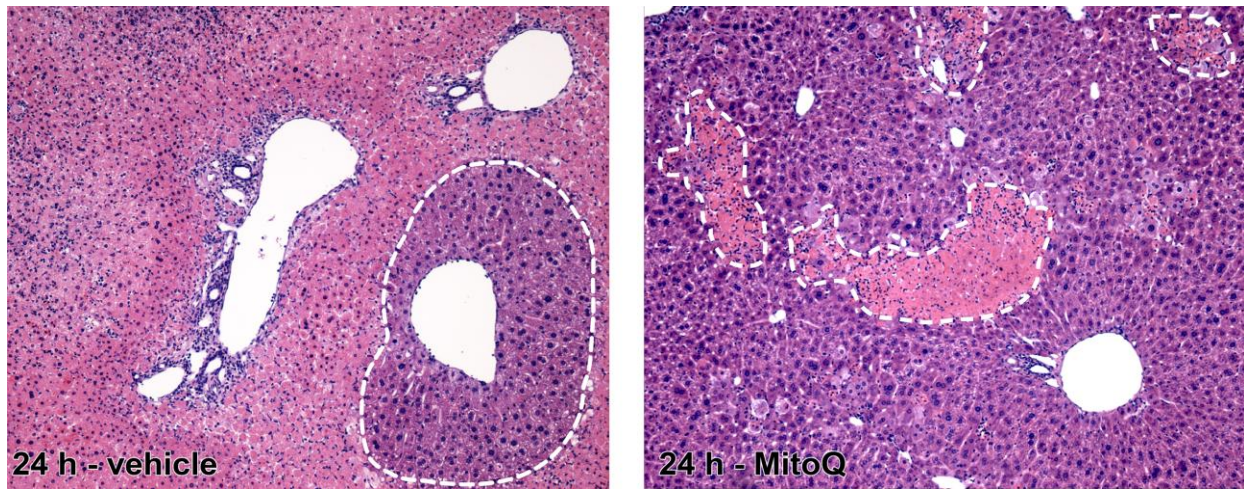
Figure S3. The duration of liver ischemia and post-operative liver injury markers do not correlate to neutrophil activation, IL-6 release, or IL-10 release in clinical liver ischemia/reperfusion injury



It was shown in Figure 1 of the main text that DAMPs (i.e., HMGB1 and nucleosomes) and cytokines (i.e., IL-6 and IL-10) are released into the circulation following major liver surgery. Of the measured parameters, only plasma HMGB1 and IL-6 concentrations increased more profoundly in patients exposed to I/R (i.e., the VIO group) than in the control group (Figure 1E and I). More importantly, postoperative plasma HMGB1 levels correlated positively to the duration of liver ischemia and postoperative ALT release (Figure 1K and L), indicating that HMGB1 release is not only characteristic for ischemic liver injury, but also reflects the extent of parenchymal liver injury. Shown here are the same correlation analyses for the pro-inflammatory and/or mitogenic cytokines IL-6, IL-1 β , and IL-12, the anti-inflammatory cytokine IL-10^{7,8}, and the marker for neutrophil activation E-AT⁹. It is shown that, in contrast to HMGB1, the release of IL-6, IL-12, and IL-10 and the formation of E-ATs do not correlate to the duration of ischemia or postoperative ALT values. A weak association was observed between peak IL-12 and peak ALT levels (F) and a moderate association was observed between peak IL-1 β levels and postoperative ALT release (H). These parameters are therefore likely non-specific inflammatory markers released or formed in response to gross surgical trauma (i.e., liver resection), and, as such, probably hold little prognostic potential. Plasma E-AT and cytokine levels were measured as described in the main text. Correlations were assessed using Spearman's r and a p -value <0.05 was considered statistically

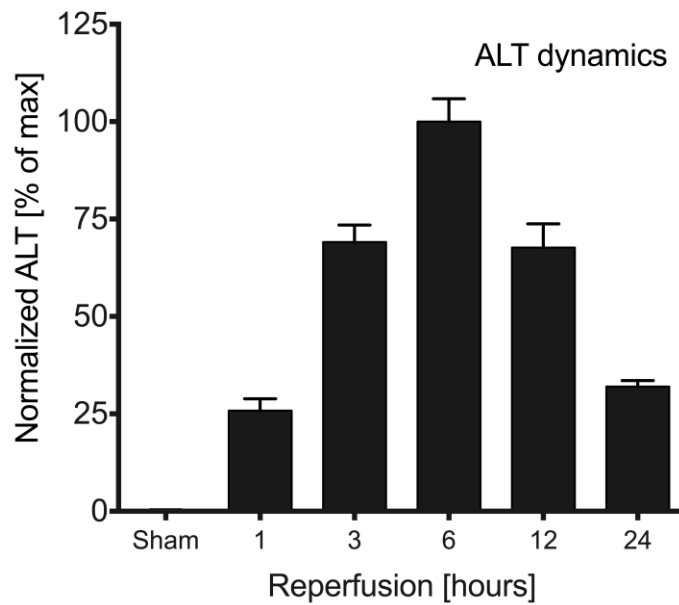
significant. ALT = aspartate alanine aminotransferase; IL-10 = interleukin 10; IL-6 = interleukin 6; HMGB1 = high mobility group box 1; E-AT = elastase- α 1-antitrypsin complexes.

Figure S4. MitoQ reduces hepatocellular necrosis at 24 h of reperfusion following mouse liver I/R.



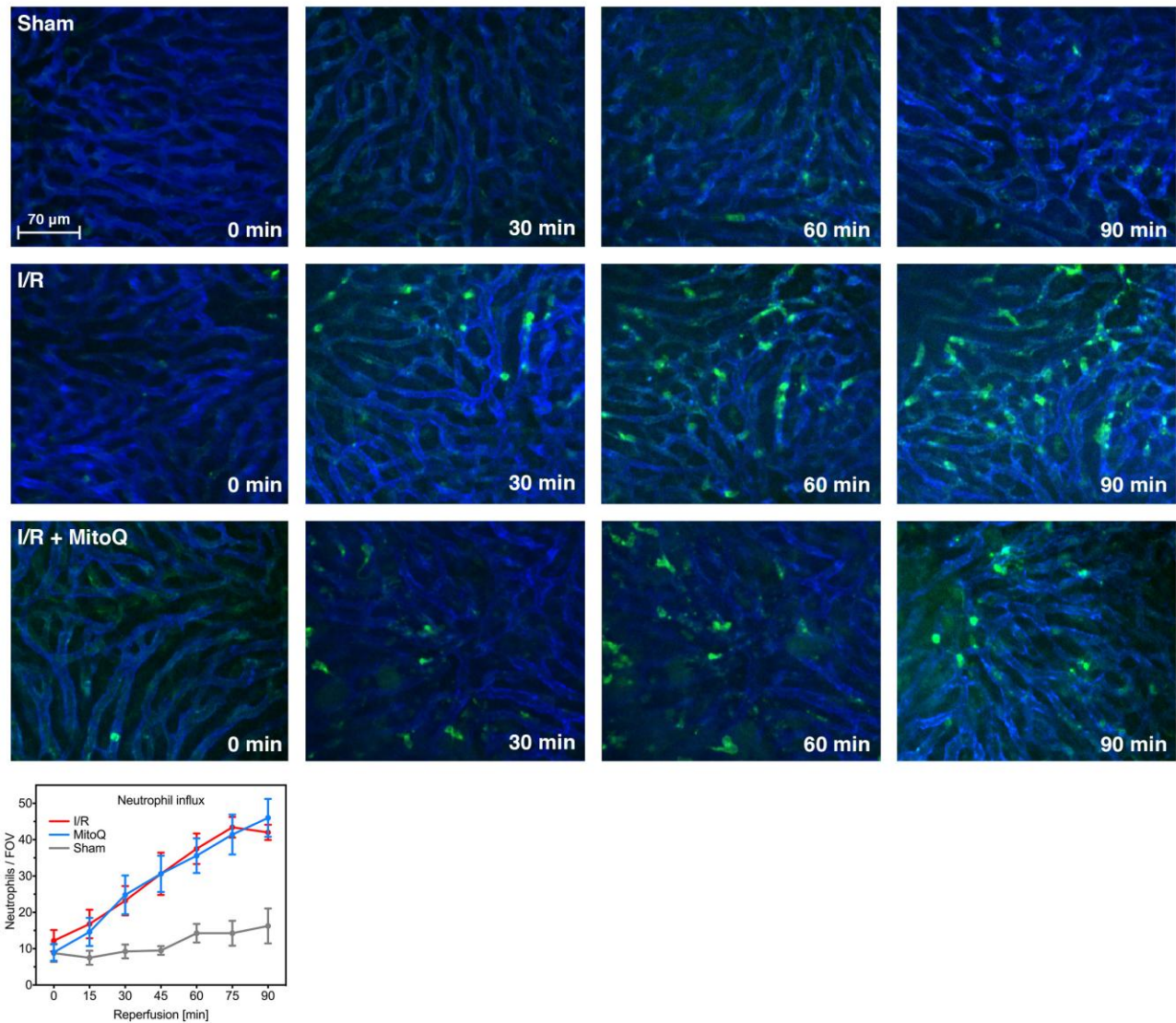
Shown are representative hematoxylin and eosin-stained histological slides of mouse livers harvested 24 h after 30 min of liver ischemia. Images were obtained with a 10x objective. Animals were either treated with sterile saline (vehicle, panel A) or 1 mg/kg of the mitochondria-targeted antioxidant MitoQ dissolved in sterile saline (panel B). A small area of remaining viable hepatocytes is encircled in white in panel A, indicating severe hepatocellular necrosis in I/R-subjected mice. In contrast, panel B shows only small patches of confluent necrosis, demarcated in white, at the same time point in MitoQ-treated animals (panel B), reflecting reduced hepatocellular necrosis in the MitoQ group. Histological quantification of necrotic areas per study arm is shown in Figure 3 of the main text.

Figure S5 – Hepatocellular injury peaks 6 h after partial liver ischemia in mice



Shown is hepatocellular injury (ALT release, y-axis) plotted as a function of reperfusion time (x-axis) following partial liver ischemia in mice. ALT values were normalized to the ALT peak values (i.e., the 6 h reperfusion time point). It should be noted that these data were generated in preliminary experiments with a more severe liver I/R model (60 min of ischemia) than is used in the main text (30 min ischemia). Besides the duration of ischemia, all experimental procedures were as described in the Materials and Methods section of the main text.

Figure S6. MitoQ does not influence the number of Gr-1-positive leukocytes circulating in the hepatic microvasculature during early reperfusion after mouse liver ischemia.

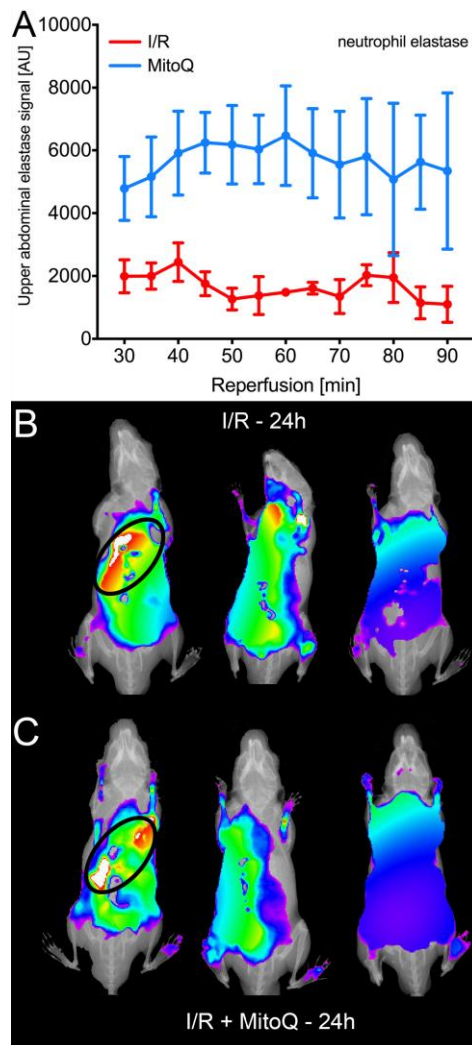


It was proposed in the main text that MitoQ ameliorates hepatic I/R injury by reducing ROS-mediated parenchymal cell death during the first minutes of reperfusion and, thereby, suppressing the release of pro-inflammatory HMGB1. The premise is supported by the reduction in I/R injury at 6 h and 24 h of reperfusion (main text). Because ROS can also propagate sterile inflammation by directly influencing leukocyte function¹⁰ and MitoQ is also taken up by leukocytes, intravital spinning disk confocal microscopy was used to investigate whether MitoQ treatment influenced the number of neutrophils circulating in early post-ischemic mouse livers. These experiments served to exclude an immediate and early effect of MitoQ on neutrophil behaviour (i.e., preceding the injury peak at 6 – 24 h of reperfusion) that could confound the premises raised in the main text. Shown are representative snapshots of leukocytes (in green, stained with anti-Gr1 antibodies) circulating in mouse sinusoids (in blue, stained with anti-CD31 antibodies). The number of GR-1-positive leukocytes per field of view (FOV) per time

point was manually counted for each animal. The traces per group are shown in the bottom panel of the figure.

As is shown in top row, sham surgery and manipulation of the mouse liver *per se* do not increase the number of Gr-1-positive leukocytes circulating in the liver microvasculature. In contrast, the number of Gr-1-positive leukocytes that pass through the liver rises steadily the first 90 min after I/R (middle row). Treatment with MitoQ (1 mg/kg) did not affect the number of circulating Gr-1-positive leukocytes during the first 90 min of reperfusion, indicating that the protective effects of MitoQ noted in Figure 3 of the main text are not attributable to direct effects on leukocyte trafficking. These data therefore support the premise raised in the main text that reducing oxidative injury in hepatocyte mitochondria during early reperfusion reduces the I/R injury peak, which follows several hours later, by limiting the release of HMGB1 and neutralizing early innate immune alarm signals. The experimental procedures are described in section S1.1.

Figure S7. MitoQ transiently increases neutrophil presence during early reperfusion after mouse liver ischemia



In extension of the intravital imaging of leukocyte accumulation (Fig. S7), neutrophil presence was additionally investigated during early (30-90 min. panel **A**) and late (24 h. panels **B** and **C**) reperfusion using non-invasive whole body fluorescence imaging in mice. Counterintuitively, elastase activity was higher during early reperfusion in MitoQ-treated animals (N=3. blue trace. mean±SEM) than in vehicle-treated mice (N=3. red trace. mean±SEM). This finding is difficult to rationalize inasmuch as the difference in neutrophil presence is already present at 30 min of reperfusion, but does not increase from that point onwards. The latter is surprising given the gradual increment in intrahepatic leukocytes numbers seen with intravital microscopy shown in Figure 2 and Figure S8.

In contrast to the early time point (panel A), the elastase signal at 24 h of reperfusion seemed comparable between groups or possibly even lower in MitoQ-treated mice (bottom 3 animals) than in the I/R group (top 3 animals). These data are in line with the improved liver histology and gross amelioration of innate immune activity shown in Figure 2 of the main text. It should however be noted that the hepatic specificity of probe fluorescence was difficult to ascertain in all animals at the 24 h time point (panels **B** and **C**, liver region encircled in black). Fluorescence data were therefore not quantified at this time point. All experimental procedures are detailed in section S1.2

SUPPLEMENTAL TABLES

Table S1 – Western blot antibodies

Antibody	Manufacturer	Cat #	Dilution
β -actin	Sigma-Aldrich	A5441	1:5000
HMGB1	Abcam	Ab18256	1:900
ICAM-1	R&D Systems	AF796	1:500
Pan-JNK-1/2	Cell Signaling	9258	1:1000
Phospho-JNK-1/2	Cell Signaling	4668	1:750
VCAM-1	R&D Systems	AF643	1:500

Supplementary Table S2 – Histopathological assessment of liver resection specimens. Liver tissue was obtained at a distance of the tumor and processed for histological analysis as part of routine clinical care. The results are provided in a descriptive manner due to the heterogeneity in histopathological profile between the resection specimen and the remnant liver. # lobular inflammation was categorized according to the number of inflammatory foci per 100x objective: grade 1 (mild) = 1 focus and grade 2 (moderate) = 2-4 foci.

Ptn.	VIO	Diagnosis	Lobular inflammation[#]	Portal inflammation	Confluent necrosis	Macrovesicular steatosis	Fibrosis	Sinusoidal dilatation[#]	Other
1	Yes	Perihilar cholangiocarcinoma	Grade 1 (mild)	Grade 1 (mild)	Absent	Absent	Bridging porto-portal fibrosis affecting <50% of vascular structures	Grade 2 (50%)	
2	No	Perihilar cholangiocarcinoma	Grade 1 (mild)	Grade 2 (moderate)	Absent	5%	Bridging porto-portal fibrosis affecting <50% of vascular structures	Grade 1 (<33%)	
3	Yes	Hepatocellular adenoma	Grade 1 (mild)	Grade 1 (mild)	Absent	5%	Some periportal/pericellular fibrosis affecting <33% of vascular structures without bridging	Grade 1 (<33%)	
4	Yes	Perihilar cholangiocarcinoma	Grade 1 (mild)	Grade 1 (mild)	Absent	Absent	Some periportal/pericellular fibrosis affecting <33% of vascular structures without bridging	Grade 2 (50%)	
5	Yes	Proximal cholangiocarcinoma	Absent	Absent	Absent	<5%	Some periportal/pericellular fibrosis affecting <33% of vascular structures without bridging	Grade 2 (50%)	

6	Yes	Intrahepatic cholangiocarcinoma	Grade 1 (mild)	Grade 1 (mild)	Absent	20%		Bridging porto-portal fibrosis affecting <50% of vascular structures	Grade 1 (<33%)	
7	Yes	Perihilar cholangiocarcinoma	Grade 1 (mild)	Grade 2 (moderate)	Absent	5%		Some periportal/pericellular fibrosis affecting <33% of vascular structures without bridging	Grade 1 (<33%)	
8	Yes	Metastasized melanoma	Grade 1 (mild)	Grade 1 (mild)	Absent	5%		Minimal periportal fibrosis	Grade 1 (>33%)	
9	No	Focal nodular hyperplasia	Absent	Grade 1 (mild)	Absent	Absent		Absent	Grade 1 (>33%)	
10	No	Chronic sclerosing cholangitis	Grade 1 (mild)	Grade 2 (moderate)	Absent	5%		Biliary cirrhosis	Grade 1 (>33%)	
11	No	Hepatocellular carcinoma	Grade 1 (mild)	Grade 1 (mild)	Absent	Absent		Some periportal/pericellular fibrosis affecting <33% of vascular structures without bridging	Grade 1 (>33%)	
12	Yes	Perihilar cholangiocarcinoma	Grade 1 (mild)	Grade 1 (mild)	Absent	Absent		Minimal periportal fibrosis	Grade 2 (50%)	
13	No	Hepatocellular carcinoma	Grade 2 (moderate)	Grade 3 (severe)	5%	20%		Porto-portal and porto-central bridging fibrosis affecting >50% of vascular structures	-	
14	Yes	Colorectal liver metastases	Grade 1 (mild)	Absent	20%	Absent		Some periportal/pericellular fibrosis affecting <33% of vascular	Grade 2 (50%)	Signs of nodular regenerative hyperplasia ¹¹ caused by preoperative chemotherapy

									(oxaliplatin)
15	No	Intrahepatic cholangiocarcinoma	Grade 1 (mild)	Grade 1 (mild)	Absent	5%	structures without bridging Absent	Grade 1 (<33%)	
16	No	Perihilar cholangiocarcinoma	Absent	Grade 2 (moderate)	Absent	Absent	Porto-portal and porto-central bridging fibrosis affecting >50% of vascular structures	Grade 1 (>33%)	
17	Yes	Hepatocellular adenoma	Grade 1 (mild)	Grade 1 (mild)	Absent	Absent	Absent	Grade 1 (>33%)	
18	Yes	Colorectal liver metastases	Grade 1 (mild)	Grade 1 (mild)	Absent	50%	Some periportal/pericellular fibrosis affecting <33% of vascular structures without bridging	Grade 2 (50%)	
19	Yes	Perihilar cholangiocarcinoma	Grade 1 (mild)	Grade 2 (moderate)	Absent	Absent	Some periportal/pericellular fibrosis affecting <33% of vascular structures without bridging	Grade 1 (<33%)	
20	Yes	Chronic/recurrent cholangitis	Grade 1 (mild)	Grade 3 (severe)	Absent	5%	Biliary cirrhosis with bridging	Grade 1 (<33%)	
21	Yes	Intrahepatic cholangiocarcinoma	Grade 1 (mild)	Grade 1 (mild)	Absent	Absent	Some periportal/pericellular fibrosis affecting <33% of vascular structures without bridging	Grade 1 (<33%)	
22	Yes	Perihilar cholangiocarcinoma	Grade 1 (mild)	Grade 2 (moderate)	Absent	Absent	Bridging porto-portal fibrosis affecting <50% of vascular	Grade 2 (50%)	

23	No	Hepatoblastoma	Grade 1 (mild)	Grade 1 (mild)	Absent	Absent	structures Some periportal/pericellular fibrosis affecting <33% of vascular structures without bridging	Grade 2 (50%)	
24	Yes	Hepatocellular carcinoma	Grade 1 (mild)	Grade 1 (mild)	Absent	Absent	Some periportal/pericellular fibrosis affecting <33% of vascular structures without bridging	Grade 1 (<33%)	
25	Yes	Perihilar cholangiocarcinoma	Grade 1 (mild)	Grade 3 (severe)	Absent	Absent	Some periportal/pericellular fibrosis affecting <33% of vascular structures without bridging	Grade 1 (<33%)	
26	No	Intrahepatic cholangiocarcinoma	Grade 1 (mild)	Grade 3 (severe)	Absent	Absent	Some periportal/pericellular fibrosis affecting <33% of vascular structures without bridging	Grade 3 (>50%)	
27	No	Chronic/recurrent cholangitis	Grade 1 (mild)	Grade 1 (mild)	Absent	Absent	Periportal and minimal pericellular and perivenular fibrosis without bridging	Grade 2 (50%)	Purulent cholangitis
28	Yes	Colorectal liver metastases	Grade 1 (mild)	Grade 1 (mild)	Absent	Absent	Some periportal/pericellular fibrosis affecting <33% of vascular	Grade 2 (50%)	

29	Yes	Perihilar cholangiocarcinoma	Grade 1 (mild)	Grade 1 (mild)	Absent	35%	structures without bridging Some periportal/pericellular fibrosis affecting <33% of vascular structures	Grade 1 (<33%)	
30	Yes	Hepatocellular carcinoma	Grade 1 (mild)	Grade 3 (severe)	Absent	20%	without bridging Bridging porto-portal fibrosis affecting <50% of vascular structures	Grade 1 (<33%)	
31	Yes	Hepatocellular carcinoma	Grade 1 (mild)	Grade 1 (mild)	Absent	Absent	Pericellular fibrosis affecting <33% of vascular structures	Grade 2 (50%)	
32	Yes	Intrahepatic cholangiocarcinoma	Grade 1 (mild)	Grade 1 (mild)	5%	Absent	without bridging Some periportal fibrosis without pericellular fibrosis or bridging	Grade 2 (50%)	
33	No	Perihilar cholangiocarcinoma	Grade 1 (mild)	Grade 2 (moderate)	Absent	5%	Some periportal/pericellular fibrosis affecting <33% of vascular structures	Grade 2 (50%)	
34	Yes	Perihilar cholangiocarcinoma	Grade 1 (mild)	Grade 2 (moderate)	<5%	5%	without bridging Bridging porto-portal fibrosis affecting <50% of vascular structures	Grade 2 (50%)	Signs of lobular atrophy
35	No	Colorectal liver metastases	Grade 1 (mild)	Grade 1 (mild)	<25%	5%	Minimal periportal/pericellular without	Grade 1 (<33%)	

36	No	Epithelioid hemangioendothelioma	Grade 1 (mild)	Grade 1 (mild)	Absent	Absent	bridging Minimal periportal	Grade 1 (<33%)	
37	Yes	Perihilar cholangiocarcinoma	Grade 1 (mild)	Grade 2 (moderate)	Absent	Absent	Some periportal fibrosis. developing bridging fibrosis	Grade 2 (50%)	
38	Yes	Perihilar cholangiocarcinoma	Absent	Grade 1 (mild)	Absent	Absent	Discrete periportal	Grade 1 (<33%)	
39	Yes	Colorectal liver metastases	Grade 1 (mild)	Grade 2 (moderate)	Absent	35%	Periportal	Grade 2 (50%)	Ballooning. borderline steatohepatitis. several Councilman bodies.

Table S3: Functional description of inflammatory messengers measured in mouse plasma.

Abbreviation	Protein	Function	Reference
Tnf α	Tumor necrosis factor alpha	Induces macrophage activation. neutrophil recruitment. and apoptosis	12
Il-1 β	Interleukin 1 beta	Induces Cox-2 and Icam-1 expression and Il-6 and chemokine production	13
Il-4	Interleukin 4	Mediates T helper 2 cell differentiation	14,15
Il-5	Interleukin 5	Stimulates proliferation and activation of eosinophils and basophils	16
Il-6	Interleukin 6	Regulates neutrophil recruitment through cytokine and chemokine signaling	17
Il-10	Interleukin 10	Inhibits activation of T cells. monocytes. and macrophages.	7,8,18
Il-12	Interleukin 12	Activates T-cells and natural killer cells and enhances proliferation of hematopoietic progenitor cells	19
Il-13	Interleukin 13	Inhibits cytokine production by monocytes and regulates lfn- γ production by lymphocytes	20
Il-18	Interleukin 18	Suppresses anti-inflammatory cytokines	21
Il-22	Interleukin 22	Promotes cell proliferation and survival	22
Ccl5	Chemokine (C-C motif) ligand 5	Regulates activation and chemotaxis of leukocytes and lymphocytes	23,24
Gm-csf	Granulocyte-macrophage colony-stimulating factor	Governs production. differentiation. proliferation. and activation of granulocytes and monocytes	16,25
lfn- γ	Interferon gamma	Activates macrophages and promotes T helper 1 cell differentiation	26
Baff	B cell activating factor	Stimulates B cell proliferation and function	27
Tslp	Thymic stromal lymphopoietin	Induces T cell signaling and enhances maturation of dendritic cells	28,29
Vegf	Vascular endothelial growth factor	Is mitogenic and angiogenic	30,31

This table was adapted from³².

Table S4 – Duration and technique of vascular inflow occlusion and removed liver segments during major liver surgery in patients.

Patient #	Cumulative ischemia time (min)	Method of vascular inflow occlusion	Couinaud segments removed
1	50	Intermittent	I-IV
2	50	Intermittent	V-VIII
3	50	Intermittent	I+V+VIII+part IV
4	43	Intermittent	I-IV
5	56	Intermittent	I-IV
6	20	Continuous	I-IV
7	65	Intermittent	I-IV
8	42	Intermittent	V-VIII
9	120	Intermittent	II-IV+wedge VI+ VII
10	52	Continuous	II+V+part VIII
11	76	Intermittent	V-VIII
12	39	Intermittent	I-IV
13	24	Continuous	V-VIII
14	26	Intermittent	II-IV
15	68	Intermittent	I-IV
16	93	Intermittent	I-IV + part VIII
17	68	Intermittent	V-VIII
18	46	Intermittent	V-VIII + part IV
19	20	Continuous	V-VIII
20	72	Intermittent	VII-VIII + I
21	43	Intermittent	II-IV
22	33	Continuous	II-IV
23	30	Continuous	V-VIII + I
24	68	Intermittent	I-IV
25	25	Continuous	V-VIII+ I
26	68	Intermittent	I-IV + wedges V+VI+VIII

The table shows the duration of ischemia, the method of vascular inflow occlusion, and the resected Couinaud liver segments for all patients included in this study that were subjected to I/R during liver resection (i.e.. the I/R group). When excessive intraoperative bleeding occurs during liver resection. the afferent vasculature is occluded with a sling to prevent hemodynamic complications. This surgical technique is known as vascular inflow occlusion or the Pringle manoeuvre³³ and induces I/R injury as side effect. Intermittent vascular inflow occlusion is the gold standard technique and consists of repetitive cycles of 20 min of ischemia followed by 10 min of reperfusion³⁴. As is shown in the table. continuous ischemia is only used if the anticipated duration of vascular inflow occlusion is short. or if the situation does not permit the 10 min reperfusion period normally used in intermittent vascular inflow occlusion (e.g.. patient #10).

Table S5 –Removed liver segments during major liver surgery in patients operated without vascular inflow occlusion (control group).

Patient #	Couinaud segments removed
27	II-IV
28	II-IV
29	II-IV
30	II-IV
31	V-VIII
32	I-IV
33	I + V-VIII + part IV
34	II-IV
35	I-IV
36	II-IV
37	I-IV
38	V-VIII
39	V-VIII

Table S6 Cytokine levels 6 h and 24 h after sham operation or liver I/R in untreated mice or mice treated with MitoQ.

	6 h sham	6 h I/R	6 h MitoQ + I/R	24 h sham	24 h I/R	24h MitoQ + I/R
IL-10	1.0 ± 0.3	9.7 ± 7.9	7.0 ± 3.3 [#]	1.0 ± 0.3	3.0 ± 1.6	6.3 ± 2.5 [#]
IL-18	134.3 ± 27.4	1034.0 ± 420.0	706.6 ± 163.2	134.3 ± 27.4	749.3 ± 212.7	611.5 ± 156.2
IL-4	1.0 ± 0.1	4.6 ± 1.5	3.7 ± 0.4	1.0 ± 0.1	4.0 ± 1.2	3.8 ± 1.6
IL-5	831.4 ± 494.0	900.3 ± 342.3	1669.0 ± 1449.0	831.4 ± 494.0	639.0 ± 567.5	449.1 ± 486.4
IL-6	831.4 ± 494.0	2396.0 ± 1929.0	915.2 ± 351.3 [#]	831.4 ± 494.0	1900.0 ± 1630.0	1229.0 ± 1719.0
TNF-a	10.0 ± 3.5	92.0 ± 52.6	49.0 ± 10.0 [#]	10.0 ± 3.5	58.0 ± 40.4	34.5 ± 26.6
IL-22	584.6 ± 521.4	4873.0 ± 2018.0	1263.0 ± 1790.0 [#]	584.6 ± 521.4	61.2 ± 48.0	42.4 ± 11.2
TSLP	4.0 ± 3.0	28.3 ± 6.8	25.0 ± 9.5	4.0 ± 2.8	19.1 ± 14.5	21.4 ± 11.1
BAFF	2166.0 ± 435.6	11141.0 ± 2556.0	10348.0 ± 2354.0	2166.0 ± 435.6	15042.0 ± 3487.0	11754.0 ± 2854.0
VEGF	12.1 ± 3.5	68.7 ± 12.4	53.4 ± 12.6	12.1 ± 3.5	60.0 ± 16.3	52.8 ± 9.3
RANTES	21.0 ± 4.0	67.3 ± 10.0	63.5 ± 13.4	21.0 ± 4.0	57.8 ± 10.2	72.2 ± 34.8
GM-CSF	0.3 ± 0.7	9.5 ± 6.6	3.7 ± 2.4 [#]	0.3 ± 0.7	6.6 ± 8.9	2.7 ± 5.2
IFN-γ	2.6 ± 1.1	19.8 ± 13.5	8.8 ± 3.0 [#]	2.6 ± 1.1	21.7 ± 32.1	9.0 ± 8.1
IL-1b	3.8 ± .3	21.4 ± 6.1	15.2 ± 3.6	3.8 ± 1.3	19.6 ± 15.0	15.5 ± 12.2
IL-12	2.5 ± 0.3	14.2 ± 1.6	10.8 ± 1.5 [#]	2.5 ± 0.3	16.1 ± 9.0	11.0 ± 6.0
IL-13	6.7 ± 0.9	29.4 ± 9.1	24.5 ± 5.9	6.7 ± 0.9	26.3 ± 9.3	19.7 ± 42

All cytokine levels are shown as pg/mL, values represent mean±SD. # indicates p<0.05 versus the I/R group. The materials and methods are included in the main text. The cytokine levels are also shown as heat map in Figure 3J of the main text.

Supplemental references

1. Committee for the Update of the Guide for the Care and Use of Laboratory Animals, Institute for Laboratory Animal Research, Division on Earth and Life Studies, National Research Council. Guide for the care and use of laboratory animals: Eighth edition. National Academies Press; 2010.
2. van Golen RF, Stevens KM, Colarusso P, Jaeschke H, Heger M. Platelet aggregation but not activation and degranulation during the acute post-ischemic reperfusion phase in livers with no underlying. *J Clin Transl Res* 2015; **1**: 107-15.
3. van Golen RF, Reiniers MJ, Olthof PB, van Gulik TM, Heger M. Sterile inflammation in hepatic ischemia/reperfusion injury: Present concepts and potential therapeutics. *J Gastroenterol Hepatol* 2012; **28**: 394-400.
4. Taub R. Liver regeneration: From myth to mechanism. *Nat Rev Mol Cell Biol* 2004; **5**: 836-47.
5. Böhm F, Köhler UA, Speicher T, Werner S. Regulation of liver regeneration by growth factors and cytokines. *EMBO Mol Med* 2010; **2**: 294-305.
6. Rehm M, Bruegger D, Christ F, Conzen P, Thiel M, Jacob M, et al. Shedding of the endothelial glycocalyx in patients undergoing major vascular surgery with global and regional ischemia. *Circulation* 2007; **116**: 1896-906.
7. Bamboat ZM, Ocuin LM, Balachandran VP, Obaid H, Plitas G, Dematteo RP. Conventional dcs reduce liver ischemia/reperfusion injury in mice via IL-10 secretion. *J Clin Invest* 2010; **120**: 559-69.
8. Dinant S, Veteläinen RL, Florquin S, van Vliet AK, van Gulik TM. IL-10 attenuates hepatic I/R injury and promotes hepatocyte proliferation. *J Surg Res* 2007; **141**: 176-82.
9. van Montfoort ML, Stephan F, Lauw MN, Hutten BA, Van Mierlo GJ, Solati S, et al. Circulating nucleosomes and neutrophil activation as risk factors for deep vein thrombosis. *Arterioscler Thromb Vasc Biol* 2013; **33**: 147-51.
10. Fialkow L, Wang Y, Downey GP. Reactive oxygen and nitrogen species as signaling molecules regulating neutrophil function. *Free Radic Biol Med* 2007; **42**: 153-64.
11. Rubbia-Brandt L, Lauwers GY, Wang H, Majno PE, Tanabe K, Zhu AX, et al. Sinusoidal obstruction syndrome and nodular regenerative hyperplasia are frequent oxaliplatin-associated liver lesions and partially prevented by bevacizumab in patients with hepatic colorectal metastasis. *Histopathology* 2010; **56**: 430-9.
12. Perry BC, Soltys D, Toledo AH, Toledo-Pereyra LH. Tumor necrosis factor- α in liver ischemia/reperfusion injury. *J Invest Surg* 2011; **24**: 178-88.
13. Dinarello CA. Immunological and inflammatory functions of the interleukin-1 family. *Annu Rev Immunol* 2009; **27**: 519-50.
14. Wynn TA. Type 2 cytokines: Mechanisms and therapeutic strategies. *Nat Rev Immunol* 2015; **15**: 271-82.
15. Li J, Zhao X, Liu X, Liu H. Disruption of TIM-4 in dendritic cell ameliorates hepatic warm IR injury through the induction of regulatory T cells. *Mol Immunol* 2015; **66**: 117-25.

16. Broughton SE, Dhagat U, Hercus TR, Nero TL, Grimbaldston MA, Bonder CS, et al. The GM-CSF/IL-3/IL-5 cytokine receptor family: From ligand recognition to initiation of signaling. *Immunol Rev* 2012; **250**: 277-302.
17. Jones SA. Directing transition from innate to acquired immunity: Defining a role for IL-6. *J Immunol* 2005; **175**: 3463-8.
18. Yoshidome H, Kato A, Edwards MJ, Lentsch AB. Interleukin-10 suppresses hepatic ischemia/reperfusion injury in mice: Implications of a central role for nuclear factor kappaB. *Hepatology* 1999; **30**: 203-8.
19. Teng MW, Bowman EP, McElwee JJ, Smyth MJ, Casanova JL, Cooper AM, Cua DJ. IL-12 and IL-23 cytokines: From discovery to targeted therapies for immune-mediated inflammatory diseases. *Nat Med* 2015; **21**: 719-29.
20. Minty A, Chalon P, Derocq JM, Dumont X, Guillemot JC, Kaghad M, et al. Interleukin-13 is a new human lymphokine regulating inflammatory and immune responses. *Nature* 1993; **362**: 248-50.
21. Takeuchi D, Yoshidome H, Kato A, Ito H, Kimura F, Shimizu H, et al. Interleukin 18 causes hepatic ischemia/reperfusion injury by suppressing anti-inflammatory cytokine expression in mice. *Hepatology* 2004; **39**: 699-710.
22. Chestovich PJ, Uchida Y, Chang W, Ajalat M, Lassman C, Sabat R, et al. Interleukin-22: Implications for liver ischemia-reperfusion injury. *Transplantation* 2012; **93**: 485-92.
23. Schall TJ. Biology of the RANTES/SIS cytokine family. *Cytokine* 1991; **3**: 165-83.
24. Bacon KB, Premack BA, Gardner P, Schall TJ. Activation of dual T cell signaling pathways by the chemokine RANTES. *Science* 1995; **269**: 1727-30.
25. Tsung A, Zheng N, Jeyabalan G, Izuishi K, Klune JR, Geller DA, et al. Increasing numbers of hepatic dendritic cells promote hmgb1-mediated ischemia-reperfusion injury. *J Leukoc Biol* 2007; **81**: 119-28.
26. Schroder K, Hertzog PJ, Ravasi T, Hume DA. Interferon-gamma: An overview of signals, mechanisms and functions. *J Leukoc Biol* 2004; **75**: 163-89.
27. Mackay F, Schneider P. Cracking the BAFF code. *Nat Rev Immunol* 2009; **9**: 491-502.
28. Reche PA, Soumelis V, Gorman DM, Clifford T, Liu Mr, Travis M, et al. Human thymic stromal lymphopoietin preferentially stimulates myeloid cells. *J Immunol* 2001; **167**: 336-43.
29. Rochman Y, Spolski R, Leonard WJ. New insights into the regulation of T cells by gamma(c) family cytokines. *Nat Rev Immunol* 2009; **9**: 480-90.
30. Ferrara N, Gerber HP, LeCouter J. The biology of VEGF and its receptors. *Nat Med* 2003; **9**: 669-76.
31. Tamagawa K, Horiuchi T, Uchinami M, Doi K, Yoshida M, Nakamura T, et al. Hepatic ischemia-reperfusion increases vascular endothelial growth factor and cancer growth in rats. *J Surg Res* 2008; **148**: 158-63.
32. Olthof PB, van Golen RF, Meijer B, van Beek AA, Bennink RJ, Verheij J, et al. Warm ischemia time-dependent variation in liver damage, inflammation, and function in hepatic ischemia/reperfusion injury. *Biochimica Et Biophysica Acta (BBA)-Molecular Basis of Disease* 2017; **1863**: 375-85.

33. Pringle JH. V. Notes on the arrest of hepatic hemorrhage due to trauma. *Ann Surg* 1908; **48**: 541-9.
34. van Riel WG, van Golen RF, Reiniers MJ, Heger M, van Gulik TM. How much ischemia can the liver tolerate during resection? *Hepatobiliary Surg Nutr* 2016; **5**: 58-71.

***Conflict of Interest Form**

[Click here to download Conflict of Interest Form: coi_disclosure.pdf](#)